

D3.1 Tangible Impacts Assessment Methods

DRAFT



D3.1 Tangible Impact Assessment Methods

Description of the methods to be applied to assess the tangible impacts in the selected trials and mini trials

Summary

The description of the selected methodologies to estimate the tangible impact damages, structured by type of Hazard and Risk Receptor, is a key piece of the project according to the ICARIA Framework. This report is expected to guide the assessment of damages in the Trials and Mini-trials for the different climate and adaptation scenarios. The outcome of deliverable 3.1 is a set of scientific methods with descriptions and references of risk models that will allow ICARIA researchers (and future external researchers across Europe) to assess the impact of Floods, Drought, Heatwaves, Forest Fires and Extreme Winds in their territories. In a changing climate context, where extreme events are becoming more frequent, the assessment of tangible damages is key to investing in effective adaptation measures and strategies that reduce damages.

| Deliverable number | Work package | |
|---|--|--|
| D3.1 | WP3 | |
| Deliverable lead beneficiary | Deliverable author(s) | Contributor(s) |
| CETAQUA | María Guerrero Hidalgo (CETAQUA) Alex De la Cruz Coronas (AQUATEC) Guillem Flor (Aigües de Barcelona) Barry Evans (University of Exeter) Albert Gili (IREC) | Eduardo Martinez Gomariz (Aigües de Barcelona) Marianne Bügelmayer-Blaschek (AIT) Jose Luis Dominguez (IREC) Nicola Addabbo (PLINIVS) Alberto Couce (CETAQUA) Thanasis Efetsos (Demokritos) |
| Internal reviewer(s) | External reviewer(s) | |
| Beniamino Russo (UPC) Mattia Leone (UNINA) | Albert Chen (UNEXE) | |
| Planned delivery date | Actual delivery date | |
| 29/12/2023 | 27/10/2024 | |
| Dissemination level | <input checked="" type="checkbox"/> PU = Public <input type="checkbox"/> PP = Restricted to other programme participants <input type="checkbox"/> RE = Restricted to a group specified by the consortium. Please specify: _____ <input type="checkbox"/> CO = Confidential, only for members of the consortium | |

Document history

| Date | Version | Author | Comments |
|------------|---------|---------------------------|---|
| 21/11/2023 | 1.0 | María Guerrero (CETAQUA) | Included outline of document and main economic methods |
| 11/12/2023 | 2.0 | Alberto Gili (IREC) | Included methods for electrical damages assessment |
| 15/12/2023 | 2.1 | Alex de la Cruz (AQUATEC) | Included methods for damages assessment for people and water sector |
| 05/01/2024 | 2.2 | Guillem Flor (AB) | Included methods for water sector damages assessment |
| 09/01/2024 | 3.0 | María Guerrero (CETAQUA) | Send for internal review |

DRAFT

Table of contents

| | |
|---|------------|
| 1 Introduction | 14 |
| 1.1 Project ICARIA | 14 |
| 1.2 Objectives of the deliverable | 15 |
| 1.3 Description of the general framework for tangible impact assessment | 16 |
| 1.4 Definitions | 20 |
| 2 Floods damage assessment methods | 22 |
| 2.1 Damage on properties | 22 |
| 2.2 Impacts in economic activity | 27 |
| 2.3 Impacts on the water sector | 33 |
| 2.4 Impacts on the electricity sector | 46 |
| 2.5 Impacts on the Transport sector | 53 |
| 2.6 Impacts on Natural areas | 67 |
| 2.7 Impacts on Pedestrians produced by urban pluvial floods | 69 |
| 3 Drought Impact Assessment | 73 |
| 3.1 Impact on aggregated Economic sectors | 73 |
| 3.2 Impact on the Water sector | 78 |
| 4 Heat waves impact assessment | 91 |
| 4.1 Impacts on people | 91 |
| 4.2 Impacts on the Electricity sector | 99 |
| 5 Forest fire impact assessment | 106 |
| 5.1 Impacts on Water sector | 106 |
| 5.2 Impacts on electricity sector | 107 |
| 6 Extreme winds impact assessment | 110 |
| 6.1 Impacts on properties | 110 |
| 6.2 Impacts on Electricity sector | 111 |
| 7 Cascading effects | 116 |
| 7.1 Cascading effects associated to the water sector | 117 |
| 7.2 Cascading effects associated to the electricity | 118 |
| 8 Conclusions | 119 |
| 9 References | 120 |
| Annex 1: Data Management Statement | 131 |

List of Figures

| | |
|---|----|
| Figure 1. Holistic modelling framework for multi-hazard risk/impact assessment, covering combined events and their cascading effects. Main elementary bricks are represented (modified after Zuccaro et al., 2018 and Russo et al., 2023). Source: D1.1 Holistic Modeling Framework, ICARIA Project. | 16 |
| Figure 2. Simplified risk/impact assessment to be implemented (Trials) and replicated (Mini-trials) within each case study region. | 17 |
| Figure 3. Flood damages classification. Source: Sharpe et al., (2012). | 18 |
| Figure 4. Sealing coefficient curves (Evans et al., 2019). | 24 |
| Figure 5. Sealing coefficient functions according to a) a specific water entry element and b) different property types. Source: Martinez- Gomariz et al., (2020). | 25 |
| Figure 6. Damage curves based on water depth inside the buildings (Evans et al., 2019). | 25 |
| Figure 7. Flowchart of the development of depth–damage curves for Spanish municipalities. Source: Martinez- Gomariz et al., 2020. | 26 |
| Figure 8. Process of methodology for indirect damages assessment. | 29 |
| Figure 9. Catalan Amplified Destination table Input-Output matrix, year 2016. Source: Catalan Statistical Office. | 31 |
| Figure 10. Exemplification of the expected depth-damage curves (vulnerability curves) (a) left side, associated with operative damage (€/m ³) and (b) right side, associated with physical damage (€/m ²). | 36 |
| Figure 11. Data flow diagram for the flood damage model in Wastewater Treatment Plants. | 38 |
| Figure 12. (a) EAD representation for several scenarios (different future climatic conditions) and (b) EAD reduction in a generic scenario with adaptation measures application. | 39 |
| Figure 13. Tertiary treatment lost revenues in coastal flooding events assessment representation in €/time. | 39 |
| Figure 14. (a) Main sewer longitudinal profile protection level evaluation per section with a generic and schematic representation. (b) Damage curve (θ - €/m) representation. | 43 |
| Figure 15. Data flow diagram representing the economical damage flooding model (own elaboration) for a coastal main sewer exposed to coastal flooding and surge impact. | 45 |
| Figure 16. Exemplification of comparative of main sewer protections in the same climate scenario. Left side with the current layout, right side with the modified layout (adaptation measure). | 46 |
| Figure 17. Fragility curves values for the elements of the grid of the FEMA study. | 49 |
| Figure 18. Thematic areas covered in flood impact assessment of the transport sector. | 53 |
| Figure 19. Hazard classifications for vehicles based on depth versus velocity of floodwater (Martínez-Gomariz et al., 2019). | 55 |
| Figure 20. Vehicle risk matrix. | 56 |
| Figure 21. Impact assessment flowchart for road networks. | 57 |
| Figure 22. Rules for governing speed of trains through flood water in the UK (Baker C. et al., 2016). | 58 |
| Figure 23. Summarised dimensions of UIC60 Rail (Source: https://railroadrails.com/railroad-rail-for-sale/uic60-rail/f) on top of EU standard sleeper (Source: https://www.buildingarena.co.uk/companies/railwaysleepers-com1/products/railway-sleeper-sizes-and-weights). | 59 |

| | |
|--|-----|
| Figure 24. Rail risk matrix. | 61 |
| Figure 25. Impact assessment flowchart for road networks. | 61 |
| Figure 26. Damages associated with the damage and risk assessment of flooding in metro systems (Forero-Ortiz et al., 2020). | 63 |
| Figure 27. Metro stations risk assessment map for a synthetic event scenario corresponding to a T20 rain event and the longitudinal profile of L3 line of the Barcelona Metro Station (from Forero-Ortiz et al., 2020a). | 66 |
| Figure 28. Hazard criterion proposed in project RESCCUE (Evans et al., 2018). | 70 |
| Figure 29. Combination of hazard and vulnerability maps to produce a flood risk map. | 72 |
| Figure 30. Criteria for assessing drought conditions in the surface water reservoirs of the AMB area. Source: ACA 2019. | 79 |
| Figure 31. Results of drought impact assessment in Sau-Susqueda reservoir system developed in project RESCCUE or the RCP 4.5 climate change scenario (RESCCUE 2019). | 80 |
| Figure 32. Organisation of the model's inputs in the different stages (in blue, essential; in grey, allow a better contextualisation to the local case). | 83 |
| Figure 33. Exemplification of expected data relationship between inflow concentration and inflow reduction (monthly data). | 85 |
| Figure 34. Exemplification of expected cost curves relating sanctions cost or extra treatment with inflow reduction (%) in each WWTP. | 86 |
| Figure 35. Data flow diagram representation of the Drought Damage Model (own elaboration). | 87 |
| Figure 36. Generic exemplification of the expected result of accumulated extra cost during an drought event related with the WWTP inflow reduction. | 88 |
| Figure 37. Tertiary treatment lost revenues in drought time assessment representation in €/time. | 88 |
| Figure 38. Identified European areas. | 97 |
| Figure 39. Spatialization the impacts of heat waves with reference to mortality. Impact is referred to RCP4.5 current period occasional frequency. | 98 |
| Figure 40. Graphical representation of the impacts of heat waves with reference to hospitalizations costs. Impact is referred to rcp scenario 4.5 current period occasional frequency. | 100 |
| Figure 41. Flowchart for the electricity sector impact assessment model. | 101 |
| Figure 42. Fragility curve of how likely the line is to fail as a function of the load it supports. | 103 |
| Figure 43. How the rated load (pu) is affected by ambient temperature (°C) for power and distribution transformers. | 104 |
| Figure 44. The effect of fire intensity and fire load density on breakdown voltage and distance in fire (You et al., 2013). | 109 |
| Figure 45. Variations in the conductor's ampacity as fire approaches the line (Choobineh et al., 2015). | 109 |
| Figure 46. Total damages due to power outages. | 110 |
| Figure 47. Fragility Curves used for assessing the impact of network components affected by extreme winds. Source: Pantelli et al. (2016) | 114 |
| Figure 48. Wind impacts on the overhead line depending on the direction of the wind. | 115 |
| Figure 49. Wind turbine efficiency to wind speed. | 115 |
| Figure 50. Water Sector Cascading Effects considered within ICARIA. | 118 |

Figure 51. Electricity Sector Cascading Effects considered within ICARIA.

DRAFT

List of Tables

| | |
|--|----|
| Table 1. Summary of methodologies classified by hazards. | 19 |
| Table 2. Data required for pluvial or fluvial flooding impact model on properties. | 23 |
| Table 3. Pluvial flooding damage model, data requirements (I). | 28 |
| Table 4. Necessary input data for the economic damage valuation model for WWTPs. | 34 |
| Table 5. Necessary input data for the economic damage assessment of the coastal flooding model on a main sewer parallel to the coast. | 41 |
| Table 6. Pluvial flooding hazard model, data requirements for electricity sector damage assessment (V). | 47 |
| Table 7. Electricity sector damage model, data requirements. | 51 |
| Table 8. Data requirements for impact assessment on road networks. | 54 |
| Table 9. Derivation criteria of vulnerability score based on VFIs along road sections (Evans 2019). | 56 |
| Table 10. Estimated Travel Cost (GBP) for cars as a function of speed per km (Penning-Rowse et al., 2010). | 57 |
| Table 11. Data requirements for impact assessment on road networks. | 59 |
| Table 12. Potential flood depth to rail disruption criteria. | 60 |
| Table 13. Derivation criteria of vulnerability score for passenger and freight flows per day. | 60 |
| Table 14. Hazard and vulnerability quantification. | 63 |
| Table 15. Hazard and vulnerability criteria for Metro stations service exposed to flooding (from Forero-Ortiz et al., 2020a). | 65 |
| Table 16. The risk matrix for Metro stations and ridership (from Forero-Ortiz et al., 2020a). | 65 |
| Table 17. Risk assessment criteria for evacuation of underground spaces through flooded stairs according to the Specific Force Per Unit Width parameter (Ishigaki et al., 2010). | 67 |
| Table 18. Impact assessment on vehicles, data requirements. | 68 |
| Table 19. Thresholds to assess human vulnerability according to different criteria (Evans et al., 2018). | 71 |
| Table 20. Formulation to compute the total vulnerability level (Evans et al., 2018). | 71 |
| Table 21. Risk matrix obtained by multiplying combined exposure/vulnerability and hazard indexes. | 71 |
| Table 22. Data requirements for the indirect tangible impact to all economic sectors of drought. | 73 |
| Table 23. Stages of the drought damage model. | 82 |
| Table 24. Necessary input data for the economic drought damage evaluation model for WWTPs. | 83 |
| Table 25. Input datasets used in the model. | 89 |
| Table 26. exponent values and type of relation. | 90 |
| Table 27. Damage typologies for the six levels of damage and the corresponding level of medical care and time of hospital stay. | 93 |
| Table 28. Data required (model inputs) for the heat wave impact model. | 94 |
| Table 29. Damage scale correlating thermal discomfort as a function of the Universal Thermal Climate Index (UTCI). | 96 |
| Table 30. Damage scale correlating thermal discomfort as a function of the Universal Thermal | |

| | |
|--|-----|
| Climate Index (UTCI). | 99 |
| Table 31. Data requirements for the electricity sector damage model. | 101 |
| Table 32. Data requirements for the electricity sector damage model. | 105 |
| Table 33. Forest fires impact on electricity infrastructures and associated threshold by Sfetsos et al 2021. | 108 |
| Forest fires impact on electricity infrastructures | 108 |
| Table 34. Data requirements for the electricity sector damage model. | 112 |

DRAFT

List of Acronyms and Abbreviations

| Acronyms Table | |
|----------------|--|
| AAR | Affected Area Rate |
| AC | Adaptive Capacity |
| ACA | Agència Catalana de l'Aigua (Catalan Water Agency) |
| ACSR | Aluminium Conductors Steel Reinforced |
| AGC | Auxiliary Generation Cost |
| AMB | Àrea Metropolitana de Barcelona (Barcelona Metropolitan Area) |
| AP | Mortality Attributable to Heat Waves |
| BAU | Business As Usual |
| BC | Business Cost |
| BHWR | Basic Human Water Requirement |
| CC | Coping Capacity |
| CCS | Consorcio de Compensación de Seguros (Insurance Compensation Consortium) |
| Cp | Coefficient of Performance |
| CS | Case Study |
| DC | Direct Current |
| DSS | Decision Support System |
| EAD | Expected Annual Damage |
| EDC | Effective Damage Cost |
| EHR | Historical Repair Records |
| EHV | Extra High Voltage |
| ENSC | Energy Non-Supplied Cost |
| EU | European Union |
| FCP | Probability of Failure for the Curve |
| FEMA | Federal Emergency Management Agency |
| FFI | Freight Flow Intensity |
| FWSI | Falkenmark Water Stress Indicator |
| GDP | Gross Domestic Product |
| GIS | Geographic Information System |
| GVA | Gross Added Value |
| HWLEM | Heat Wave Local Effect |
| Idescat | Instituto de Estadística de Cataluña (Catalonia Statistical Institute) |
| IDF | Intensity Duration Frequency |
| IPCC | Intergovernmental Panel on Climate Change |
| IT | Information Technology |
| LRG | Losses Related to the Grid |
| LRG | Losses Related to the Grid |
| MD | Number of Average Deaths |

| | |
|------|---|
| OSM | Open Street Map |
| PD | Predicted Deaths |
| PDF | Probability Distribution Function |
| PFI | Passenger Flow Intensity |
| PLI | Protection Level Index |
| PPIC | Public Policy Institute of California |
| RCP | Representative Concentration Pathways |
| RWH | Human Water Requirement |
| SAR | South Aegean Region |
| SBG | Salzburg |
| SLR | Sea Level Rise |
| SPI | Standardised Precipitation Index |
| SSO | Strategic Sub Objectives |
| TC | Transformative Capacity |
| TMB | Transporte Metropolitano de Barcelona (Barcelona Public Transport Operator) |
| UCTI | Universal Thermal Climate Index |
| UPC | Universitat Politècnica de Barcelona (Technical University of Catalonia) |
| VA | Added Value |
| VFI | Vehicular Flow Intensity |
| WDA | Water Depth Average |
| WP | Work Package |
| WWTP | WasteWater Treatment Plant |

DRAFT

Executive summary

This document presents the ICARIA approach for impact assessment methodology from a multi-hazard perspective, following the Holistic Modelling framework that provides consistency across selected climate-related hazards categories (i.e. heat waves, forest fires, droughts, floods, storm surges and storm wind). The proposed approach guarantees solid results since it is constructed, in its majority, from previous EU projects (i.e. RESCCUE, CLARITY, etc.) and International frameworks and metrics for risk/impact assessment in the context of climate change.

The present deliverable aims to set the rules for the following impact assessments in the 3 study regions (Barcelona Metropolitan Area, South Aegean Region and Salzburg Region) in the form of implementation in the project trials and mini-trials. The document is structured by climate hazard and provides significant aspects to build robust results, proposing clear steps from collecting essential data, to referenced assessment methods for damages to critical sectors and services at risk (e.g. related to urban water, transport, energy, waste, natural areas and tourism sectors), to expected outcomes. Therefore, it is expected to provide comprehensive guidance to ICARIA consortium researchers to assess the expected climate related damages for several risk receptors within the ICARIA project .

The methodologies proposed have been selected following the criteria of: i) robustness; ii) suitability to the hazards and risks receptors within ICARIA, including cascading effects; iii) adaptability to the different case studies; iv) technical capability of the Consortium members; v) expected data availability required to carry out the assessments.

The tangible impact assessment methods described in this deliverable are key to assess tangible damages expected from the most relevant climate hazards in the selected critical sectors and, under different climate and adaptation scenarios.

The final outcomes will give a better understanding of any possible consequences in monetary terms, that allow to define and compare suitable, sustainable and cost-effective adaptation solutions, from a climate resilient development perspective.

1 Introduction

1.1 Project ICARIA

The number of climate-related disasters has been progressively increasing in the last two decades and this trend could be drastically exacerbated in the medium- and long-term horizons according to climate change projections. It is estimated that, between 2000 and 2019, 7,348 natural hazard-related disasters have occurred worldwide, causing 2.97 trillion USD losses and affecting 4 billion people. These numbers represent a sharp increase of recorded disaster events by comparison with the previous twenty years. Much of this increase is due to a significant rise in the number of climate-related disasters (heatwaves, droughts, flooding, etc.), including compound events, whose frequency is dramatically increasing because of the effects of climate change and the related global warming. For the future, by mid-century, the world stands to lose around 10% of total economic value from climate change if temperature increase stays on the current trajectory, and both the Paris Agreement and 2050 net-zero emissions targets are not met.

In this framework, Project ICARIA has the overall objective to promote the definition and the use of a comprehensive asset level modelling framework to achieve a better understanding about climate related impacts produced by complex, compound and cascading disasters and the possible risk reduction provided by suitable, sustainable and cost-effective adaptation solutions.

This project will be especially devoted to critical assets and infrastructures that are susceptible to climate change, in a sense that its local effects can result in significant increases in cost of potential losses for unplanned failures, as well as maintenance – unless an effort is undertaken in making these assets more resilient. ICARIA aims to understand how future climate might affect life-cycle costs of these assets in the coming decades and to ensure that, where possible, investments in terms of adaptation measures are made up front to face these changes.

To achieve this aim, ICARIA has identified 7 Strategic Sub Objectives (SSO), each one related to one or several work packages. They have been classified according to different categories: scientific, corresponding to research activities for advances beyond the state of the art (SSO1, SSO2, SSO3, SSO4, SSO5); technological, suggesting and/or developing novel solutions, integrating state-of-the art and digital advances (SSO6); societal, contributing to improved dialogue, awareness, cooperation and community engagement as highlighted by the European Climate Pact (SSO7); and related to dissemination and exploitation, aimed at sharing ICARIA results to a broader audience and number of regions and communities to maximise project impact (SSO7).

- SSO1.- Achievement of a comprehensive methodology to assess climate related risk produced by complex, cascading and compound disasters
- SSO2.- Obtaining tailored scenarios for the case studies regions
- SSO3.- Quantify uncertainty and manage data gaps through model input requirements and innovative methods

- SS04.- Increase the knowledge on climate related disasters (including interactions between compound events and cascading effects) by developing and implementing advanced modelling for multi-hazard assessment
- SS05.- Better assessment of holistic resilience and climate-related impacts for current and future scenarios
- SS06.- Better decision taking for cost-efficient adaptation solutions by developing a DSS to compare adaptation solutions
- SS07.- Ensure the use and impact of the ICARIA outputs

The ICARIA project focuses on three case study regions with profound geographical, environmental, and socio-economical differences which will necessarily be taken into account for the holistic modelling framework development in a multi-hazard risk/impact assessment perspective. The Barcelona Metropolitan Area (AMB) and the Archipelago of South Aegean Region, are located in the coastal area of the Mediterranean Sea and are facing increasingly climate extremes (e.g., storm surges, pluvial floods, heatwaves, drought and forest fire) with huge impacts in socio-economic and environmental terms. The third one, the Salzburg Region, is located in Austria and is particularly sensitive to the effects of climate change (e.g. glacier melt and heatwaves) that directly impact the prevailing energy production assets (extremely critical infrastructures) and other important sectors. Seven additional follower regions will be considered for replication beyond the project.

Across different climate-related hazard categories and their multiple interrelations (e.g. complex, compound and cascading disasters), case studies will be used to test the risk/impact modelling methodology and technical solutions primarily through Trials. Secondly, the development and execution of Trials will be used to implement Mini-trials and will be planned for “demonstrators”.

1.2 Objectives of the deliverable

The main outcomes of Work Package 3 are:

- Development and testing of frameworks and methods for tangible impacts assessment (including direct and indirect damages)
- Development and testing of a holistic framework and a tool focused on the analysis of climate resilience of strategic services and infrastructures
- Decision Support System (DSS) Conceptualization, development and testing of a Decision Support System to assess climate related impacts and prioritise sustainable and cost-efficient adaptation measures

Task 3.1 focuses on the first objective, aiming to develop a framework to assess the tangible impacts caused by the hazards covered in the Project ICARIA (pluvial and coastal floods, drought, forest fires, heatwaves and extreme winds). In this context, tangible impacts assessment considers both direct and indirect damage, from single and compound events (multi-hazard perspective).

In general terms, the methodologies try to include several types of costs associated with the damages caused by the hazards, such as reconstruction costs, the costs of not providing the intended service, the knock-on effects on other systems and the results of exposure and vulnerability functions.

This task runs closely with WP1, in particular T1.1 ICARIA Holistic Modelling Framework, where a harmonised and consistent holistic modelling framework to support the impact and resilience assessments across different climate-related hazard categories has been presented.

Considering the outcomes of D1.1, the mentioned hazards and several assets and services of interest to be assessed were selected. Within the ICARIA context, critical assets and services have been defined as those infrastructures and buildings that cause a high impact to the system, society and economy if they fail due to a climate hazard. In ICARIA, the assets to be studied are related to urban water cycle, transport system, energy infrastructure, waste system, natural areas and the tourist sector. Regarding services, most of them will be analysed in terms of expected damage and resilience performance. Tourism, however, will be included both as a risk factor (e.g., increased tourism increases water supply demands, thus increasing vulnerability to droughts) and as a consequence of an event (e.g., civil society organisations prevent usage of bathing areas, thus reducing tourism).

During the first year of the project, this task has supported several discussions between researchers and the different Communities of Practices (CoP) to select all methodologies that will serve to evaluate the impacts of the aforementioned hazards and critical assets.

This deliverable collects all the methodologies that have been agreed in a structured manner so they can be implemented in the following years by the experts in the trials and mini-trials.

1.3 Description of the general framework for tangible impact assessment

The general framework of the tangible impact assessment has been built from the agreed design of the Holistic Modeling Framework (Deliverable 1.1, D1.1 onwards) to be applied in ICARIA. The model follows the developments made in EU-FP7 SNOWBALL (Zuccaro *et al.*, 2018), CLARITY (Zuccaro and Leone, 2021) and RESCCUE projects (Russo *et al.*, 2023), summarised in Figure 1.

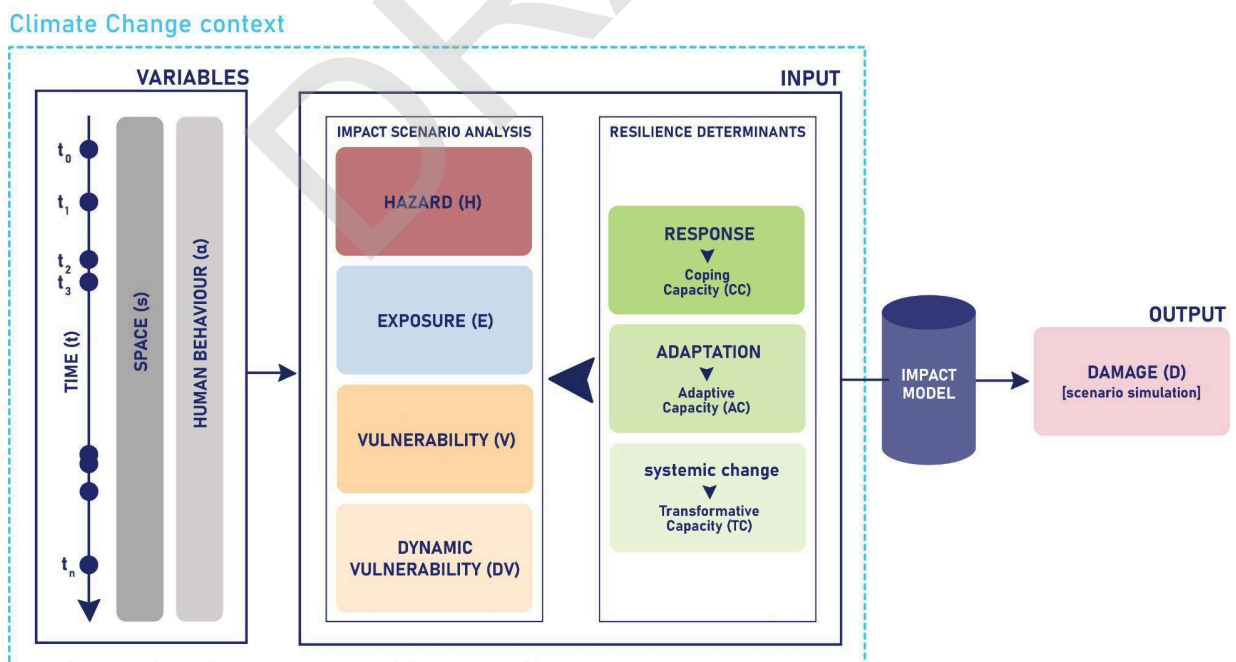


Figure 1. Holistic modelling framework for multi-hazard risk/impact assessment, covering combined events and

their cascading effects. Main elementary bricks are represented (modified after Zuccaro et al., 2018 and Russo et al., 2023). Source: D1.1 Holistic Modeling Framework, ICARIA Project.

The ICARIA holistic modelling framework assumes “elementary bricks” as units of analysis: *Hazards (H)* (within a complex scenario characterised by compound coincident or consecutive events), initial *Exposure (E)*, initial *Vulnerability (V)* and *Dynamic Vulnerability (DV)*, expected to produce an impact of a given intensity (*Damage - D*) in a window of analysis depending on *Time (t)* and *Space (s)* variables, and influenced by *Human Behaviour (α)* (intended as influence of decisions taken by local authorities, risk managers and/or communities along the DRM cycle). The key dimensions of resilience – *Coping Capacity (CC)*, *Adaptive Capacity (AC)*, *Transformative Capacity (TC)* – interact with the elementary bricks determining a change in the impact scenario (see D1.1 and D3.2). Both Time and Space represent the reference frame of the other elementary bricks. Hazard, initial Exposure and initial Vulnerability represent the input data in “peace time”, while Dynamic Vulnerability manifests itself gradually, as a consequence of subsequent combined phenomena. Coping, Adaptive and Transformative Capacities represent those elementary bricks through which identifying actions that can improve resilience, considering combined phenomena. Damage on risk receptors is the output data of the cascading effects scenario assessment. Human behaviour, as an additional factor within the procedure, has the capacity to drastically influence the other elementary bricks (except time and space). Further details about the ICARIA methodological framework can be found in D1.1.

Distribution of damage occurred on one or more risk receptors, expressed in the number of damaged elements for each damage class and/or monetary value of their restoration. Providing the time-space distribution of damage to the exposed elements caused by an “interactive causal chain” timeline of events, it represents the output of the ICARIA holistic modelling framework: $D(t,s)$. The damage scenario, resulting from the modelling procedure applied to the chain, takes into account i) the temporal distribution of the damage level for each element in all time steps of analysis, and ii) the spatial distribution of the damage level (e.g., number of deaths, number of collapsed buildings, sec./min./hours of power line interruption, etc.) for each elements within exposure categories.

Further, the three case studies - Barcelona Metropolitan Area (AMB), Salzburg Region (SALZ) and South Aegean Region (SAR) - have evaluated their most important hazards and assets in order to select the related tangible impacts to be assessed. The summarised assessment for each case study can be seen in Figure 2. The decision process considered the three Community of Practice (CoP) priorities and concerns collected during sessions and surveys, data availability, expertise required and alignment with ICARIA’s strategy and objectives.

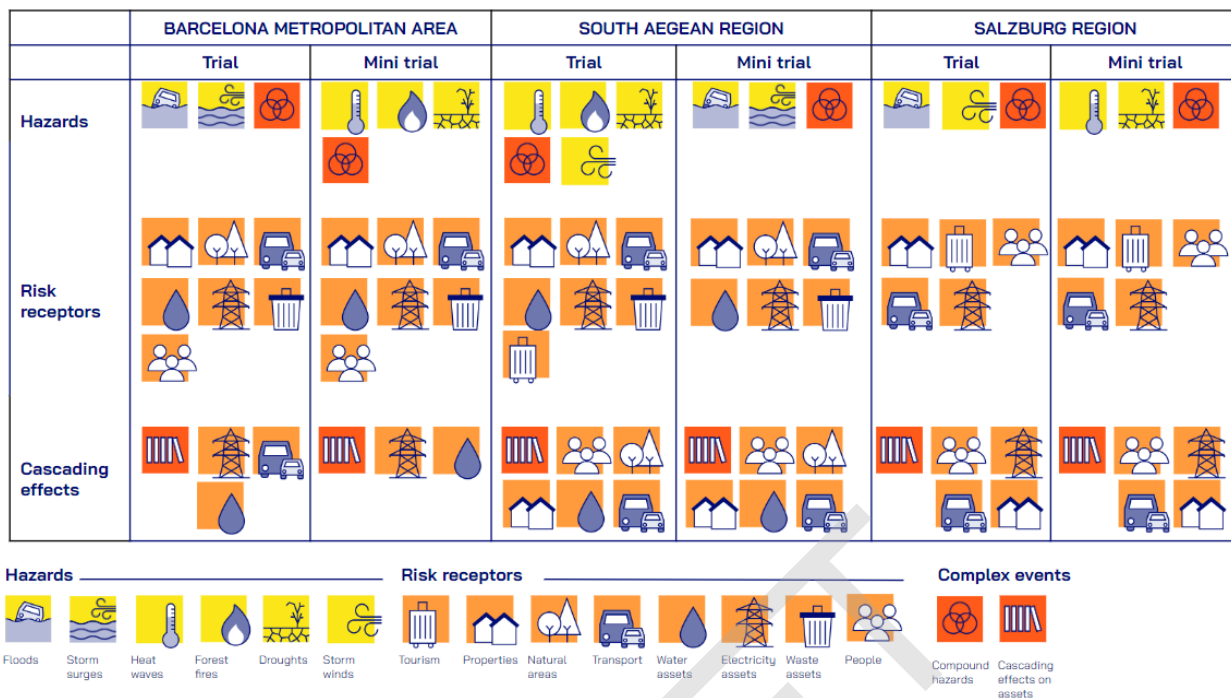


Figure 2. Simplified risk/impact assessment to be implemented (Trials) and replicated (Mini-trials) within each case study region.

The three case studies defined their assessment architecture for both the trial and the mini-trial. The trials are the main studies to be carried out in each case study, based on priorities for the region, previous expertise, data availability or other relevant criteria. Mini-trials replicate the studies made in the trials in other case studies, with the goal of helping to assess and improve the replicability of the methods and tools developed in the trials.

To understand the damage that an impact can cause, it can be useful to define and categorise them. Within the literature, there is a broad consensus on the categorization of damage. The first distinction that is commonly made is between tangible and intangible damage, displayed in Figure 3. A tangible damage is a damage that is easily capable of being assessed in monetary terms (Smith and Ward, 1998). Intangible damages arise from adverse social and environmental effects caused by climate hazards, including factors such as loss of life and injury, stress and anxiety (Sharpe et al., 2012). ICARIA focuses on tangible damages specifically, since they are easier to communicate to and understand by stakeholders, the transference of their values to other locations is more systematic and, generally, the methods for assessment are more developed compared to the intangible damages. There are, however, exceptions to this scope, in cases where the intangible damages assessment was found to be relevant for the CoP or for the methodological development perspective. For example, damages on people caused by flood impacts were considered as relevant to the AMB case study and, also considering the recent background from RESCCUE project, it was decided to consider them within the trial.

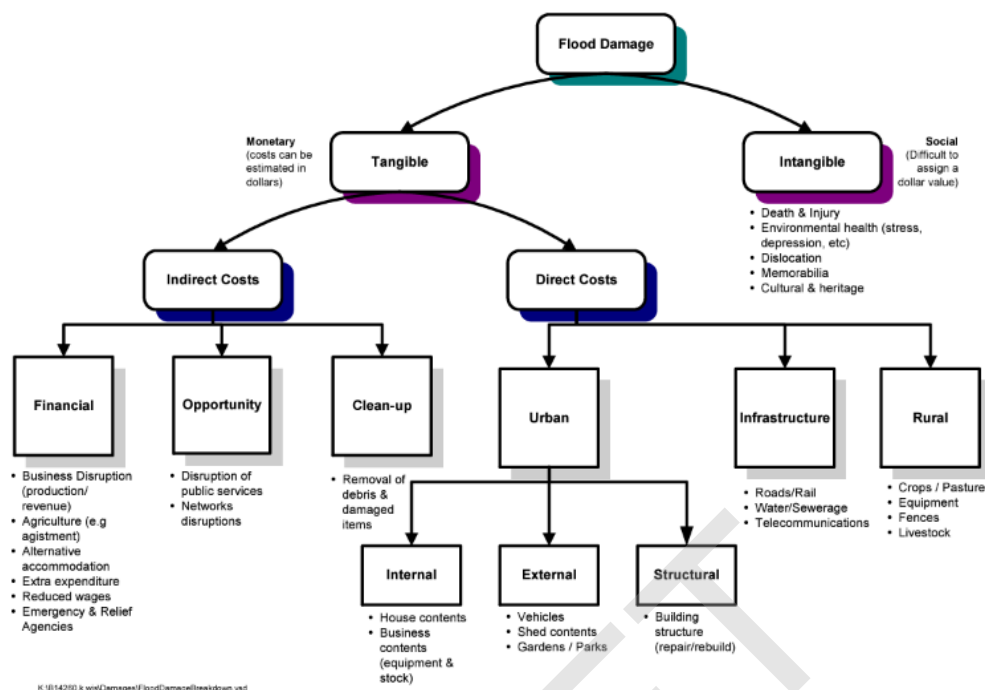


Figure 3. Flood damages classification. Source: Sharpe et al., (2012).

The second common distinction is between direct and indirect tangible damages. Typically, direct damage is defined as any loss that is caused directly by a hazard event naturally occurring or manmade. In case of flooding, for example, direct damage is defined as any loss that is caused by the immediate physical contact of flood water with humans, property and the environment. An indirect damage is induced by the direct impacts and may occur – in space or time – outside the flood event. The indirect damages are a cascading effect of the direct damages. The indirect damages try to assess how the direct damages are spread across the closer economic agents (Sharpe et al., 2012).

The following table describes the hazards, the selected damages included to be assessed and the main method of assessment of the latter, summarising the content of this deliverable.

Table 1. Summary of methodologies classified by hazards.

| Hazard | Asset | Damage | Key parameter of the methodology | Trial | Minitrial |
|--------|--------------------|----------------------------------|---|-----------|-----------|
| Flood | Properties | Direct | Depth-Damage curves & EAD function | AMB & SBG | SAR |
| | Economic sectors | Indirect | Input-Output Model /econometric regression | AMB | SBG |
| | Water Sector | Direct - WWTP Indirect - WWTP | Depth-Damage curves & EAD function | AMB | SAR |
| | | Direct - Main Sewer | <i>Oceanographic range and level change intensity</i> -Damage curves & EAD function | AMB | |
| | Electricity Sector | Direct | Fragility Curves and Intensity Duration Frequency Curves. | SBG & AMB | SAR |
| | | Indirect | Vulnerable points cascading effects evaluation starting from the direct impact assessment method. | SBG | AMB |
| | Transport | Direct - Traffic | Combined flood velocity and depth impact assessment. Vehicular flow intensity (VFI) | SBG | AMB & SAR |
| | | Direct - Railroads | Passenger flow intensity (PFI) and freight flow intensity (FFI) - Flood Depth | SBG & AMB | SAR |
| | | Direct - Metro | Metro service disruption due to flooding - Flood Depth | AMB | SAR |

| | | | | | |
|---------------|--------------------|--------------------------------------|--|-----------|------------|
| | | | Ridership evacuation due to floodings - Flood Depth and Flood velocity | | |
| | Natural areas | Direct- agriculture | Depth - damage curves & EAD function | AMB | SAR |
| | Pedestrians | Direct | 1D/2D urban drainage model + Pedestrian hazard classification . | AMB & SBG | |
| Drought | Economic sectors | Direct - aggregated economic sectors | Cobb douglas | SAR | SBG & AMB |
| | | Indirect - all sectors | General equilibrium modelling | SAR | AMB |
| | Water sector | Direct | Drought risk assessment through the evaluation of the state of surface water reservoir | SAR | AMB |
| | | Indirect - WWTP | Inflow-Operative extra cost curves | AMB | SAR |
| Heat Waves | Pedestrians | Direct | HWLEM simulations + UTCI indicator. | SAR | AMB SGB |
| | Electricity Sector | Direct | Electric demand oscillations related to Heatwave temperature variation. | SAR | AMB SGB |
| | | Indirect | Economic costs due to service disruption model. | SAR | AMB SGB |
| Forest Fire | Water Sector | Direct | Wildfire simulation from the WRF-FIRE | SAR | AMB |
| | Electricity Sector | Direct | Burned electricity network assets. | SAR | AMB |
| Extreme Winds | Properties | Direct | CLIMADA Assessment model. | SAR & SBG | |
| | Electricity Sector | Direct | Fragility Curves of network components | SAR & SBG | |

1.4 Definitions

Before the description of the methodologies, basic definitions related with the scope of the deliverable are provided:

Direct Damage relates to damage that results directly from a defined hazard; for example a flood event could cause direct physical damage to an infrastructure due to the immediate physical contact of flood water with humans, property and the environment. The terms 'loss' and 'damage' are used synonymously in the literature.

Disaster refers to "severe alterations in the normal functioning of a community or a society due to hazardous physical events interacting with vulnerable social conditions, leading to widespread adverse human, material, economic, or environmental effects that require immediate emergency response to satisfy critical human needs and that may require external support for recovery" (Field et al.,2012).

Exposure refers to the risk of a service, infrastructure and or population being adversely affected by an impact.

Hazard refers to "the potential occurrence of a natural or human-induced physical event that may cause loss of life, injury, or other health impacts, as well as damage and loss to property, infrastructure, livelihoods, service provision, and environmental resources" (IPCC 2012). A hazard could, for example, be a flood event, coldwave, heatwave, risk of terrorism and/or cyber-attack.

Impact refers to the effect/influence of an event (naturally occurring or manmade) that results in a consequence such as causing damage and/or disruption to a service or infrastructure. An example of an impact could be a flood event causing damage to an energy substation resulting in a localised power cut. The term 'impact' refers to the broad effects that an event can have on people, to property and to the environment. These impacts can be both positive and negative, although it is common in the literature to see the term used in a purely negative sense, especially in relation to human health, where health impact assessments are conducted.

Indirect Damage is induced by the direct impacts and may occur – in space or time – "outside" the event. In the context of this document refers to the detrimental effect on a system. Infrastructure refers to physical buildings and objects that provide or facilitate the distribution of a service. Again in the example of "Energy Supply" an infrastructure could be a power station, power lines, power substation etc. and in the context of "Health Care" an infrastructure could be a hospital, clinic, blood bank etc. Intangible damage refers to damages that cannot be expressed in monetary values, for example the loss of life or the deterioration of health as a result/consequence of an impact.

Tangible damage refers to monetary damage that has occurred as a result of an impact.

Vulnerability refers to the propensity of exposed elements (such as human beings, their livelihoods and assets) to suffer adverse effects when impacted by hazard events. Vulnerability is related to predisposition or capacities that favour, either adversely or beneficially, the adverse effects on the exposed elements. Vulnerability refers to exposure, susceptibility and resilience (BINGO, 2016).

The structure of the document is as follows: it starts with the introduction to the Project ICARIA, the deliverable objectives and the methodological background that sets the approach followed throughout the document. It is followed by the explanation of the methodologies to assess the selected impacts, structured by hazards - i.e. floods, drought, heatwaves, forest fires, and extreme winds.

DRAFT

2 Floods damage assessment methods

White (1945) considered that flooding causes four types of impacts on communities: (a) damage to physical property; (b) interruption of the production of goods and services; (c) loss or impairment of human life; and (d) reoccupation and rehabilitation of flooded areas (Chen et al., 2016). These impacts have been classified differently across literature, although they remain valid conceptually. The four types of impacts have been considered, in different combinations, to propose methods to estimate tangible damages caused by flooding events and, considering the differences of the geographic contexts.

2.1 Damage on properties

In this section the focus is put on the tangible damages caused by floods to properties, which can be classified as direct and indirect damages. Direct tangible damages to properties are defined as any loss caused by the physical contact of flood water with properties or any other asset, while indirect damages are induced by the direct damage and may occur outside the flood affected area or after the flood event (Chen et al., 2016).

2.1.1 Direct damage - Pluvial and fluvial flooding

Urban areas are vulnerable to pluvial and fluvial floods (Chen et al., 2010). Whereas fluvial floods only occur in riverine floodplain areas and tend to be more damaging, they do not occur as often as pluvial ones. An urban drainage system deals with stormwater, or the combination of stormwater and wastewater. The drainage networks are considered as two subsystems for modelling: major (overland flow paths), and minor (underground sewer pipes). Heavy rainfall may lead to pluvial floods in many cities once the drainage system is overloaded. In hydrological terms, fluvial floods are generally characterised by high flow depths and low water velocity, since they are mostly caused by river systems exceeding the conveyance of the channel that causes overbanking. It may be caused by flow coming from upstream. Whereas urban pluvial floods, due to the low roughness of the overland surfaces present low flow depths and high velocity (up to 3-4 m/s), mainly due to intense rainfall in the local region that overwhelms the drainage capacity.

The proposed method to assess the direct effects of floods on properties for the Project ICARIA is based on the flood-depth-damage curves, also known as vulnerability curves, which are an essential element of many flood damage models. In particular, the method was developed by CETAQUA researchers in Project RESCCUE and allows to transfer the depth-damage curves developed for Barcelona municipality to other urban areas (Martínez-Gomariz et al., 2020; Martínez-Gomariz et al., 2021). The methodology allows to estimate the damage of both flood types and can be applied in all the provinces of Spain when tailored flood-depth-damage curves can be obtained.

2.1.1.1 Scope and objectives of the impact assessment

The objective of this method is the assessment of expected economic damages for different kinds of properties (i.e. housing, commercial buildings, industrial warehouses), relative to the return period of flooding events with tailored flooding damage curves. The methodology source for the development of the damage curves is presented in Deliverable 3.4 of the RESCCUE Project and Evans et al., (2019) and Martínez-Gomariz et al., (2020), which were developed to be replicable in any other urban area in Spain. The advancement of this iteration lays on the possibility of adapting the curves to other types

of areas (rural or islands) and other types of properties not considered previously, such as the waste treatment infrastructures for the case of this project.

2.1.1.2 Input datasets used in the flood impact model on properties

Table 2. Data required for pluvial or fluvial flooding impact model on properties.

| Data requirements for the pluvial flooding damage | | |
|---|---|--|
| Data group | Description | Source |
| Urban flooding maps | Local flood maps from 1D/2D hydrodynamic flooding model | Results Task 2.1 |
| Land use and parcel information | Classification of land use and buildings in the study area to determine the sealing coefficient and the depth inside the building | Satellite information/ Public cadastre |
| Insurance payouts from past flood events | The Public Insurance Company of Spain, which covers extraordinary risks, provided data on the payouts for properties and businesses related to all extreme events that occurred in the past 25 years. | Local insurance organization: Consorcio de Compensación de Seguros (AMB)/ Catastrophe Fund Austria (SBG) |
| Depth-Damage curves | Matrix to associate certain water depths with economic damages | Project RESCCUE (Martinez-Gomariz et al., 2020) |

In summary, this methodology involves three main groups of information: (1) urban flooding maps, (2) land use and parcel information and (3) depth damage functions. In addition, the damage curves can be updated or validated with new information from past flood events payouts from extreme events insurance databases.

2.1.1.3 Impact assessment model setup

For the estimation of tangible direct damages caused by pluvial and fluvial floods, depth-damage curves are used. They are useful to represent the vulnerability of elements at risk, and to assess the damage caused by pluvial or fluvial floods and other hazards, matching the magnitude of the flood with the economic damage caused to buildings.

First, flood maps are the results of the 1D/2D hydrodynamic flooding models (hazard assessment). However, although these maps provide information about water depths and velocity in streets and open areas of the city, in fact, most damages are associated with the intrusion of water to the inside buildings. As a result of the existence of physical barriers that prevent its intrusion and the short duration of flash floods, the residence time of the floodwater in streets is not enough for the water levels outside and inside to become equal. Therefore, in the context of urban flash floods it is not adequate to consider that the water levels inside properties are equal to the depth of water surrounding buildings. In order to develop more accurate damage quantification it is recommended to consider correction parameters such as the Sealing Coefficient (S_c) (Martinez-Gomariz et al., 2019). It is a function that relates water level outside and inside properties depending on the type of land use

assessed. By applying this coefficient to the 1D/2D hydrodynamic model results, it is possible to estimate the water depth inside each parcel of the city (Martinez-Gomariz et al., 2019).

The figure below depicts the tailor-made Sealing Coefficient curves developed in project RESCCUE for the city of Barcelona (Evans et al., 2019). It is important to consider that these curves were developed for specific kinds of land uses based on estimations of the structure of their entrances since these are the preferential pathways of floodwater (Martinez-Gomariz et al., 2019).

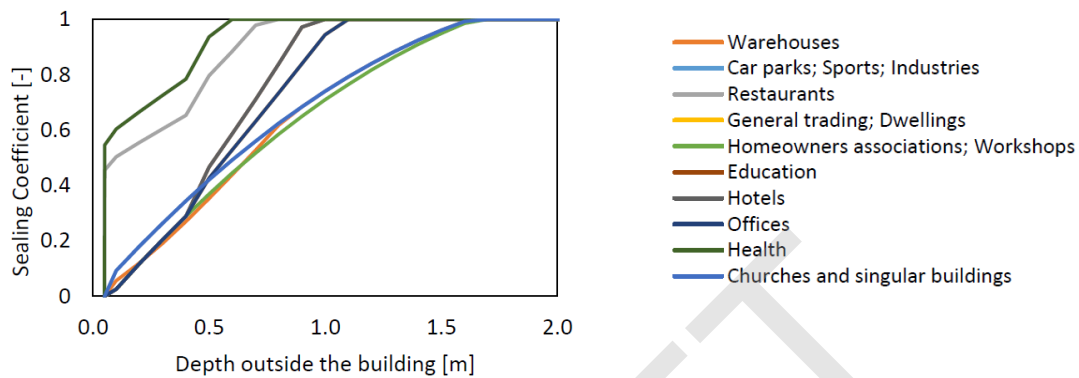


Figure 4. Sealing coefficient curves (Evans et al., 2019).

As mentioned earlier, urban areas are diverse environments with multiple types of buildings dedicated to different activities and purposes. Therefore, in order to assess the economic damage of floods, it is necessary to account for this diversity. The methodology suggested to follow in ICARIA, based on the RESCCUE project, accounts for this reality. To this end, it is necessary to gather detailed land use information of all the terrain parcels in the risk assessment model domain.

As for the damage curves, the suggested approach was also applied in project RESCCUE (Evans et al., 2019). In this sense, Martínez-Gomariz et al.,(2020) proposed a methodology to develop land use specific damage curves based on the analysis of records of losses on properties damaged during floods (representing different kinds of land use) issued by insurance companies. Martínez-Gomariz et al.,(2020) considered 14 typologies of properties covering warehouses, car parks, restaurants, general buildings, homeowners, sport facilities, education facilities, hotels, industries, offices, health, workshops, dwellings and churches according to the classification criteria used by the insurance companies.

In order to deal with the differences between fluvial and pluvial floods, determined by depth, water velocity and residence time of water in the streets, affecting the depth inside the buildings, the method provides a sealing or permeability coefficient that determines the difference between the water depth outside and inside the buildings (Martinez- Gomariz et al., 2020).

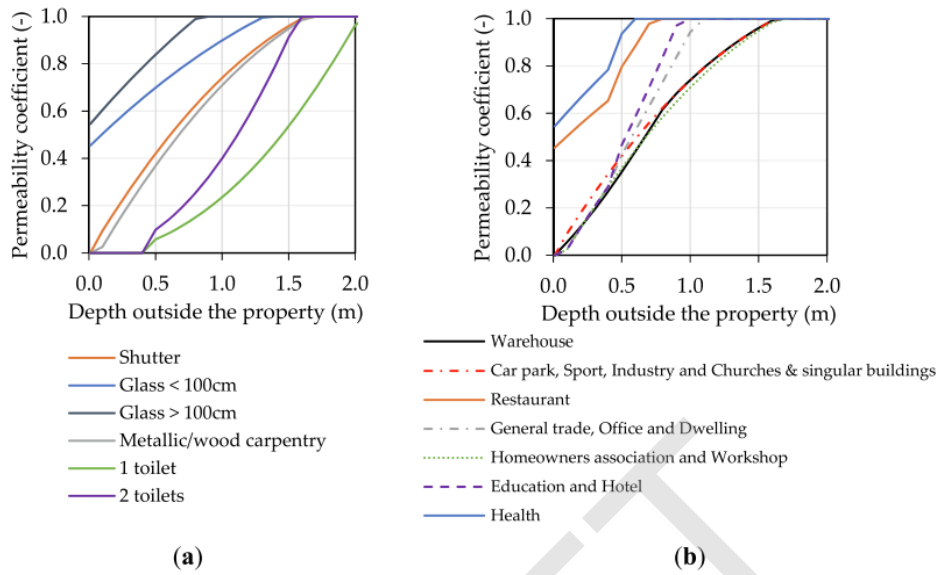


Figure 5. Sealing coefficient functions according to a) a specific water entry element and b) different property types. **Source:** Martinez- Gomariz et al., (2020).

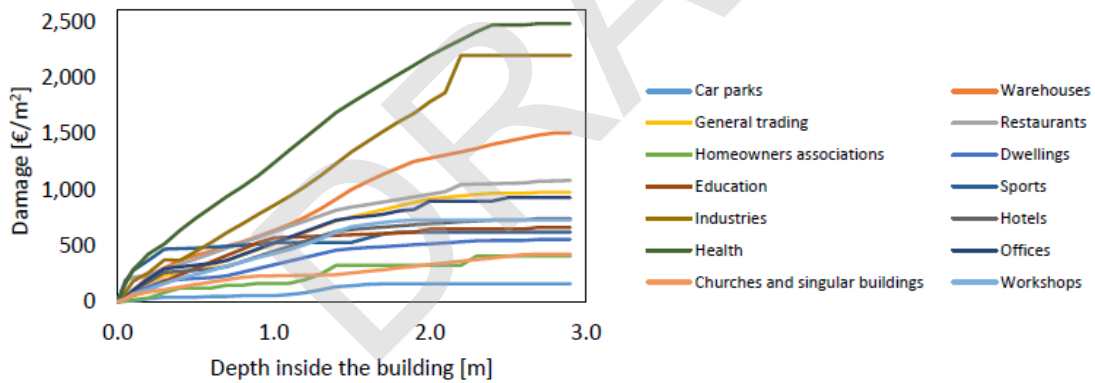


Figure 6. Damage curves based on water depth inside the buildings (Evans et al., 2019).

The values of these damage curves are normalised per surface unit (e.g. €/m²) to make them comparable among property types and flooding events.

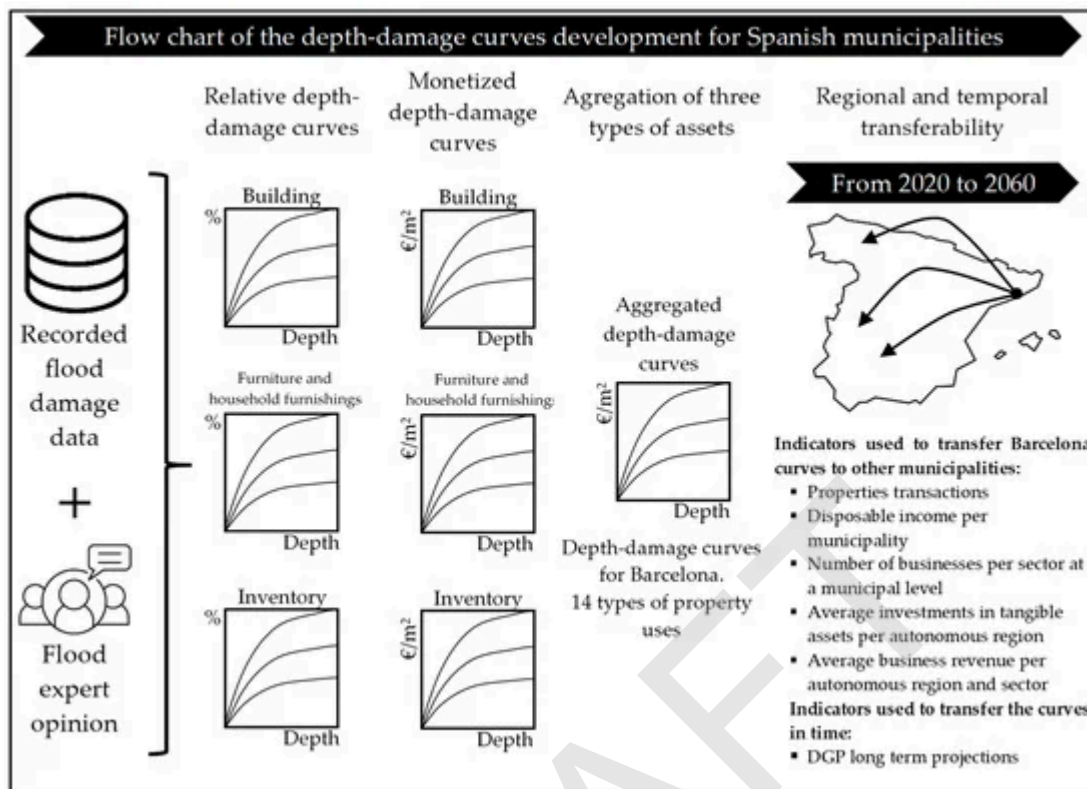


Figure 7. Flowchart of the development of depth–damage curves for Spanish municipalities. **Source:** Martinez-Gomariz et al., 2020.

In ICARIA, these curves will be updated and adapted with the new socio-economic climate projections and new insurance data. They will be transferred from the original study to the 3 Case Studies of ICARIA using the transferability method developed by Martinez-Gomariz et al.,(2020) as, summarised in Figure 7 below. Compared to other available methods, such as the Global Flood Depth Damage Functions developed by the JRC (Huizinga et al., 2017), there are two main improvements. First, the JRC curves are based on construction cost surveys from multinational construction companies, although it provides a coherent set of detailed building cost data across dozens of countries, it does not consider the current added value of the building. Whereas the semi-empirical model proposed by Martinez-Gomariz et al. (2020) provides a value based on the loss caused by the flooding event, which is more likely to consider the added value of the building or household, as is based on the estimation for the reimbursement of the insurance, including in the value concepts beyond the price tags on construction costs, i.e. location, furniture or stock. Second, the geographical top-down approach of JRC does not allow specifying the differences in economic development between regions of the same country. The proposed model is built to satisfy this condition specifically.

The regional transferability to other Spanish urban areas considered demographic, economic and geographical factors, as they substantially influence the prices of goods and services across the country. Regional adjustment indices are available, taking as a reference Barcelona, based on indicators that are used as proxies of the expected regional price variability for the different assets' curves. The method will be adapted to transfer the curves to other regions in Europe and also to cover other types of land use, such as rural areas or islands.

The original 14 types of property uses were grouped into three general sectors: commercial, industrial, and residential and others. Furthermore, the researchers divided the damage within each property by 3 different types of assets in order to obtain three indicators (i.e., building, furniture and household furnishings and inventory). The indicators were selected, so they can both relate to the original curves and change with local data to the rest of municipalities. In Figure 7 the indicators used to adapt the curves to other municipalities are shown.

From each curve, the expected annual damage is estimated, which is the annual average monetary costs of flood damage estimated by multiplying all the probabilities of events of different magnitudes to occur, by their associated damage cost.

In addition, and as another novelty within ICARIA project, a special curve will be developed to represent the waste sector, considered as a critical local service. The infrastructure is related to the industrial properties sector, although its service interruption due to an extreme flooding event can cause damages that impact the public sector. Therefore, the adaptation of this curve will consider the available data from past extreme events in the municipal waste treatment infrastructures to adapt from the industrial properties curves for the relevant case studies.

The experts will review the need for an update of the values used in 2020 for the transfer of the curves from Barcelona to other regions with new estimates and variables if relevant data sources are found.

2.1.1.4 Expected outputs of the model

The previously mentioned methodology will allow to obtain quantitative flood damage maps and the Expected Annual Damage (EAD) (in terms of absolute values and maps) for the return periods of pluvial flood T1, T10, T50, 100 and T500 and current (baseline) and future (Business as Usual and Adaptation) scenarios. These results could be aggregated for each district/municipality/region.

The results will allow a geographic overview about the flood economic impacts distribution and the comparison, in terms of EAD, among the actual scenario, future scenario without any adaptation measure (Business as Usual) and different adaptation scenarios (implementing different adaptation strategies, such as nature-based solutions, grey infrastructure or hybrid solutions).

2.2 Impacts in economic activity

The focus of this section is on economic losses from business interruption specifically related to flooded business, including many economic sectors, such as agriculture, construction, industry or retail, among others. Using the previous methodology to evaluate the impact on properties as a baseline, an indirect damage method is proposed to further understand the costs of floods in the regional economy.

2.2.1 Indirect damage

2.2.1.1 Scope and objectives of the impact assessment

As explained in the previous section, while direct flood damage occurs due to the physical contact of objects with the flood water, indirect damage is not directly induced by flooding, but occurs - in space or time - due to the propagation of the impacts. The focus of this section is to estimate the cost generated indirectly in the regional economy when a flood occurs. For that purpose, a methodology is

proposed based on the combination of input-output analysis with econometric models. Different econometric approaches are proposed with the aim of selecting the one that better fits the data by considering Akaike and Bayesian criterion (Cavanaugh & Neath, 2019).

2.2.1.2 Input datasets used in the model

Table 3. Pluvial flooding damage model, data requirements (I).

| Data requirements for the pluvial flooding damage model | | |
|---|---|--|
| Data group | Description | Source |
| Historical Insurance payouts from extraordinary events | The Public Insurance Company of Spain, which covers extraordinary risks, provided data on the payouts for properties and businesses related to all extreme events that occurred in the past 25 years. | Consorcio de Compensación de Seguros (AMB) / Catastrophe Fund (SBZ) |
| Employment historical data | Employment rates by economic sectors | Statistical office - Idescat (AMB) / Austrian Statistical office (SBZ) |
| Climate data | Historical pluvial flood events that allow relating damage claims with pluvial floods return periods. Future climate scenarios selected for each case study | D1.2 ICARIA |
| Input-output tables | Regional/National economic activity matrix of the productive process flow of good and services | Statistical office - Idescat (AMB) / Austrian Statistical office (SBZ) |

For the AMB CS, data collection has already been carried out: historical flood damage data has been obtained from damage compensations paid by the Spanish Insurance Compensation Consortium (CCS). The CCS compensates for damage caused to people and property by floods and other adverse weather events covered by an insurance policy. The database includes records of related paid claims for the 1996-2022 period in Catalonia at the municipality level. Employment and input-output tables are obtained from Catalonia’s statistical institute (Idescat). All economic data is adjusted to current prices using the consumer price index method, provided by the National Institute of Statistics (INE).

In order to homogenise the data, the method proposes to downscale the Input-Output table to the lowest scale possible by using the most appropriate method from the ones available, such as regional input-output tables, employment data from Census 2021, or other economic data indicator that is available at both scales and allows downscaling. Insurance data has been aggregated by the sum of the 36 Municipalities inside the AMB.

The SBZ and SAR CS will carry out the same data collection and adaptation process in order to complete the indirect impact of flooding analysis, adapting when needed to their local characteristics.

2.2.1.3 Impact assessment model setup

For the estimation of indirect effects, the methodological framework developed in RESCCUE project is proposed (D3.4 RESCCUE), given that it satisfies two relevant criteria. The first one is simplicity, which means that it can be easily transferred to other locations or case studies aimed at estimating indirect effects of different types of climate hazards. The second is that it is robust and meets the objective of delivering reliable estimates.

The method follows a two-step approach: First, ex-post indirect damages are calculated through input-output method, using the database of insurance claims from past floods events as a proxy for direct damages (Barredo et al., 2012). Second, using the preceding results, an econometric regression is carried out to estimate the relation between indirect and direct damages. It provides coefficients that are estimators applicable to future direct damages obtained in the previous section for design floods on selected return periods (to be defined, but likely T2, T10, T100 and T500). To conclude, the expected annual damage (EAD) is calculated using the previously estimated indirect damages. The methodology is summarised in Figure 8.

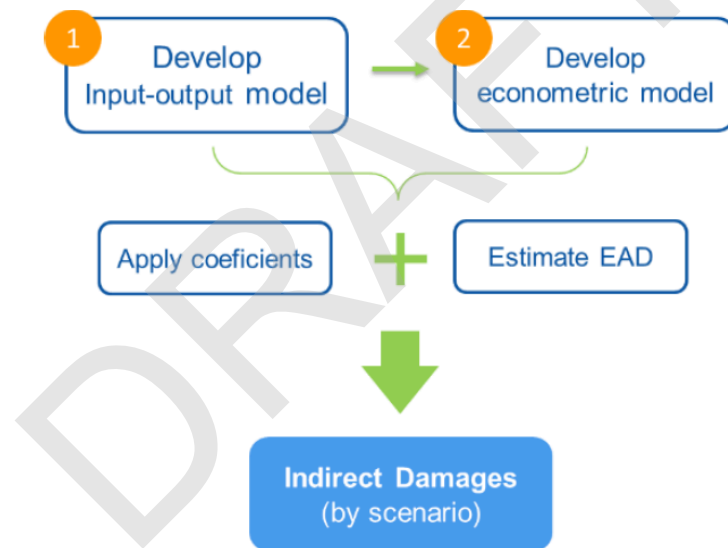


Figure 8. Process of methodology for indirect damages assessment.

Input-Output model

The Input-Output model developed by Leontief (1941) is an analytical framework to examine the interdependencies of industries within an economy (Jenkins et al., 2021). The fundamental information used in I-O are flows of products from each sector as producers to each of the other sectors and itself considered as consumers. This information is summarised in a transaction table where the rows describe the distribution of producer's output and the columns describe the composition of inputs required by a particular industry to produce its output (Miller & Blair, 2009).

The Leontief model is a demand-side model and the indirect effects are calculated after an exogenous change in final demand. For the purpose of this analysis, a supply side model is more suitable as it

captures the interrelations after an exogenous shock in gross value added. The Ghosh (1958) model has been considered which has the same basic formulation but in which the coefficients are horizontally determined rather than vertically (González, 2011).

The model relies on a set of assumptions which some of them can be considered as weakness (Jenkins et al., 2021). According to González (2011) the assumptions can be summarised as:

- Constant allocation coefficients. This implies no technical change which is a weakness for long term analysis
- Correspondence between number of products employed in production and the number of sectors that produce them
- Linear and homogeneous production functions
- Exogeneity of value added

Consider, for example, the Regional I-O table depicted in Figure 9. The total production x of a sector j can be defined as the column sum of the inputs coming from the different sectors z_{ij} plus its added value v_j (see Eq. 1):

$$x_j = z_{1j} + z_{2j} + \dots + z_{nj} + v_j \text{ (Eq. 1)}$$

In matrix term Eq. 2 can be written as:

$$x' = i'Z + v' \text{ (Eq. 2)}$$

Instead of calculating technical coefficients, in Ghosh (1958) an allocation coefficient matrix B is calculated. The coefficients b_{ij} represent the distribution of sector i 's outputs across sectors j that purchase interindustry inputs from i (Miller & Blair, 2009). The allocation coefficients matrix is calculated as follows:

$$B = x^{-1}Z \text{ (Eq. 3)}$$

By clearing z in Eq. 5 and replacing it in Eq. 4 we get:

$$x' = v'(I - B)^{-1} \text{ (Eq. 4)}$$

Where $(I-B)^{-1}=G$. G being the matrix containing the Gosh results as the output inverse analogue to the Leontief demand sided model and such providing the results from a supply sided oriented model. By using this matrix we can get the total effect in output given an exogenous change in the value added by economic activity as defined in Eq. 6:

$$\Delta x' = (\Delta v')G \text{ (Eq. 5)}$$

Indirect effects can be calculated by subtracting the allocation coefficient matrix to the Gosh matrix.

As a novelty, at least as a trial in the AMB CS, an estimation will be carried out of the indirect effects from an exogenous shock derived from the paid claims of CCS historical data from 1996 to 2020 using all the available input-output tables for the period instead of only one. This would allow capturing the registered technological change over the period of analysis. In addition, regional tables will be

downscaled to the lowest area possible by using the most adequate regionalization method, based on available data and CS suitability. The most common method employs regional total production data.

The IO tables with 64 products and sectors will be used. The estimated indirect effects perceived by economic activity are then used as inputs for an econometric model that relates direct with indirect effects.

Econometric model

The final database is a panel data of 64 cross sectional observations (the economic activities) and 24 years from 1996 to 2020 which allows for different specifications. The first econometric specification relies on the model used in RESCUE project but with a slight modification. The specification is as follows:

$$Indirect_{t,i} = \beta_1 * Direct_{t,i} + \beta_2 * N^oClaims_{t,i} + \beta_3 * GDP_{t,i} + \beta_4 * Unemp_{t,i} + \gamma_i * Econsector_{t,i} + \varepsilon_t \text{ (Eq. 6)}$$

Where the *Indirect* dependent variable measures the indirect damages, *Direct* variable measures the direct damages, *N^oClaims* is the number of claims registered per flood event, *Unemp* is the unemployment rate, and *Econsector* is the 64 economic sectors considered or the corresponding aggregation in 10 sectors. The model does not contemplate constant terms as all sectors are included in the *Econsector* variable which is the alternative to use the baseline category when working with dummies (Gujarati et al., 2021). Different variations of the specification are tested and the best model is selected according to Akaike's and Bayesian criteria. This specification is known as a *Pooled Panel data model* (Gujarati et al., 2021). Following the standard approach in Panel data econometrics (Baltagi, 2021), Hausman and Lagrange Multiplier tests will be performed to see the suitability between different models, including but not exclusive to pooled, fixed and random effects models.

Time fixed effects are introduced in all specifications to capture trends in the economic variables. In the case of a random effects estimation, as coefficients for economic sectors are needed, a Mundlak regression would be performed (Mundlak, 1978).

2.2.1.4 Expected outputs of the model

The model will provide the economic value of the indirect effects of the return periods and scenarios selected for the CS applying it. From the econometric regression, the resulting coefficients can be translated as ratio of direct damages, differentiating by economic sector, return period and economic growth. These results can later be adapted to the climate and adaptation scenarios to estimate variations in expected damages in each scenario.

| Núm. | Codi | BRANQUES (CCAE) | CONSUMS INTERMEDIIS PER BRANQUES D'ACTIVITAT | | | | | | | | | | 11 | 21 | 22 |
|------|------------|---|--|-------------------------------|-------------|--------------------------------|----------------------------|--|--------------------------|---|---|--|--------------------------|---------------------|---------------------------|
| | | | 1 | 2 | 3 | 4 | 5 | 6 | 7 | 8 | 9 | 10 | | | |
| | | | A | B, C, D, E | F | G, H, I | J | K | L | M, N | O, P, Q | R, S, T, U | | | |
| | | PRODUCTES (CPA) | Agricultura, ramaderia, silvicultura i pesca | Indústria, aigua i sanejament | Construcció | Comerç, transport i hostaleria | Informació i comunicacions | Activitats financeres i d'assegurances | Activitats immobiliàries | Activitats professionals, científiques, administratives i auxiliars | Administració pública, educació i sanitat | Activitats artístiques, d'entreteniment i altres serveis | Total demanda intermèdia | Total demanda final | Total usos a preus bàsics |
| 1 | A | Productes agraris i pesquers | 521 | 6.696 | | 661 | 1 | | | 2 | 21 | 9 | 7.911 | 3.152 | 11.063 |
| 2 | B, C, D, E | Productes industrials i sanejament | 1.438 | 70.230 | 4.121 | 10.243 | 1.656 | 263 | 65 | 2.252 | 2.046 | 904 | 93.219 | 114.046 | 207.265 |
| 3 | F | Treballs de construcció | 89 | 1.192 | 6.450 | 1.775 | 139 | 194 | 2.314 | 360 | 542 | 184 | 13.238 | 14.553 | 27.791 |
| 4 | G, H, I | Serveis de comerç, transport i hostaleria | 435 | 11.862 | 1.818 | 17.100 | 725 | 254 | 31 | 1.778 | 1.538 | 538 | 36.080 | 70.416 | 106.496 |
| 5 | J | Serveis d'informació i comunicacions | 4 | 730 | 234 | 1.039 | 2.627 | 406 | 19 | 955 | 948 | 163 | 7.125 | 9.829 | 16.954 |
| 6 | K | Serveis financers i d'assegurances | 61 | 840 | 501 | 1.529 | 98 | 2.502 | 2.077 | 480 | 217 | 174 | 8.478 | 5.203 | 13.681 |
| 7 | L | Serveis immobiliaris | 8 | 1.156 | 420 | 5.207 | 243 | 466 | 139 | 892 | 829 | 509 | 9.867 | 21.820 | 31.687 |
| 8 | M, N | Serveis professionals, científics, administratius i auxiliars | 72 | 7.382 | 2.741 | 9.891 | 1.174 | 962 | 536 | 5.950 | 2.118 | 817 | 31.644 | 16.223 | 47.868 |
| 9 | O, P, Q | Serveis d'Administració pública, educació i sanitaris | 1 | 59 | 9 | 151 | 14 | 29 | | 131 | 1.736 | 103 | 2.232 | 35.876 | 38.108 |
| 10 | R, S, T, U | Serveis artístics, d'entreteniment i altres serveis | 1 | 130 | 11 | 353 | 161 | 75 | | 144 | 332 | 1.212 | 2.419 | 11.020 | 13.439 |
| 11 | | Total | 2.630 | 100.277 | 16.305 | 47.948 | 6.837 | 5.151 | 5.181 | 12.945 | 10.328 | 4.612 | 212.214 | 302.139 | 514.353 |
| 12 | | Impostos nets sobre productes | 10 | 117 | 484 | 685 | 15 | 69 | 14 | 123 | 1.357 | 248 | 3.124 | 12.936 | 16.060 |
| 16 | | Total consum intermedi / consum final a preus d'adquisició | 2.641 | 100.395 | 16.788 | 48.634 | 6.851 | 5.220 | 5.195 | 13.068 | 11.685 | 4.860 | 215.337 | 319.360 | 534.698 |
| 20 | | Valor afegit brut a preus bàsics | 1.916 | 39.021 | 9.054 | 49.478 | 7.053 | 7.390 | 23.371 | 17.644 | 27.736 | 7.945 | 190.608 | | |
| 21 | | Producció a preus bàsics | 4.557 | 139.416 | 25.842 | 98.111 | 13.905 | 12.610 | 28.566 | 30.712 | 39.421 | 12.805 | 405.945 | | |

Figure 9. Catalan Amplified Destination table Input-Output matrix, year 2016. Source: Catalan Statistical Office

2.3 Impacts on the water sector

2.3.1 Direct and indirect effects

Wastewater Treatment Plant

Wastewater Treatment Plants (WWTP) are public service infrastructures that are exposed to different types of flood-related hazards (pluvial, fluvial, coastal and its combinations) due to their location. These facilities are usually located at low-lying areas close to large bodies of water such as seas or rivers (Burian et al., 2013). There are two principal reasons for locating these facilities in these near-water environments: first, the low elevations enable wastewater to be conveyed to the treatment point by gravity, thereby reducing the energy cost of transportation; second, the WWTPs' usual proximity to natural water bodies allows an efficient discharge of treated water into them. Therefore, WWTPs' location makes them highly susceptible to flood hazards (Friedrich et al., 2012).

In general, the characterisation of flooding is based on the estimation of water depths and velocities for certain flood events (Martínez-Gomariz et al., 2020 citing White, 1945). Therefore, there are few differences between coastal flooding and other types of flooding; for instance, their potential direct impact of waves on the asset and the effect of elevated salt concentrations in seawater. Even so, different consequences have also been defined that can occur especially for coastal flooding, such as elevated levels of groundwater, inflow and infiltration, surge inundation and coastal erosion, following the division used by Spirandelli et al., (2018) in a coastal vulnerability assessment project in Hawaii (USA). This section focuses on the characterisation of tangible impacts resulting from pluvial and coastal floods (fluvial floods are not considered as they are not part of the ICARIA hazard framework).

2.3.1.1 Scope and objectives of the impact assessment

A transversal methodology is developed for the assessment of flood risks for any Wastewater Treatment Plant anywhere in the world. Vulnerability assessment will be carried out using sector-specific depth-damage curves. Due to the lack of literature in this sense, empirical assessment will be done, based on the recorded flood events at the facilities operated by Aigües de Barcelona within the Metropolitan Area of Barcelona. Therefore, curves will be created on the basis of the expert knowledge through interviews with plant managers, maintenance managers and other experts from inside and outside Aigües de Barcelona company, making them available to be adapted to other CS.

Existing vulnerability assessment of wastewater infrastructure to climate change and, in particular, to flood events focus on qualitative assessment and vulnerability function (Spirandelli et al., 2018; Burian et al., 2013; Friedrich et al., 2012; Choi, 2019 and Hughes et al., 2021). As a novelty, in ICARIA, a study of depth-damage curves and evaluation of EAD will be carried out for a new complex and specific asset such as WWTPs.

Two specific studies in the WWTPs of China and Butarque (Comunidad de Madrid, Spain) have been used as reference to develop this method. In both projects (Gámez, 2021a and Gámez, 2021b), a pilot programme of adaptation to flood risk (in this case fluvial) is being developed for both WWTPs. The study, developed in collaboration with the Ministry of Ecological Transformation and Demographic Challenge in the framework of the Flood Risk Management Plan, produces flood maps (water depth) for different return periods for the area of the WWTPs, enumerates an inventory of risk elements and defines unit costs for damage assessment according to land use (€/m²). Damage associated with flooding, called Total Risk Value (€) in the study, is quantified for different return periods.

2.3.1.2 Input datasets used in the model

Inputs of the model for the assessment of the flood impact on WWTPs are classified in two main categories: 1) inputs needed for the model development (facilities heights, treatment process composition and possible impact affectations, experts knowledge and recorded historical data), and 2) inputs required for the model application (georeferenced location, result of previous ICARIA project tasks and hazard models outputs carried out by other partners). Table 4 shows a description of the inputs to the economic damage estimation model.

In addition, expert opinion-based information will be obtained from interviews with the WWTP Plant Managers and other professionals to understand the consequences of the floods on the elements of the WWTP. These interviews will be used to define the internal processes of the model (vulnerability assessment), but are also intended to be established as input (Table 4). Through the responses from the interviews, the parameters used for calculating the damage estimation will be proposed. Finally, vulnerability curves will be validated based on historical data inputs from the Insurance sector.

Table 4. Necessary input data for the economic damage valuation model for WWTPs.

| Data requirements for the flood damage model on WWTP | | |
|---|---|---|
| Data group | Description | Source |
| WWTP surroundings Elevation map | Terrain elevation map (raster format in GIS support) to locate WWTP facilities. | Local cartographic information database |
| Flood Depth maps (pluvial) | ICARIA project 2D shapefiles of pluvial flooding. Made for different return periods. | ICARIA Task 4.2 and 4.3 results |
| Flood Depth maps (coastal) | ICARIA project 2D shapefiles of coastal flooding. Made for different return periods. | ICARIA Task 4.2 and 4.3 results |
| Food Depth maps (comb.) | ICARIA project 2D shapefiles of combined flooding events. Made for different return periods. | ICARIA Task 4.2 and 4.3 results |
| INTERNAL INFORMATION (vulnerability curves development) | | |
| WWTP Locations and extents | 2D rendering (GIS support files) of all WWTPs and building height information (plans). | WWTPs operator internal information |
| Experts information Indirect historical data | Results of the interviews with WWTPs Plant Managers and other professionals. These allow the model to be specified for each study case (transferability). | WWTPs personnel On-site interviews |
| Industrial Historical Insurance Payments | Model validation data. History of extraordinary damage (natural catastrophes) covered by the insurance in facilities related to extreme events. | National insurance for extraordinary catastrophes |

2.3.1.3 Impact assessment model setup

Methodology used in the impact assessment model is developed following the usual steps in other previous studies related to flooding in other assets. The usual **Risk (Impact) = Hazard x Exposure x Vulnerability** scheme (see D1.1) is used in a similar way as done in several studies on vehicles (Martínez-Gomariz et al., 2019), properties (Martínez-Gomariz et al., 2020), dams (Martínez-Gomariz et al., 2023) or linear infrastructures such as major roads (Douglass et al., 2014).

The model is developed based on depth-damage curves (vulnerability curves) methodology and subsequently EAD assessment (risk assessment). Based on the overlapping of flood maps and WWTP locations, it is possible to establish the damage scale for each event. The methodology employed is based on the procedure used in the RESCCUE project, where Martínez-Gomariz et al. (2020) proposed a methodology based on water depth (m) / damage (€/m²) curves for properties. Other flood damage-related studies in the city of Barcelona have also used the EAD as an indicator to quantify flood risks (Velasco et al., 2013). The model proposed here is based on the previous methodology although assessing instead the impact on a new asset such as WWTPs, vulnerable facilities, close to water bodies and complex infrastructures with high socio-economic value, thus being a novel approach. The modelling will be developed on the basis of the data provided mainly by the experts interviewed.

Hazard assessment

Two types of floods are differentiated for this study: coastal floods and pluvial floods. The main difference between both types is the salinity of the water. Possible harmful effects associated with corrosion, differences in cleanliness or other occurrences related to the effect of salinity will be evaluated using a salt water coefficient (C_{SAL}). Salinity impact and its coefficient will be defined based on the knowledge of experts specialised in flood events in sanitary system facilities. The hazard evaluation parameter will be the flood depth (h , in m) for all types of floods. Water depth assessment (h) will be obtained from the superposition of terrain and WWTP plans with the water heights in floods, data provided as outputs of the flood models generated by ICARIA project partners in the different study areas.

Exposure and Vulnerability assessment

In this model, the exposure information is simply represented by the location of WWTPs and their treated water volume. Regarding the vulnerability study, depth-damage curves (also called vulnerability curves in more general terms) will be developed in the same way as in previous projects already mentioned in previous paragraphs (RESCCUE). Two vulnerability curves will be developed: the first associated with indirect damage as cost increase or service interruptions of the treatment operative (m - €/m³). The second, associated with direct physical damage, which includes damage caused by the flood that requires replacement of equipment parts, actuations derived from impacts on civil works or extra cleaning among others. These curves will be represented based on the associated cost to the facility surface (m - €/m²).

Depth-damage curves applied to WWTPs are intended to be distinguished for the different types of treatment existing in the facilities (i.e. pre-treatment and primary treatment, secondary treatment and tertiary treatment). Regarding the model application, curves will be selected and aggregated according to the treatments performed in each WWTP. An example of the expected damage curves associated with the vulnerability assessment in WWTP is shown in Figure 10.

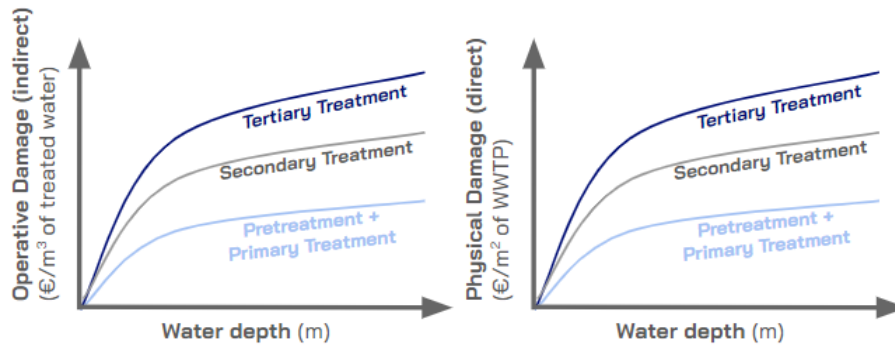


Figure 10. Exemplification of the expected depth-damage curves (vulnerability curves) (a) left side, associated with operative damage (€/m³) and (b) right side, associated with physical damage (€/m²).

WWTPs operated by Aigües de Barcelona within the Metropolitan Area of Barcelona have not suffered from flooding events during the last decades. The absence of historical records makes the expert opinion in the sector the main source of information for the curves elaboration. In this regard, the information is extracted from interviews from several expert personnel such as: plant managers of the different facilities, maintenance managers, flood experts specialised in the asset of WWTPs and professional technicians from Aigües de Barcelona with decades of experience in engineering and operations at the facilities, among others. These curves can be replicated in the different CS by following the same interviewing process with local stakeholders, or by adapting using the curves designed for the AMB CS.

For a better characterisation of the curves, data provided by the national insurance for extraordinary catastrophes (in this case the *Consorcio de Compensación de Seguros de España*, CCS from now on) are studied for different historical events around Spain. All WWTPs have very similar hazard exposure and construction design characteristics. This similarity allows the validation of the model with information on floods in other parts of the Spanish territory. The same curve calibration exercise can be developed in any EU country based on information from historical events recorded by the local insurance sector.

Impact assessment

Impact assessment for flooding on WWTPs in this project is exclusively economic, being tangible impacts the focus of the ICARIA project. The internal process of the model consists of an overlay of the results of the ICARIA WP2 with the two-dimensional planes of the WWTPs. Flooded and damaged infrastructures are identified for each flood map generated from different return periods, and the impact is assessed for each WWTP. A damage assessment formulation is proposed as follows:

$$\text{Damage for a treatment type } j \text{ associated with a climatic event } i: D_{TREAT_i}^j = D_{OP_i}^j + D_{PHY_i}^j$$

Where $D_{TREAT_i}^j$ is the damage in treatment j for event i , as the sum of the outputs of the operating cost vulnerability curves ($D_{OP_i}^j$) and the direct and physical flood damage ($D_{PHY_i}^j$). Then, the total damage in a

facility for event i (D_{TOT}^i) is the sum of the damages in the different treatment types j . Some studies

suggest increased damage in coastal flooding due to salinity of the water (Flood et al., 2011 and Hummel et al., 2018). The final cost is multiplied by a salinity coefficient C_{SAL} if it is a coastal flooding. C_{SAL} will be determined on the basis of expert knowledge and comparison of historical pluvial and coastal events damage. A value range cannot be specified yet.

Total damage for climatic event i :
$$D_{TOT}^i = \left(\sum_{j=1}^3 D_{TREAT,i}^j \right) \times C_{SAL}$$

Finally, the EAD will be calculated using data of different flood maps (water depth) corresponding to design rainfalls related to different return periods (i events) in a similar way as done in other assets in urban floods (Martínez-Gomariz et al., 2019, Velasco et al., 2016 and Velasco et al., 2013). The different results provided associated with different climate scenarios will be compared using the results of the EAD. More details on these results are given in the expected outputs section below. Figure 11 shows a data flow diagram of the performance of the coastal or pluvial flooding impact in a WWTP.

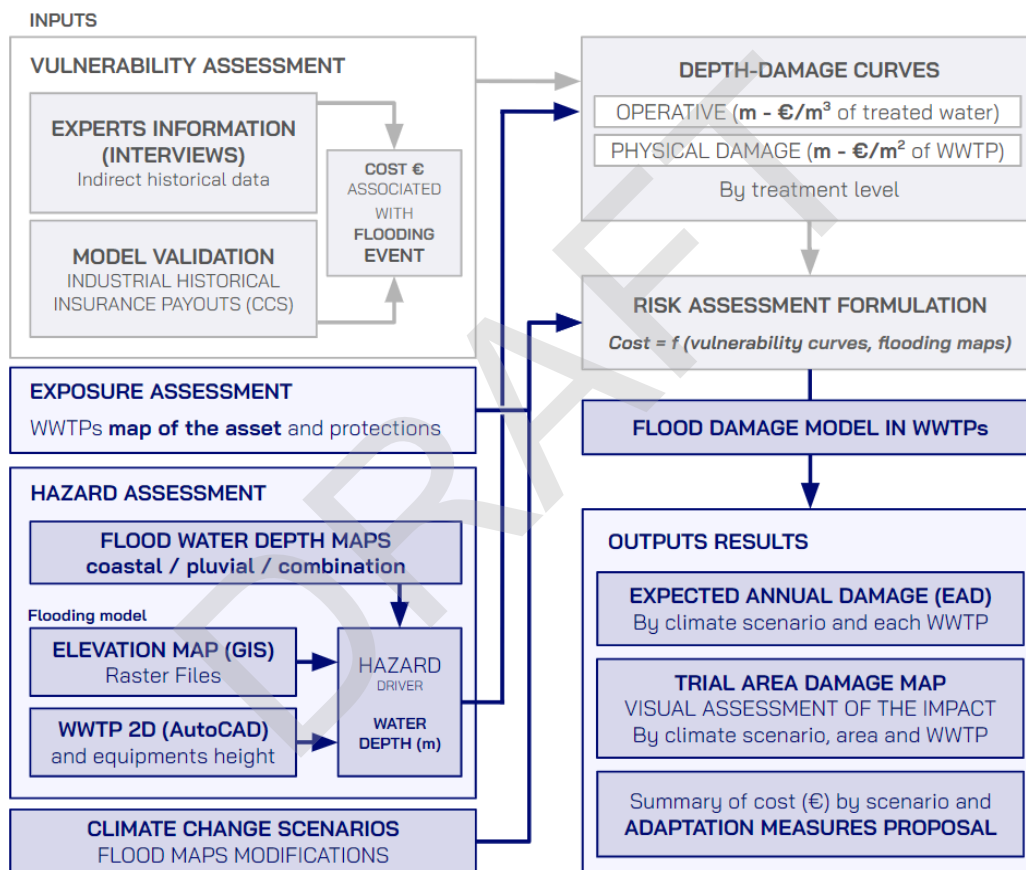


Figure 11. Data flow diagram for the flood damage model in Wastewater Treatment Plants.

2.3.1.4 Expected outputs of the model

The objective of the model is the evaluation of the results on the basis of the assessment of the different EADs for each climate scenario. The total costs associated with the events for the available return periods will be provided. Additionally, the percentage of costs associated with operational and physical damage will be plotted and classified by treatment level. These classifications enable the identification of high cost processes, which can be used to prioritise adaptation scenarios. Figure 12(a) shows a schematic of the possible outcomes of the EADs. Additionally, a trial area map will be provided to

visualise the results, highlighting the distribution of hazard level and their impact on WWTPs. Possible adaptation measures will be proposed for each scenario and will be compared with the initial configuration as shown in Figure 12(b). EAD is used as an indicator to compare the efficiency of different adaptation (EAD reduction) scenarios in terms of risk reduction.

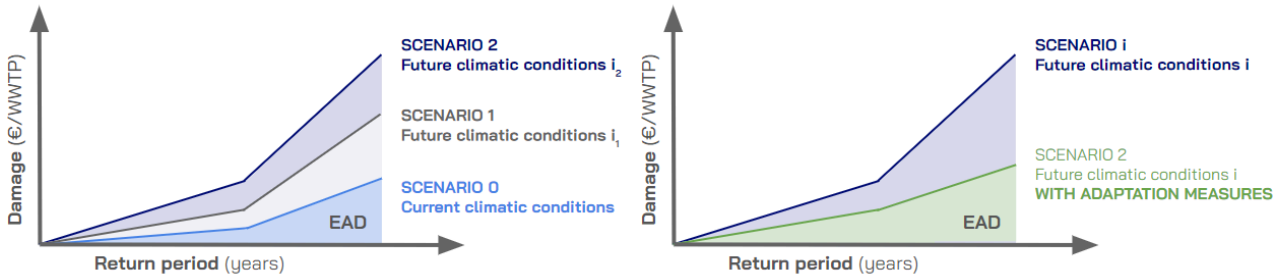


Figure 12. (a) EAD representation for several scenarios (different future climatic conditions) and (b) EAD reduction in a generic scenario with adaptation measures application.

Finally, an assessment of the cost of the feasibility of regeneration in WWTPs with tertiary treatment is added. Coastal flooding produces saltwater inflows into WWTPs, increasing the salinity of the water to be treated. High salinity water cannot be treated (tertiary treatment). For the purposes of this study, untreated water volume is related to the consecutive treatment interrupted time. Then, by relating the cubic metre price of regenerated water (€/m³) to the time of service interruption, the lost revenue due to non-treatment is shown, as is presented in Figure 13. Regenerated water is used for a large number of purposes (e.g. industrial or municipal) and for consumption by the population after a drinking water treatment process (Agència Catalana de l'Aigua, 2023). This treatment limitation increases its importance in times of drought, when regeneration is one of the main sources of water availability.

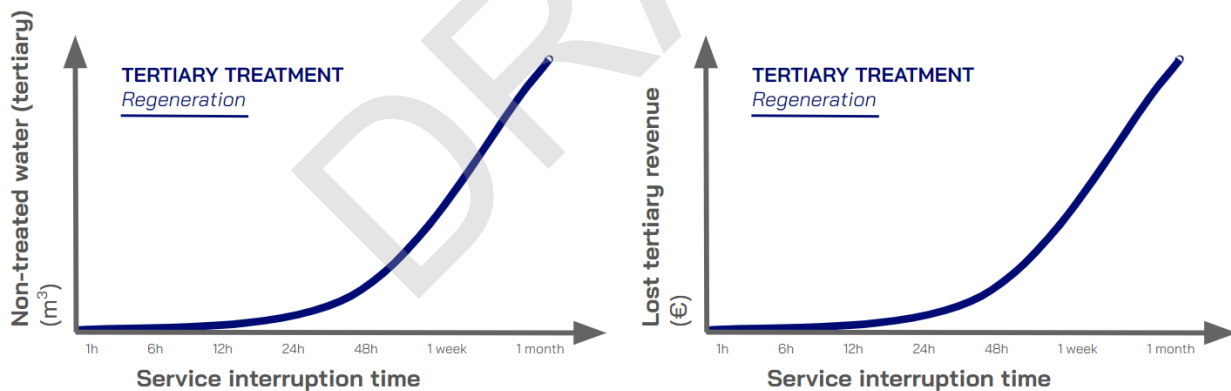


Figure 13. Tertiary treatment lost revenues in coastal flooding events assessment representation in €/time.

Coastal Main Sewer

A main sewer parallel to the coastline is a common infrastructure in the environment of drainage systems. In coastal areas, the lowest point of a territory is the coastline, which makes it an optimal location for these infrastructures. Impacts on coastal sewers usually trigger knock-on effects, mostly occurring in the Wastewater Treatment Plants (Friedrich et al., 2012) as they are the destiny of the wastewater conveyed. The sewer system can be separate (domestic and pluvial flow conveyed in different systems) or combined (using the same system for all water). The main sewer is expected to have higher dimensions when it comes to combined sewers and the impacts on them are more relevant due to

higher conveyed flows. Climate change projections, particularly those of Sea Level Rise (SLR), advocate the need to know in detail the risk of these coastal infrastructures, due to the expected increased exposure (Mestre et al., 2013 and IPCC, 2023).

Generally, these infrastructures are mostly exposed to coastal flooding hazards (i.e., joint effect of wave impact and surge sea water inundation) and combined flooding (e.g., coastal and pluvial flooding) under storm events. Several authors have evaluated this combination of effects in some sites, such as South Africa (Friedrich et al., 2012), Taiwan (Hsiao et al., 2021) and California (Sangsefidi et al., 2023). Most of them are based on the assessment of the differences in the concentration of pollution : on the one hand, evaluating the water flowing into the main sewer (increased salinity) and on the other hand, assessing the polluted water discharged into the environment through cracks in the sewer walls.

2.3.1.5 Scope and objectives of the impact assessment

A transversal and replicable methodology for different case studies will be developed for the assessment of damage in a combined main sewer parallel to the coastline. As the infrastructure is highly specific, it is inevitable to develop a strategy based on a real case study. In this case, the assessment is based on the detailed analysis of the *Llevant* Main Sewer, an infrastructure managed by Aigües de Barcelona that conveys wastewater from Maresme area (northeast of Barcelona) to the *Besòs* WWTP, east of Barcelona (Barcelona Metropolitan Area ICARIA trial). The development of the case study methodology and the infrastructure details will be exposed and carried out in the ICARIA deliverable 4.2 Trial Assessments. The aim of the project is to develop a methodology applicable to other coastal CS.

Many articles in the literature attempt to assess, in a quantitative way, the impacts of coastal flooding on near shore drainage systems. Most of them try to measure the possible increases in flow due to infiltration and inflow due to ruptures in the sewer (Spirandelli et al., 2018 and Sangsefidi et al., 2023). In this case, thanks to the historical data available from Aigües de Barcelona on the damage to the main sewer over the last few decades and interviews developed to different company experts, the approach focuses on the physical damage that the main sewer has suffered and the repair needs that have derived from it. Consequently, the main objective of this vulnerability study is based on the development of damage curves relating some oceanographic results variables (sources of coastal flooding and impact of the water on the asset) with an economic quantification.

2.3.1.6 Input datasets used in the model

Necessary information for the model development is divided into two main categories: data needed for the elaboration of the model (internal and based on the *Llevant* main sewer) and data needed for the application of the model (for any main sewer parallel to the coast). Regarding the first block, the main input to the vulnerability study is the approximation of the intervention costs associated with the events based on expert knowledge obtained from interviews with the Sewer System Personnel and other professionals in the Aigües de Barcelona company sector. In addition, damage data of the *Llevant* Main Sewer by Aigües de Barcelona will be used to validate the internal processes of the model (damage assessment).

On the other hand, necessary data for the application of the model are described. The oceanographic intensity parameters data associated with these events are provided from WP1 and WP2, and are expected to be extracted from a coastal hydrodynamic model. If this information is not available, websites with interactive oceanographic information on the sewer coastal area can be used to obtain the maximum sea level and event duration. Other inputs are those related to the current situation (georeferenced sewer location and elevations) and those related to climate projections associated with flood events. Table 5 shows a description of the inputs to the economic damage quantification model.

Table 5. Necessary input data for the economic damage assessment of the coastal flooding model on a main sewer parallel to the coast.

| Data requirements for the flood damage model on the main sewer | | |
|---|--|---|
| Data group | Description | Source |
| Main Sewer surroundings Elevation map | Terrain elevation map (raster format in GIS support) to locate the main sewer and surroundings. | Local cartographic information database |
| Oceanographic events data (H_s, E_D) | Wave height (H _s) data and event duration (E _D) in the near-shore bays for each of the damage events recorded in the study case area. | Local oceanographic registers database |
| Sewer location | 2D rendering (GIS support files) of sewer to locate flooded areas and facilities by overlaying mapping with climate flood projections. | Local sewer system operators or municipalities |
| Flood Water Depth maps (coastal) | ICARIA project 2D water depth raster files of coastal flooding in the case study trial area (hazard intensity parameter). Made for different return periods. | ICARIA Task 4.2 and 4.3 results |
| Flood Water velocity maps (coastal) | ICARIA project 2D water velocity raster files of coastal flooding in the case study trial area (hazard intensity parameter). Made for different return periods. | ICARIA Task 4.2 and 4.3 results |
| Experts information Indirect historical data | INTERN INFORMATION (vulnerability curve) Results of the interviews with AB Personnel and other professionals. | Local main sewer operator On-site interviews |
| Economic information Direct historical data | INTERN INFORMATION (vulnerability curve) Results of interventions to de sewer to protect or repair damage resulting from extreme historical climatic events. | Local main sewer owner or operator Internal projects |
| Protection Level Index Protection and distance | Assessment of the protection of the infrastructure in each case based on the coastal protection measures and the distance of the asset from the sea. | Local information and ICARIA Task 4.2 and 4.3 results |

2.3.1.7 Impact assessment model setup

First of all, a brief summary of the impact assessment of a coastal event on an exposed main sewer parallel to the coast line is developed below, following the scheme proposed in ICARIA for a generic asset (see D1.1). However, adapting to specific infrastructures, such as a sewage collector parallel to the coastline and its unique characteristics, may require slight modifications to the initial project framework.

Hazard assessment

The primary hazard in this case study is coastal flooding and the resulting wave impacts. Typically, a wave event is described by its significant wave height (H_s) and the event duration (E_D). However, it is intended to emphasise the hazard assessment in the wave impact and storms in the main sewer. To achieve it, hazard characterisation will be defined by the event intensity parameter (θ), that can be described as:

$$\theta = f(v, h, E_D)$$

The parameter relates water velocity (v) and water depth (h) at the main sewer exposed points, variables obtained as outputs of the coastal hydrodynamic model developed by WP2, and the duration of the event (E_D), variable defined by the same hydrodynamic model or obtained in other oceanographic records in the area. An initial event threshold must be defined in both cases. If the hydrodynamic model is not available, hazard characterisation will be developed through hydrostatic results: flood water depth will be obtained from the model and velocity will be replaced by another variable that could define the hazard intensity as the significant wave height (H_s). H_s will be characterised by the local oceanographic records database.

Exposure and vulnerability assessment

Exposure assessment is characterised by the location of the main sewer in each section referring to the hazard (probability of contact between the coastal flooding and the infrastructure). Although it is not the same methodology employed, the vulnerability assessment is based on the procedure used in the RESCCUE project, where Martínez-Gomariz et al. (2020), proposed a water depth - damage curves (m - €/m²) methodology for vehicles and properties (Martínez-Gomariz et al., 2021, Martínez-Gomariz et al., 2020b and Martínez-Gomariz et al., 2019). In this case, the damage curves (also known as vulnerability curves) relate the oceanographic event intensity (θ) and the cost associated with the impact of the intensity level to the main sewer.

Vulnerability curves correlate in this case the intensity of the event (θ) with the repair cost per linear metre of the main sewer (θ - €/m), as shown schematically in Figure 14b.

In order to define the damage curves, a complete exposure of the main sewer is assumed. The costs associated with the oceanographic hazard variables are defined by using information obtained from sector experts interviews in the Barcelona Metropolitan Area (AMB) trial. In addition, the events historical repair records (EHR) of the main sewer will also be used as a validation source of the results. For the validation of the recorded historical events, Aquatec partner will be required to provide results from the coastal hydrodynamic model with the oceanographic conditions associated with the event for a future characterisation of the associated damage.

Existing adaptation measures (main sewer protection) assessment

Usually, adaptation measures for an asset that is affected by the impact of a climatic hazard are evaluated after the risk assessment in the current situation. In this case, the main sewer under study already has protection mechanisms that reduce the exposure of the asset in some sections and must be introduced into the model for a correct interpretation of the recorded events. Sections are classified into five categories according to the degree of protection or Protection Level Index (PLI):

- **PROTECTION LEVEL 0. Unprotected areas**

The main sewer is visible to the naked eye from the waves.

- **PROTECTION LEVEL 1. Sand protection**

The main sewer remains buried or semi-buried in sand against the waves and is exposed with the first coastal sand erosion.

- **PROTECTION LEVEL 2. Breakwater protection**

The main sewer remains protected by a breakwater embankment that reduces the impact, if any, of wave intensity of the main sewer.

- **PROTECTION LEVEL 3. Breakwater and sand protection**

Sum of two previous protections.

- **PROTECTION LEVEL 4. Protection by urban infrastructure**

The main sewer is buried and protected by structural elements such as buildings or the promenade in the area.

Exposure of the different sections of the sewer is assessed. The length of each section is defined irregularly, associating its length with sections with similar protection level. An exemplification of the protection assessment is shown in Figure 14a. Damage (vulnerability) curve is made at protection level 0 (100% exposure) but possible adaptations are shown in Figure 14b depending on the level of protection of each section.

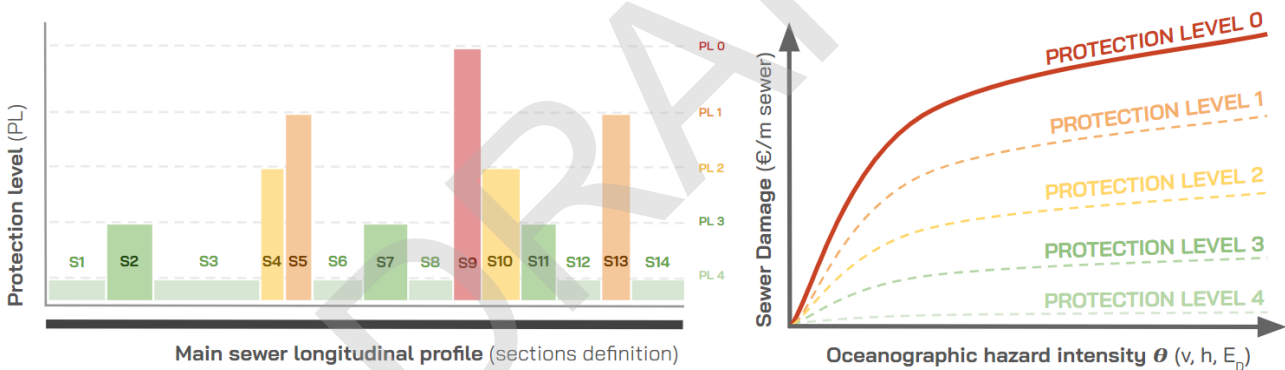


Figure 14. (a) Main sewer longitudinal profile protection level evaluation per section with a generic and schematic representation. (b) Damage curve (θ - €/m) representation.

Impact assessment

Risk assessment for coastal flooding impacts on the main sewers parallel to the coast in this project is exclusively economic, being tangible impacts the focus of the ICARIA project. The internal process of the model consists of an overlay of climate projection mappings with the two-dimensional planes (in GIS format) of the coastal main sewer. Flooding and water impact for different events and for climate projections (related to Sea Level Rise SLR) are correlated with the intensity parameter (θ). In this case, a first assessment of the resulting cost of repair for each section is expressed as follows:

Total section cost related with an event:
$$C_{sec \theta Ei} = f(D_{\theta Ei} \times PLI)$$

Where $C_{sec \theta Ei}$ is the total damage per each section in the particular event i associated to its oceanographic situation θ , $D_{\theta Ei}$ is the cost associated with the oceanographic variation (vulnerability

curve) of the event i and PLI is the protection level index value for each section. Total economic cost associated with an event storm is made up of the sum of costs of all main sewer sections related to the intensity of the storm (θ) and the protection level of each of the sections, as expressed in the equation:

Total main sewer cost related with an event:

$$CTOT_{\theta Ei} = \sum_{i=1}^n Csec_{\theta Ei}$$

Finally, the model develops an approximation of the EAD for the null protection scenario (main sewer fully exposed) from the data of different coastal storms (and different oceanographic variables) related to different return periods in a similar way as done in other assets in urban floods (Martínez-Gomariz et al., 2019, Velasco *et al.*, 2016 and Velasco et al., 2013). The return periods (Tr) are directly related to the intensity of the event (θ). The exposure of the asset is evaluated for each case indirectly with the hazard evaluation parameter (θ), since if the draft is 0 (no exposure), the intensity is null and consequently the cost is null as well.

In addition, to allow impact assessment in locations where a hydrodynamic model of the coast is not available, a relationship between the variables obtained in the model (velocities and water depth) with the significant wave height (H_s) associated with those characteristics is proposed. With this information, indirect curves (H_s - €/m) can be generated for a wave height assessment, being a more accessible variable at the recording buoys close to the study area. Conversely, if the curve construction data is obtained from a hydrostatic model, the intensity parameter will be estimated by the oceanographic wave height data rather than by the velocity. Different adaptation measures of the collector will be presented and the EAD generated in each case will be compared. The adaptation measures will include modifications of the protection levels or modifications of the layout (reduction of exposure to protection level 4). More details on these results are given in the expected outputs section below. Figure 15 shows a data flow diagram of the performance of the flooding and coastal surge storm model.

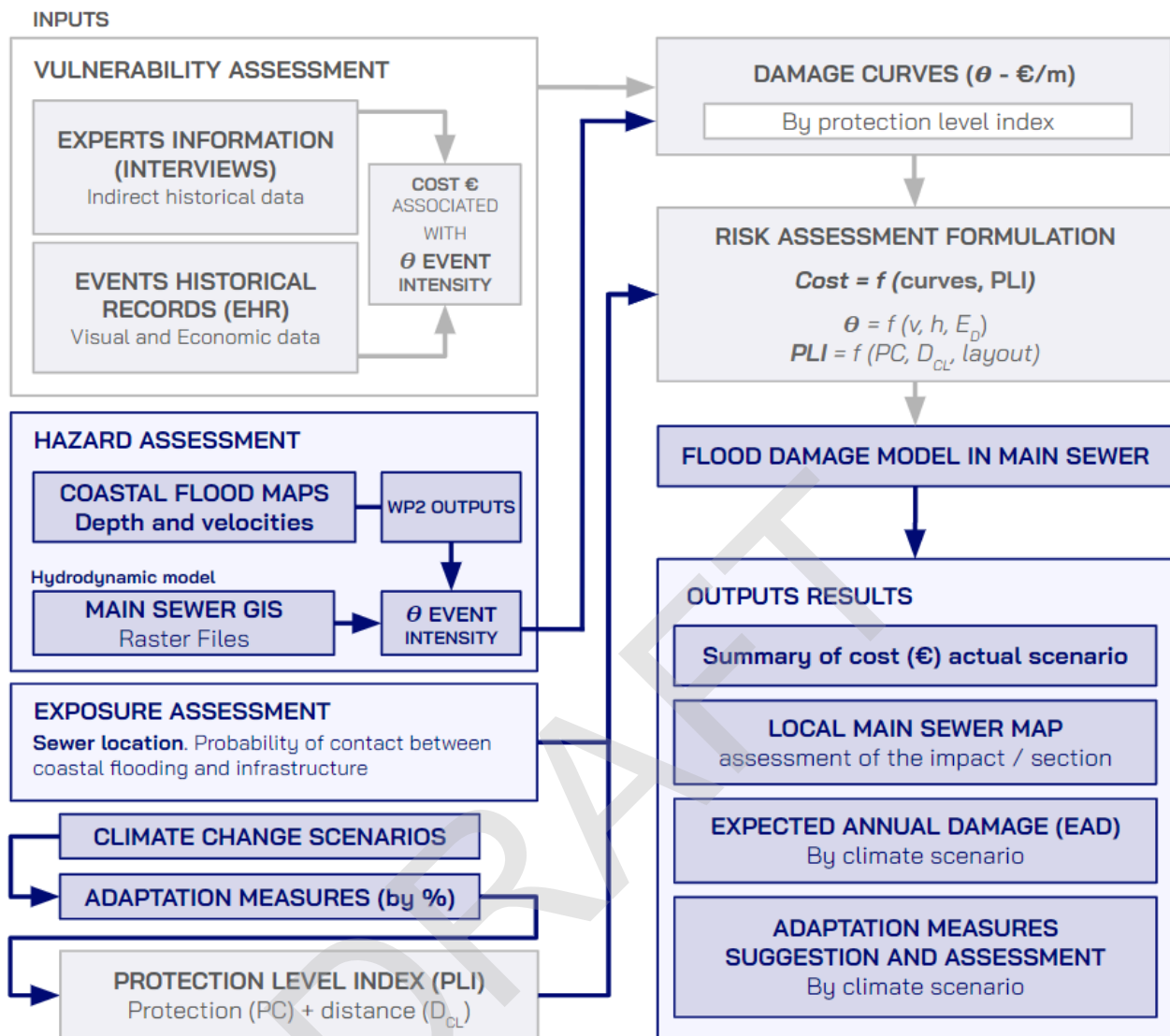


Figure 15. Data flow diagram representing the economical damage flooding model (own elaboration) for a coastal main sewer exposed to coastal flooding and surge impact.

2.3.1.8 Expected outputs of the model

The expected model outputs for the main sewer are a succession of maps and economic results about different protection levels and climate projections. The first output is a summary of costs for a fictitious sewer without coastal protection (100% exposure) in the current scenario. This is evaluated by considering different oceanographic storms with different return periods (Tr) from the hydrodynamic model results provided by WP2. The study was adapted to the current situation of the main sewer by applying the coastal exposure reductions associated with the current PLI. An economic assessment will be combined with a linear map of the main sewer showing the expected impact on the different sections.

The assessment of the different climate scenarios will be carried out in a systematic way. Variations in oceanographic intensity and SLR directly affect the intensity parameters (θ), which consequently affect

the associated costs. The results of the evaluation and comparison of different climate scenarios will be presented through the creation of EAD, as described in the risk assessment.

Finally, adaptation measures associated with the impacts of the various climate scenarios will be proposed. The assessment will consider two measures: modifying the protection level and modifying the layout of the main sewer. In each case, an EAD assessment will be conducted to evaluate the economic impact of the proposed measures on risk reduction. Figure 16 provides an example of increasing coastal protection or shifting the layout of a generic sewer.

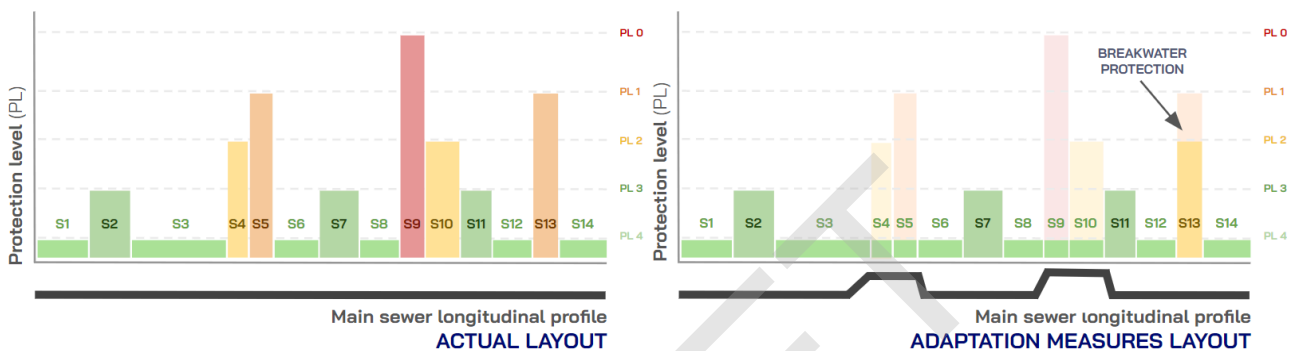


Figure 16. Exemplification of comparative of main sewer protections in the same climate scenario. Left side with the current layout, right side with the modified layout (adaptation measure).

2.4 Impacts on the electricity sector

The electricity sector is a critical infrastructure as its correct functioning is key to maintain the rest of critical sectors, which people's health, basic services provision and security depend on, such as health care infrastructures, water distribution and sanitation networks, public transport, etc. Therefore, the assessment of the electricity distribution network has been pointed out as key in the 3 CoP workshops, when defining the expected contributions for their CS.

In this section, the expected assessment methods for direct and indirect tangible impacts are presented. The direct effects method is expected to estimate the damage caused to the distribution network per se, whereas indirect damages focus on cascading effects to water and transport sectors.

2.4.1 Direct Impact

2.4.1.1 Scope and objectives of the impact assessment

Electrical grids are not immune to the impacts of floods, which can lead to direct consequences that are not only potentially fatal in themselves but can also trigger cascading failures. Any outdoor network element is susceptible to failure due to the presence of water, and therefore, it can be asserted that this event affects the electrical system at various levels: in electricity generation (such as ground-level generation plants like photovoltaic facilities), in transmission (evident in electrical power lines), and in electrical distribution (including electrical substations). The objective of impact assessment within the electrical sector is to evaluate the potential repercussions caused by floods.

The physical scope of this study pertains to the power grid within large territories containing urban and non-urban areas such as the AMB, marking a significant difference with the RESCCUE project, which exclusively considered cities such as Barcelona or Bristol. In this case, only electrical substations were considered potential elements susceptible to failure due to heavy rains. This assumption was based on the understanding that the low-voltage lines in the cities were assumed to be underground. Additionally, all-electric generation plants were neglected due to their limited representation. The ICARIA project, with its broader scope, allows for the consideration of both the probability of failure in overhead power lines and electric generation plants, in addition to considering the loss of power capacity that the elements may have due to external conditions. The technical scope involves the calculation, based on climatic maps, of the probability of failure for network elements derived from their fragility curves. The purpose is to ascertain the likelihood of service interruption in the electrical supply.

Once the parameters for this part of the study are established, the main objective can be computed: the direct economic damage. By identifying which elements of the electrical grid fail, the locations of these failures, and which portion of the network experiences an interruption in electrical supply, the impact of the flood event on the electrical system can be monetized, as explained in the subsequent sections.

2.4.1.2 Input datasets used in the model

To create the modelling of the system for evaluating the direct impacts induced by floods on the power grid, the following data as input variables are considered.

Table 6. Pluvial flooding hazard model, data requirements for electricity sector damage assessment.

| Data requirements for the electricity sector damage model | | |
|---|---|--|
| Data group | Description | Source |
| Historic climate data | Historic datasets of rainfall data with the highest time resolution possible (mm / 1 to 5 min resolution) | EU/National/Regional meteorological agencies Meteorological databases (e.g. Copernicus) |
| Future climate projections | Local downscaled precipitation projections of different climate change scenarios | Results Task 1.2 |
| | Future IDF curves considering different change scenarios and time horizons | |
| Power grid map | Power grid geolocation map of the elements that compounds it with their electrical data related to them | ENTSO-E OpenStreetMap E-distribución (for AMB case of study) |
| Fragility curves data | Fragility curves of the elements participating in the study. | Federal Emergency Management Agency FEMA (2009) |

2.4.1.3 Impact assessment model setup

For the setup of the impact assessment model on the electrical grid, a similar approach is adopted as in the RESCCUE project due to the nature and the similarity of the available data, although with an expanded territorial scope and the inclusion of additional elements within the electrical network.

Hence, the first step is to create a sampling shape layer of all the vulnerable elements of the grid by using an average diameter according to each type. In the RESCCUE project, the average diameter for the electrical direct current (DC) substations was 20 metres based on the recommendation in the Energy Networks Association article (ENA 2018), distributed uniformly with a cloud of 106 sampling points. The diameter has two functions: the first helps to define the influence area for each location, while the second allows the tool to cope with location uncertainty in GIS data.

The second step involves cross-referencing the sampling layer with the detailed flooding map, which delineates the water depth in each flooded region. Following the intersection of these two datasets, specific parameters are derived, including the measurement of water depth in metres.

The third step involves calculating the Affected Area Rate (AAR) by floods for each element and their Water Depth Average (WDA) using the following equations. The first one counts the points affected by the flood (n_{γ}) and divides them by the total number of sampling points (n_{total}) of the sampling shape layer generated in the first step. The second one calculates the average of the flood depth for every sampling point to obtain a general representative number of each location.

$$AAR = \frac{n_{\gamma}}{n_{total}} \cdot 100 \text{ (Eq. 7)}$$

$$WDA = \frac{1}{n} \sum_{i=1}^n \gamma_i \text{ (Eq. 8)}$$

With the parameters AAR and WDA established, the subsequent step involves the incorporation of fragility curves into the model. The curves compiled by FEMA (2009) represents a table of the study with the values of the curve for each element, are utilised, and through a sensitivity analysis, a better resolution is attained by considering a broader spectrum. Once the final curves are determined, the Probability of Failure for the Curve (FCP) can be derived, taking into account the WDA of the element.

Finally, the last step involves calculating the probability of failure (P_F) for the element, considering its area affected by flooding (AAR). P_F thus indicates how likely the studied element is to fail on a scale from zero to one.

$$P_F = AAR \cdot FCP \text{ (Eq. 9)}$$

2.4.1.4 Expected outputs of the model

With the model setup done, it is possible to identify which elements are most vulnerable, how likely they are to fail, the location where they are malfunctioning, and subsequently, the points in the network where the power supply may be disrupted by flooding. Considering all these aspects, to economically quantify the direct impact on the electrical grid, four economic loss categories are taken into consideration, following the methodology outlined by (Sánchez-Muñoz et al., 2020). Two of them are presented here and assumed as direct impacts, and the other two are explained and considered in the section on indirect impacts 2.4.

- Damages over electrical assets:** the Effective Damage Cost (EDC) for each element is calculated by considering three parameters, to monetize the potential damages caused to them. The first one is the failure probability (P_F) calculated in the previous section. The second one is the Damage ratio (D_{ES}) of the element caused by the flood, obtained from damage curves of FEMA-HAZUS and shown on Figure 17. The last parameter is the price of the corresponding element in € (p_s).

$$EDC = P_F \cdot D_{ES} \cdot p_s \quad (Eq. 10)$$

| Label | Earthquake Classification | Specific Occupancy | Functionality Threshold Depth | Percent Damage by depth of flooding in feet ² | | | | | | | | | | | Comments |
|-------|---------------------------|--|-------------------------------|--|-----|---|-----|----|------|----|------|----|----|----|--|
| | | | | 0 | 1 | 2 | 3 | 4 | 5 | 6 | 7 | 8 | 9 | 10 | |
| ESSL | ESS1, ESS2 | Low Voltage Substation | 4 | 0 | 2 | 4 | 6 | 7 | 8 | 9 | 10 | 12 | 14 | 15 | Control room damaged starting at 0 feet, and maximized at 7' depth. Additional damage to cabling and incidental damage to transformers and switchgear. |
| ESSM | ESS3, ESS4 | Medium Voltage Substation | 4 | 0 | 2 | 4 | 6 | 7 | 8 | 9 | 10 | 12 | 14 | 15 | |
| ESSH | ESS5, ESS6 | High Voltage Substation | 4 | 0 | 2 | 4 | 6 | 7 | 8 | 9 | 10 | 12 | 14 | 15 | |
| EDC | EDC1, EDC2 | Distribution Circuits Elevated Crossings | N/A | 0 | 0 | 0 | 1 | 1 | 1 | 1 | 2 | 2 | 2 | 2 | Low vulnerability due to flooding of ends of buried cables and possible barge traffic impacting transmission towers |
| EDC | EDC1, EDC2 | Distribution Circuits Buried Crossings | N/A | 0 | 0 | 0 | 0 | 0 | 0 | 0 | 0 | 0 | 0 | 0 | No damage due to submergence. |
| EDC | EDC1, EDC2 | Distribution Circuits (non-crossing) | N/A | 0 | 0 | 0 | 0 | 0 | 0 | 0 | 0 | 0 | 0 | 0 | No damage due to submergence. |
| EPPS | EPP1, EPP2 | Small Power Plants | 4 | 0 | 2.5 | 5 | 7.5 | 10 | 12.5 | 15 | 17.5 | 20 | 25 | 30 | Support facilities damaged on ground level. Control and generation facilities damaged when water elevation reaches 2nd level. |
| EPPM | EPP3, EPP4 | Medium Power Plants | 4 | 0 | 2.5 | 5 | 7.5 | 10 | 12.5 | 15 | 17.5 | 20 | 25 | 30 | |
| EPPL | EPP3, EPP4 | Large Power Plants | 4 | 0 | 2.5 | 5 | 7.5 | 10 | 12.5 | 15 | 17.5 | 20 | 25 | 30 | |

Figure 17. Percent damage curves values for the elements of the grid of the FEMA study.

- Non-supplied electricity:** In order to quantify the Energy Non-Supplied Cost (ENSC) it is the need to specify the 5 parameters involved with its equation (see Eq. 11, Eq. 12): probability of failure of the electrical element (P_F), the period without energy (t_{WE}), the repair time (t_R), the non-supplied power (P_{ES}) and the energy price (p_E).

$$ENSC \left\{ P_F \cdot P_{ES} \cdot t_R \cdot p_E, t_R \leq t_{WE} \right\} \quad (Eq. 11)$$

$$ENSC \left\{ P_F \cdot P_{ES} \cdot t_{WE} \cdot p_E, t_R > t_{WE} \right\} \quad (Eq. 12)$$

2.4.2 Indirect Impact

2.4.2.1 Scope and objectives of the impact assessment

Electric grids constitute critical infrastructure, and in the face of disruptive events such as floods, it is imperative not only to consider their direct impacts but also to emphasise their indirect effects on other sectors such as water and transportation.

To conduct this study, this section adopts the same territorial scope as the section on direct impacts. Moreover, from a technical standpoint, the focus is on identifying points along the electrical lines where critical infrastructures from other sectors are connected, which are likely to experience electrical supply disruptions due to the failure of one or multiple elements within the electric grids (calculated in the section on direct impacts of floods).

2.4.2.2 Input datasets used in the model

For the assessment of indirect impacts, it is necessary in this instance to consider the direct impacts. Therefore, the same inputs are taken into account as in the evaluation of direct impacts, with the addition of new ones for the indirect assessments. Consequently, to create the modelling of the system for evaluating the indirect impacts induced by floods on the power grid, it is necessary to consider the following data as input variables.

Table 7. Electricity sector damage model, data requirements.

| Data requirements for the electricity sector damage model | | |
|---|---|---|
| Data group | Description | Source |
| Historic climate data | Historic datasets of rainfall data with the highest time resolution possible (mm / 1 to 5 min resolution) | EU/National/Regional meteorological agencies Meteorological databases (e.g. Copernicus) |
| | IDF curves of historic rain events | |
| Future climate projections | Local downscaled precipitation projections of different climate change scenarios | Results Task 1.2 |
| | Future IDF curves considering different change scenarios scenarios and time horizons | |
| Fragility curves data | Fragility curves of the elements participating in the study. | FEMA (2009) |
| Connection points of the water infrastructures | Connection points of critical water infrastructures to the power grid. | Water operators (e.g.. AMB case study: |

| | | |
|--|--|--|
| | | Aigües de Barcelona) |
| Connection points of the transport infrastructures | Connection points of critical transport infrastructures to the power grid. | Transport operators or local risk owner (e.g. AMB case study: Transports Metropolitans de Barcelona (TMB) and AMB Transport unit) |

2.4.2.3 Impact assessment model setup

Thanks to the model assessing direct impacts on the electrical grid due to a flood case study, the identified vulnerable points in the network serve as the starting point for estimating a potential cascading effect on other sectors. By establishing if there is a direct connection between the elements likely to fail or lose the capacity of energy supply with the new inputs for the model, which are the connection points of the critical infrastructures of interest to the grid, it can be determined how much energy is lacking to the infrastructure while the electrical elements are malfunctioning.

To calculate the Energy Loss (EL) in the critical infrastructure, Eq. 13 and Eq. 14 try to quantify it in case of a flood event by summing up the total energy lost by all the substations and elements connected to them, affecting the critical infrastructure. Eq. 13 and Eq. 14 are derived from Eq. 11, in which we calculate the costs for non-supplied energy without the energy price element, thus obtaining the energy lost in the power grid.

$$EL \left\{ P_F \cdot P_{ES} \cdot t_R, t_R \leq t_{WE} \right\} \quad (Eq. 13)$$

$$EL \left\{ P_F \cdot P_{ES} \cdot t_{WE}, t_R > t_{WE} \right\} \quad (Eq. 14)$$

2.4.2.4 Expected outputs of the model

The outputs of the model for indirect impacts are threefold. The first consists of detecting points where critical infrastructures of other sectors are connected to the power grid. The second entails quantifying the energy that these infrastructures could potentially not receive during a flood event in the territory. The third includes the identification of these critical infrastructures and the subsequent analysis of the potential consequences in the event of efficiency downturns in the electrical system: assessing whether they would withstand the impact and continue operating normally or if there is a possibility of a cascading failure.

On the economic side, the two remaining impacts of the Sánchez-Muñoz et al.,(2020) study are calculated.

- **Businesses earning losses provoked by the shortage:** For the monetization of the business cost (BC) an equation (Eq. 15) is considered. The formula employs the Gross Domestic Product (GDP) of the analysed region, multiplying it by the probability of failure of the electrical element (P_F). Additionally,

it incorporates a factor determined by the ratio of the affected population (number of people affected by the shortage, n_p) to the total population (n_{tot}), further multiplied by the fraction of the year during which the shortage occurs (shortage duration in days, t_{WE} , divided by 365).

$$BC = GDP \cdot P_F \cdot \frac{n_p}{n_{tot}} \cdot \frac{t_{WE}}{365} \quad (Eq. 15)$$

- **Expenditures associated with the renting of emergency electrical supply appliances:** The Auxiliary Generation Cost (AGC) formula is segmented into four intervals. The first interval determines if the repair time is less than the shortage time, in which case, it would not be necessary to lease auxiliary equipment to support the network. The remaining three intervals are divided based on the equipment rental cost, which is inversely proportional to the duration of the lease (C_{Rt}). Each interval considers the probability of failure (P_F), the cost of transporting the generators (C_{AGT}), the fuel cost required for their operation (C_{FC}), and the number of auxiliary generators (n_{AG}) needed to supply the energy that the network cannot provide. See Eq. 16, Eq. 17, Eq. 18 and Eq. 19.

$$AGC\{0, t_R \leq t_{WE}\} \quad (Eq. 16)$$

$$AGC\{P_F \cdot C_{AGT} \cdot n_{AG} + C_{FC} + C_{Rt1} \cdot n_{AG}, t_{WE} < t_R \leq 1 \text{ week}\} \quad (Eq. 17)$$

$$AGC\{P_F \cdot C_{AGT} \cdot n_{AG} + C_{FC} + C_{Rt2} \cdot n_{AG}, 1 \text{ week} < t_R \leq 3 \text{ weeks}\} \quad (Eq. 18)$$

$$AGC\{P_F \cdot C_{AGT} \cdot n_{AG} + C_{FC} + C_{Rt3} \cdot n_{AG}, t_R > 3 \text{ weeks}\} \quad (Eq. 19)$$

The calculation of the auxiliary generators involves dividing the distribution centre power consumption (P_{ES}) by the maximum active power provided by the generator (P_{AG}) and rounding up the result to the nearest whole number, as expressed in Eq. 20:

$$n_{AG} = \left\lceil \frac{P_{ES}}{P_{AG}} \right\rceil \quad (Eq. 20)$$

Ultimately, with all the partial costs of the direct and indirect impacts at various levels of the electrical grid considered, the total economic cost of the flood's direct impact can be calculated by summing up all the partial costs. The equation for the Losses Related to the Grid (LRG) is as follows:

$$LRG = EDC + BC + ENSC + AGC \quad (Eq. 21)$$

2.5 Impacts on the Transport sector

The transportation sector plays a crucial role within regions and cities facilitating the movement of goods, services and populations. Flood events can have significant impacts upon this sector directly through damages caused to buildings and physical infrastructures, and potential injuries and loss of life to people caught within the flood water, and indirectly through service disruption affecting businesses resulting in economic losses.

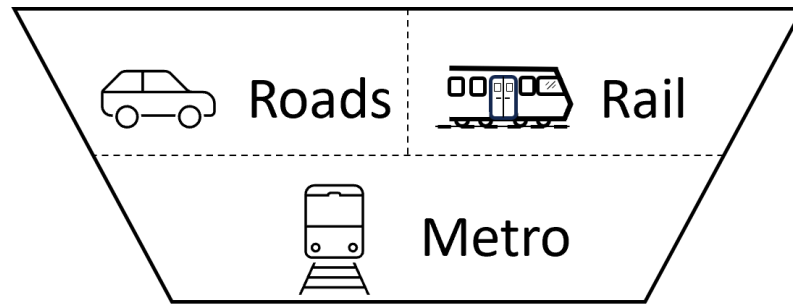


Figure 18. Thematic areas covered in flood impact assessment of the transport sector.

Within the framework of the ICARIA project, one of the impact models will focus on the assessment of direct and indirect impacts of flooding on the transportation sector regarding both above ground and below ground assets. These assets are analysed in the context of three thematic areas, as shown in Figure 18. This assessment will help us to understand the risks posed to the transportation network by flooding, considering current and future climate scenarios along with compound hazard events.

2.5.1 Impact assessment on Road Network

2.5.1.1 Scope and objectives of the impact assessment

Direct impacts to the road network are commonly derived through the analysis of inundation of flood waters on the road surfaces making them either unsafe or impassable for traffic flows. Previous works by Pregolato et al. (2017), and Pyatkova et al. (2019) analysed the relationship between what is perceived to be the maximum safe speed of vehicles travelling through flood water and the minimum depths that could result in the vehicle stalling.

In modelling disruption to traffic flows, two of the commonly used methods are graph theory approaches (Bíl et al., 2015; Pregolato et al., 2016) and loosely coupling of traffic models to Pyatkova, (2018) and Evans et al., (2020). Whilst coupling of traffic models allow for simulation of disruption to traffic outside of flood extents due to vehicles re-routing they require a pre-existing or the development of a traffic model for the region. In the absence of model and/or data required for this process, a graph-theory approach becomes a preferential alternative.

Within the scope of ICARIA in the absence of traffic models at regional level, a graph-theory approach is being adopted building on the approaches used within the Lisbon case study in RESCCUE (Deliverable 2.4. RESCCUE) whilst integrating novel approaches for determining the potential impacts flood and compound flood events will have on traffic flows.

2.5.1.2 Input datasets used in the model

Table 8. Data requirements for impact assessment on road networks.

| Data requirements for impact assessment on vehicles | | |
|---|---|---|
| Data Group | Description | Source |
| Flood Depth Maps | Spatial data output of flood models | Hazard models implemented in Task 4.2 and 4.3 |
| Flood Velocity Maps | Spatial data outputted from flood models that contains surface flow velocities of flood water | Hazard models implemented in Task 4.2 and 4.3 |
| Vehicle Stability Curves | Empirically defined stability curves for range of vehicle types | Data available from previous studies/literature (Martínez-Gomariz et al., 2017) |
| Road Usage Statistics | Traffic counts/estimates across road network | Hazard models implemented in Task 4.2 and 4.3 |
| Speed Vs Cost Estimates | Data that can be utilised to express operational costs of vehicles per km as a function of their speed | Adjusted values derived from Multi-colour handbook (Penning-Rowse et al. 2010) |
| Road Network Maps | Geographical data depicting road networks within respective case studies along with any accompanying data relating to road use and types (e.g. major highway, minor road, access road etc.) | Data can either be provided by case studies or publicly available sources, e.g. OpenStreetMap (https://www.openstreetmap.org/) |

2.5.1.3 Impact assessment model setup

Whilst the approaches outlined in Pregolato et al. (2017), Pyatkova et al. (2019), and Evans et al. (2020) analysed the potential disruptions to traffic flows as a result of flood water depths they did not consider the potential effects of flow velocities. In Martínez-Gomariz et al. (2017) the relationship between water-depth and flow velocity were assessed in the derivation of stability curves for a range of vehicle classes. These curves highlight the potential hazard induced by flood on vehicles, affecting their stability due to buoyancy and/or sliding, in relation to water depths and flow velocities. In this approach, even relatively low water depths can pose potential risks to vehicles when the flow velocity is high. Using a generic vehicle as reference (in this instance a Seat Ibiza), three hazard bands, Low, Medium, and High, were derived, see Figure 19.

- **Low:** likelihood of vehicle instability due to combination of depth-velocity values
- **Medium:** Due to uncertainty/variations in friction coefficient there is an increased likelihood that vehicles may become unstable within this range of depth-velocity values
- **High:** High likelihood of vehicle instability due to combination of depth-velocity values

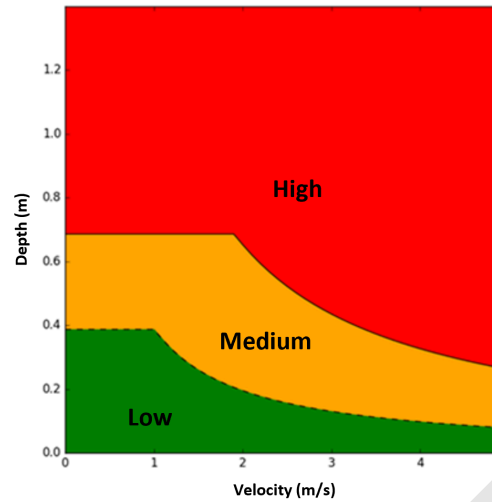


Figure 19. Hazard classifications for vehicles based on depth versus velocity of floodwater (Martínez-Gomariz et al., 2019).

To derive a risk/impact assessment on traffic flows along the road network, information relating to exposure and vulnerability is required. In Evans et al. (2018) this was determined by considering Vehicular Flow Intensity (VFI) along roads within the transport network where roads with higher traffic flows are considered to be more vulnerable. Table 9 shows an example of vulnerability scores based on VFIs for the city of Barcelona from Evans (2019). The criteria for these vulnerability classes were originally derived via expert opinion from the municipality and can be adjusted accordingly for other regions based on road usage.

Table 9. Example criteria of vulnerability score based on VFIs along road sections (Evans 2019).

| Vulnerability index/score | Vehicle flow intensity (VFI) (veh/day) |
|---------------------------|---|
| 1 (Low) | < 5,000 |
| 2 (Medium) | $5,000 \leq x \leq 10,000$ |
| 3 (High) | > 10,000 |

Using the classification methods for defining hazard and vulnerability along road sections, a qualitative risk matrix is defined in Figure 20.

| | | Hazard | | |
|---------------|------------|---------|------------|----------|
| | | Low [1] | Medium [2] | High [3] |
| Vulnerability | Low [1] | 1 | 2 | 3 |
| | Medium [2] | 2 | 4 | 6 |
| | High [3] | 3 | 6 | 9 |

Figure 20. Vehicle risk matrix.

To assess the final impact, the Exposure information (i.e. the number of cars expected to be present in a given road characterized by a given VFI index) must be also considered. This can be determined by Road Usage Statistics (Traffic counts/estimates across road networks) provided by case studies.

To quantify monetary impacts, it is necessary to define the relationship between vehicle speed and estimated costs. For this, revised (inflation adjusted) data from Penning-RowSELL et al., (2010) (Table 10) along with road use statistics and estimated speed restrictions, will be used. These cost estimates will be compared against baseline (dry weather) estimates. To define speed reduction, Eq. 22 from PregNolato et al. (2017) will be used where:

$$v(w) = 0.0009w^2 - 0.5529w + 86.9448 \quad (\text{Eq. 22})$$

- **w**: flood water depth (mm)
- **v(w)**: maximum safe travel speed (km/h)

Table 10. Estimated Travel Cost (GBP) for cars as a function of speed per km (Penning-RowSELL et al., 2010).

| Vehicle | Speed (km/h) | | | | | | | | |
|---------|--------------|------|------|------|------|------|------|------|------|
| | 1 | 2 | 5 | 10 | 20 | 40 | 50 | 80 | 100 |
| Car | 10.23 | 5.15 | 2.10 | 1.09 | 0.57 | 0.31 | 0.25 | 0.17 | 0.15 |

Summary flow process view:

Figure 21 outlines the flow of data and processes that will be used to carry out the risk/impact analysis of flooding to vehicles utilising the road network. Here flood model outputs combined with data pertaining to stability functions shown in Figure 21 will be utilised to spatially define the hazards that flood water poses to vehicles across the road network. This hazard data combined with road vulnerability data (that depicts vehicle flows along road sections) will be used to spatially define risk/impact scores

across the network. For the monetary impact assessment, the use of relative speed reduction maps will be employed along with cost speed relationships to define potential financial losses.

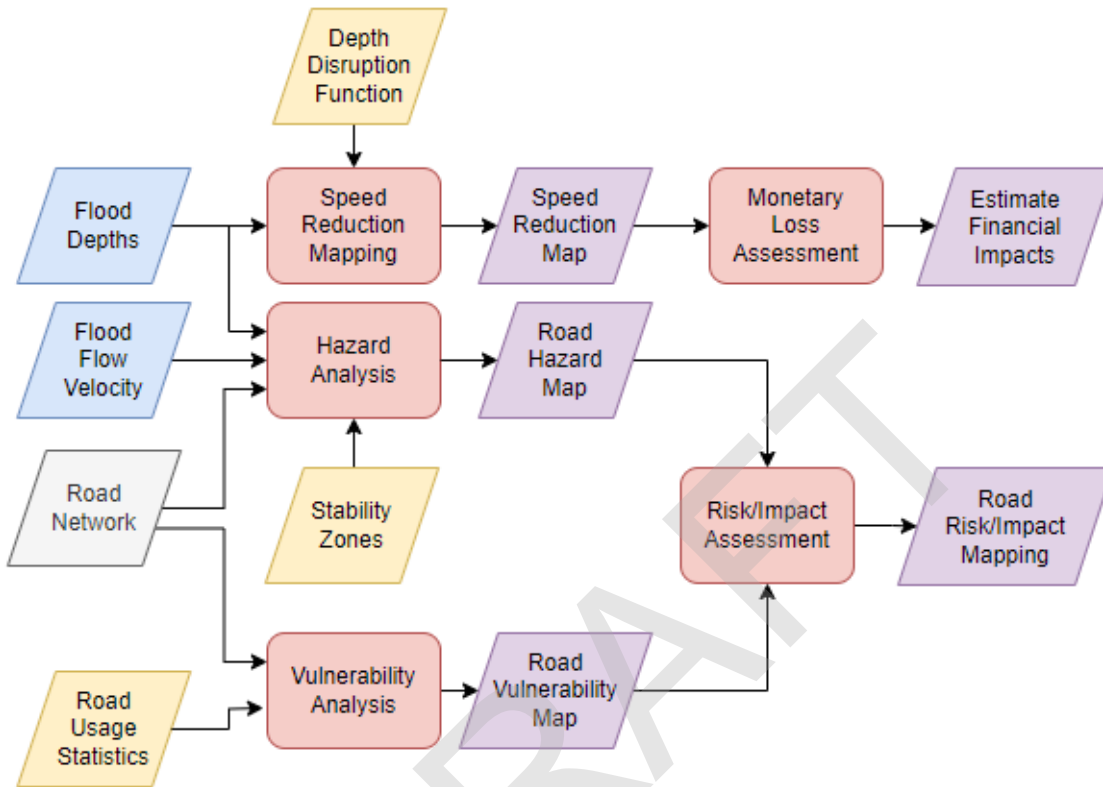


Figure 21. Impact assessment flowchart for road networks.

2.5.1.4 Expected outputs of the model

Road network risk maps: These will identify sections of the road network that pose potential risks to traffic flows along them for each of the modelled return periods from the flood models for both current (baseline) and future (BAU) scenarios.

Monetary impacts: Through the analysis of road network risk maps and potential speed reductions associated with said risks, estimates as to potential monetary losses will be derived. Through the analysis of accumulative financial impacts for the modelled return periods for both baseline and BAU scenarios, respective exceedance probability curves will be derived along with average annual loss values.

2.5.2 Impact assessment on rail network

Like that of the road network infrastructure, rail networks play a vital role in the mobilisation of people and freight. Within the RESCCUE project, the city of Lisbon analysed the disruption to the rail network through the spatial analysis of flooding that intersects rail tracks and transport user interfaces such as

train stations; this approach will be adopted within ICARIA to assess potential disruption to overground rail travel. The following sections outline how flood model outputs are used to define hazards posed to the above ground rail network.

2.5.2.1 Scope and objectives of the impact assessment

The rail safety and standards board within the UK (2015) outlines some operational constraints on train speeds when there is flood water present upon the tracks. Figure 22 defines the operational speed constraints for trains traversing partially flooded track sections where if the water depth is above sleeper level but below the bottom of the rail head, trains can proceed at line speed. If the water depth is between the bottom and top of the rail head, speed is limited to 5 mph (8 km/h), and if it is above the rail head, permission to proceed must be obtained from Operational Control.

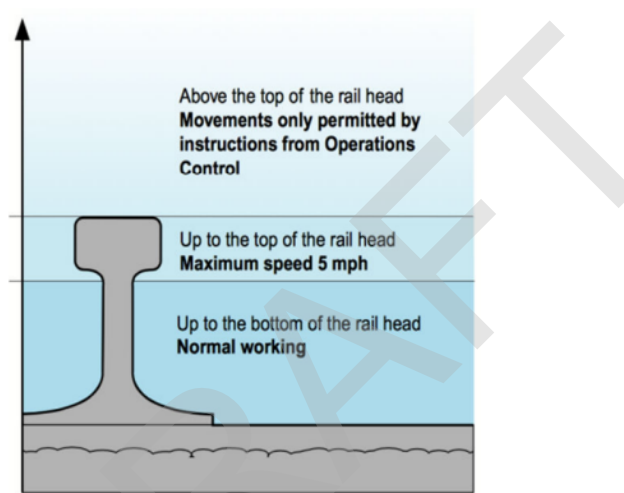


Figure 22. Rules for governing speed of trains through flood water in the UK (Baker C. et al., 2016).

To simulate impacts/disruption to train services within ICARIA, a simplified GIS based approach will be applied assessing flood depths along track sections to define whether services are disrupted due to speed reductions or due to temporary suspension due to track closures.

2.5.2.2 Input datasets used in the model

Table 11. Data requirements for impact assessment on road networks.

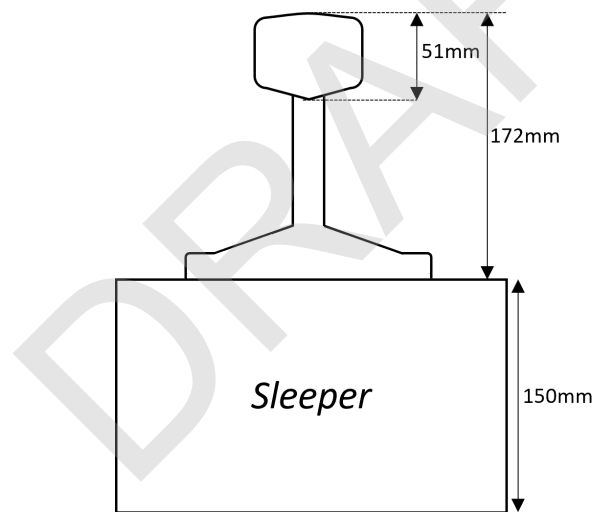
| Data requirements for impact assessment on road networks | | |
|--|---|---|
| Data Group | Description | Source |
| Flood Depth Maps | Spatial data outputted by flood models relating to depth of flood water | Hazard models implemented in Task 4.2 and 4.3 |

| | | |
|-----------------------|--|---|
| Rail Network Maps | Geographical data depicting rail networks within respective case studies along with any accompanying data relating to transport user interfaces. | Data can either be provided by case studies or source via OpenStreetMap (https://www.openstreetmap.org/) |
| Rail Usage Statistics | Passenger and/or freight counts/estimates across rail network | Hazard models implemented in Task 4.2 and 4.3 |

2.5.2.3 Impact assessment model setup

Using the rail profile of a UIC60 Rail that complies with European Standard EN 13674-1 ("UIC60 Rail for Sale," 2020) as and estimate for track height we have rail configuration that consists of a rail height of 172mm and head height with a head size of 51mm, on top of a Sleeper with a height of 150mm "Railway Sleeper Sizes and Weights," 2023.).

Figure 23. Summarised dimensions of UIC60 Rail (Source:



<https://railroadrails.com/railroad-rail-for-sale/uic60-rail/f>) on top of EU standard sleeper (Source: <https://www.buildingarena.co.uk/companies/railwaysleepers-com1/products/railway-sleeper-sizes-and-weights>).

Based on this track specification and the operational parameters outlined in Baker et al.,2016, we can define the potential disruption in terms of speed reduction and track closures for standing water on train tracks, see Table 12.

Table 12. Potential flood depth to rail disruption criteria.

| Water Depth Description | Water Depth (mm) | Permitted Speed (km/h) | Hazard Classification |
|-------------------------|------------------|------------------------|-----------------------|
|-------------------------|------------------|------------------------|-----------------------|

| | | | |
|---|-------------------|---|--------|
| Above sleeper level but below bottom of rail head | Depth < 271 | Normal line speed | Low |
| Between bottom and top of rail head | 271 ≥ Depth < 322 | 8 km/h | Medium |
| Above rail head | Depth ≥ 322 | 0 km/h (Permission needed from Operational Control) | High |

The vulnerability assessment will be defined considering two types of flows, passenger and freight, where the vulnerability scores will be expressed in terms of passenger flow intensity (PFI) and freight flow intensity (FFI) to assess the risks, see Table 13. The risk derivation will use the rail risk matrix (Figure 24).

Table 13. Derivation criteria of vulnerability score for passenger and freight flows per day.

| Vulnerability index/score | Passenger flow intensity (PFI) (people/day) | Freight flow intensity (FFI) (freight value/day) |
|---------------------------|--|---|
| 1 (Low) | < p1 | < f1 |
| 2 (Medium) | p1 ≤ people ≤ p2 | f1 ≤ freight value ≤ f2 |
| 3 (High) | > p2 | > f2 |

Summary flow process view:

Similar to the approach outlined in the assessment impacts to road networks, the rail impact assessment model will analyse the potential disruption caused due to flood waters interacting railway tracks. Figure 25 outlines the flow process where hazard and vulnerability data are used to estimate potential disruptions to rail services.

| | | Hazard | | |
|---------------|------------|---------|------------|----------|
| | | Low [1] | Medium [2] | High [3] |
| Vulnerability | Low [1] | 1 | 2 | 3 |
| | Medium [2] | 2 | 4 | 6 |
| | High [3] | 3 | 6 | 9 |

Figure 24. Rail risk matrix.

To assess the final impact, the Exposure information (i.e. the number of trains expected to be present in a given rail section characterised by a given PFI/FFI index) must be also considered. This can be determined by Rail Usage Statistics (passenger and/or freight counts/estimates across rail network) provided by case studies.

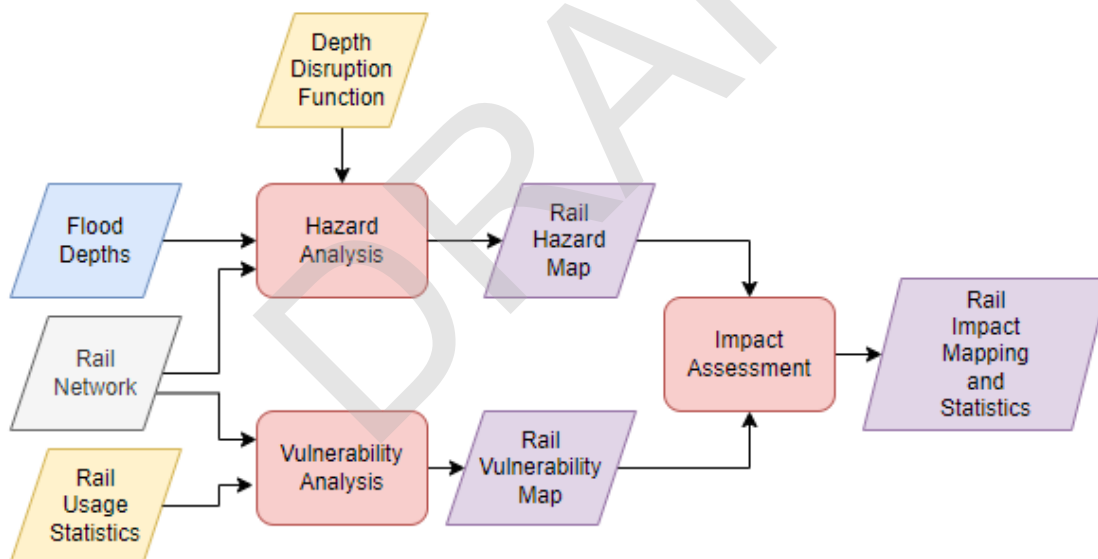


Figure 25. Impact assessment flowchart for road networks.

2.5.2.4 Expected outputs of the model

Rail network risk maps:

These will identify sections of the rail network that pose potential risks to passenger and freight flows along rail network for the modelled return periods based on flood model outputs for both current (baseline) and future (BAU) scenarios

Monetary impacts:

Through the analysis of rail network risk maps and potential speed reductions associated with said risks, estimates as to potential monetary losses will be derived. Through the analysis of accumulative financial impacts for the modelled return periods for both baseline and BAU scenarios, respective exceedance probability curves will be derived along with average annual loss values.

2.5.3 Flood impacts on metro

Underground metro (or subway) transportation is an essential infrastructure of most major urban areas worldwide to ensure that citizens are able to travel across metropolitan areas. Besides being a sustainable and efficient means of transport in densely populated regions, it also contributes to reducing private car usage and consequently helps to decrease pressure on road traffic infrastructure (Forero-Ortiz et al., 2020).

However, just as any other asset, metro networks are affected by extreme weather events, a situation that will be aggravated in the coming decades due to the effect of climate change. Several authors indicate that the intrinsic characteristics of this transport means, such as its subterranean location, the dependence on electricity or the fact that metros are located in flash flood prone environments, make this asset especially vulnerable to flooding events (Lyu et al., 2019; Huang et al., 2017 and Sugimoto et al., 2017). Nevertheless, literature reflects the fact that references that address risk assessment of metro infrastructure against flooding events are limited (Forero-Ortiz et al., 2020).

2.5.3.1 Scope and objectives of the impact assessment

Risk assessment of floodings in metro facilities can address several different problematic phenomenons. As in other infrastructures, on the one hand we have direct impacts that can be further subdivided into tangible (e.g. damaged facilities and equipment, reparation costs) and intangible impacts (e.g. public reliance on the service, potential death or injuries, need to evacuate facilities). On the other hand, indirect damages can also be split into tangible (e.g. decrease in number of passengers due to service disruption, economic loss due to delay in transport times) and intangible (e.g. risk perception) (Forero-Ortiz et al., 2020).

Even if for all the above damages, the hazard driver is the presence of water in the metro premises, for each specific case, this hazard is associated with the presence of water in different spaces of the metro network facilities. Furthermore, since different risk receptors are relevant in the context of risk assessment of metro flooding, different vulnerability criteria have to be considered in each case.

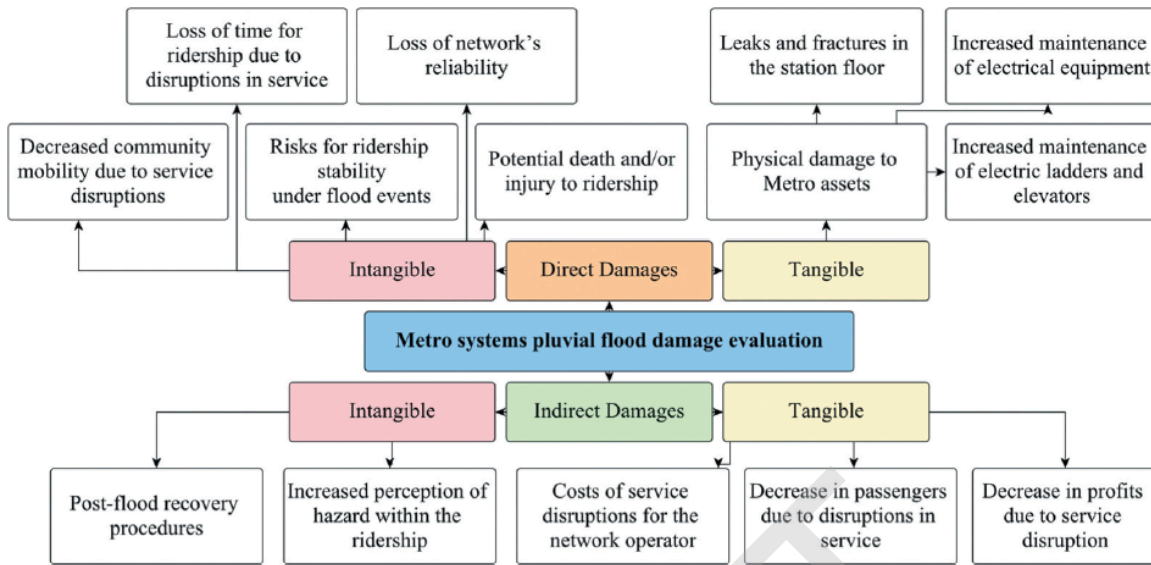


Figure 26. Damages associated with the damage and risk assessment of flooding in metro systems (Forero-Ortiz et al., 2020).

2.5.3.2 Impact assessment model setup

In the context of project ICARIA, the impact of flooding in the metro network will be addressed from two points of view:

- Service disruption of the metro network (Direct tangible impact)
- Risk for the ridership in case of evacuation (Direct intangible impact)

The table below summarises the hazard and vulnerability qualification criteria that should be considered for the mentioned risk assessments.

Table 14. Hazard and vulnerability quantification.

| Index / Score | Service disruption perspective | Service users safety perspective |
|-------------------------------------|---|--|
| Hazard quantification | Level of water in the railways | Level and speed of water in access stairs and platforms |
| Vulnerability quantification | Critical water level at which metro convoy operation is constrained | Critical point at which evacuation of metro users is constrained |

Importantly, the monetization of these risks has not yet been investigated as far as the authors of this section know. Therefore, this section will focus on evaluating the above mentioned impacts in a quantitative manner that is not quantified in monetary terms.

Direct Tangible impact method: Metro service disruption due to flooding

Forero-Ortiz et al. (2020a) proposes a methodology for a flood risk assessment in underground metro systems to evaluate the disruption of this service during flash flood events. Such methodology was developed and tested for the city of Barcelona in the context of the EU research project RESCCUE (Velasco et al., 2018).

Hazard assessment

The hazard assessment dimension of this model is based on the coupling between a 1D/2D hydrodynamic urban drainage model and a representation of the metro underground network. This representation can be done in different ways and using various softwares.

In the suggested methodology this coupling is based on generating a parallel sewer system with the exact same characteristics as the metro facilities in the actual urban drainage model.

In this step, it is essential to adequately represent the structural elements through which the water overflow, generated during the flash floods, enters into the metro network. These elements, (e.g. ventilation grates, access stairs, access elevators, hallways) can be modelled as drainage network inlets that enable the exchange between the 1D and the 2D domains of the model. The hydraulic behaviour of such islets can be approximate to gated inlets based on the findings of experimental characterization campaigns (Russo et al., 2021). Tunnels and stations can be modelled as pipes with the adequate dimensions and geometry. As a result of this coupling, it becomes possible to assess the accumulation of water in the metro facilities and, especially, in the level of water in the rails platform.

The quantification of hazard for this specific risk assessment can become a complex matter due to the diversity of operational systems in metro networks around the world. Forero-Ortiz et al. (2020a) suggests quantifying hazard based on the water level in the rails platform at which the electric signalling devices, which regulate the safe circulation of convoys, begins to malfunction.

Based on this principle, and in cooperation with the Barcelona public transport operator (TMB), the following hazard quantification thresholds were defined.

Vulnerability assessment

With regards to vulnerability, Forero-Ortiz et al. (2020a) suggests quantifying this parameter based on the number of ridership affected by potential service disruption. Importantly, given the important fluctuation of passenger numbers between peak hours and the rest of the day, different vulnerability criteria are defined depending on the hour of the day (dynamic exposure). Such creations were determined based on a statistical analysis of the average hourly ridership in two metro stations of interest.

Risk assessment

Based on the above quantifications of hazard and vulnerability, Forero-Ortiz et al.,(2020a) suggests a matrix based qualitative approach to evaluate the risk of metro service disruption in different parts of the Barcelona metro infrastructure. Table 15 and Table 16 summarise the mentioned risk assessment criteria.

Table 15. Hazard and vulnerability criteria for Metro stations service exposed to flooding (from Forero-Ortiz et al., 2020a).

| Index / Score | Hazard (Water Depth) | Vulnerability for Non-Peak Hours (Ridership Flow) | Vulnerability for Peak Hours (Ridership Flow) |
|---------------|----------------------|---|---|
| 1 (low) | 0 - 0.15 m | 116 - 578 users/h | 96 - 591 users/h |
| 2 (medium) | 0.15 - 0.30 m | 578 - 1075 users/h | 591 - 1244 users/h |
| 3 (high) | > 0.30 m | 1075 - 1516 users/h | 1244 - 2701 users/h |

The hazard classification in the above table reflects the fact that, according to this methodology, with a water level lower than 15 cm in the railway platform, the metro service will be able to carry on. Above 15 cm, service disruption begins, so its operation will be constrained. With a water level higher than 30 cm, the rails are expected to be covered by water, so the service will be interrupted. As for the vulnerability, it can be observed that a higher score has been assigned to specific infrastructures (e.g. metro stations) with a more intense ridership.

Table 16. The risk matrix for Metro stations and ridership (from Forero-Ortiz et al., 2020a).

| Vulnerability | Hazard | | |
|---------------|------------|------------|------------|
| | Low (1) | Medium (2) | High (3) |
| Low (1) | Low (1) | Low (2) | Medium (3) |
| Medium (2) | Low (2) | Medium (4) | High (6) |
| High (3) | Medium (3) | High (6) | High (9) |

Based on this risk criteria, it is possible to develop risk maps according to the index assigned to each station and section of a metro line.

The study presented in Forero-Ortiz et al. (2020a) focused on the line L3 of the Barcelona metro network. Applying the explained methodology, it was possible to identify the section of this line with a higher risk of service disruption for rain events with different return periods. The figure below shows the results for a T20 event.

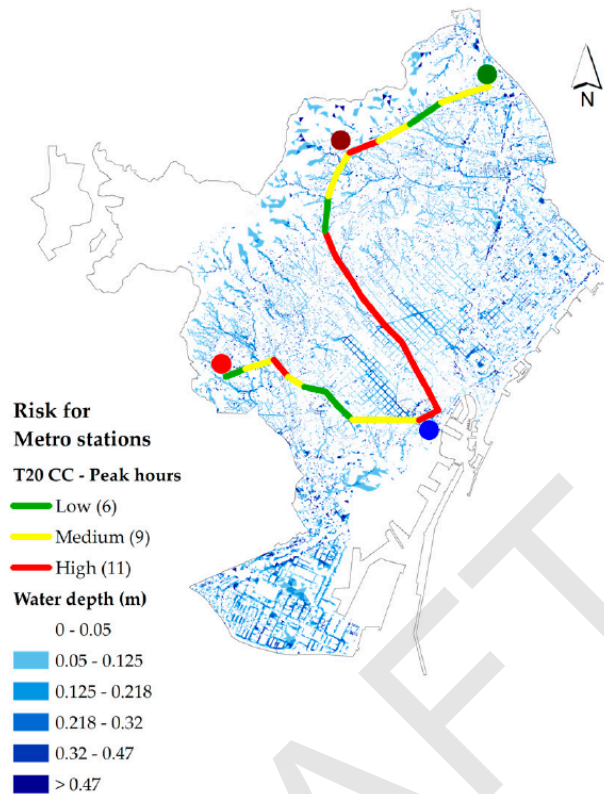


Figure 27. Metro stations risk assessment map for a synthetic event scenario corresponding to a T20 rain event and the longitudinal profile of L3 line of the Barcelona Metro Station (from Forero-Ortiz et al., 2020a).

Direct intangible impact method: Ridership evacuation due to flooding

Forero-Ortiz et al.,(2020b) presents an extensive literature review on scientific activities related to assessing conditions for citizen evacuation during flooding of underground metro infrastructure. Most investigations concluded that the presence of water above a certain level in stairs and platforms in underground environments pose a serious threat to citizens safety and difficult evacuation protocols. However, research in this field is quite limited and, so far, it is not clear which is the most adequate methodology to quantify the risk associated with these events.

Nevertheless, given the relevance of this for the AMB case study, the risk assessment methodology described in Aparicio-Urbe et al.,(2023) will be applied in project ICARIA.

Hazard assessment

Hazard assessment from the ridership evacuation perspective is focused on evaluating the amount of water that intrudes the metro network during flash flood events and quantifying the height and speed of water in access stairs to the metro stations. Therefore, it is necessary to couple a 1D/2D hydrodynamic urban drainage model with a 3D hydrodynamic model. On one hand, the 1D/2D model will determine the amount of water that can enter metro facilities located in areas affected by floods based on the water flood depth and velocity results in the area where the metro station accesses are located. On the other

hand, the 3D model will use the results of the 1D/2D model as the water input and compute the behaviour of water in typical access stairs to simulate the behaviour of water in these environments to be able to quantify relevant hydraulic parameters such as the water height and velocity in each step of the stairs (Aparicio-Urbe et al., 2023).

Hazard assessment criteria for this specific risk assessment is based on the “Specific Force Per Unit Width” (M_o) developed by Onishi et al.,(2008). The Eq. 20 below shows the calculator of this parameter:

$$M_o = \frac{V^2 * H}{g} + \frac{H^2}{2} \quad (Eq. 20)$$

where M_o is the Specific Force Per Unit Width, V is the water speed, H is the water height and g is the force of gravity.

Vulnerability assessment

The intrinsic characteristics of passengers (e.g. age, gender) can determine their vulnerability to be affected by this hazard. Ishigaki et al.,(2010) proposed a hazard classification of M_o based on real scale experimentation considering different population groups with different vulnerabilities. This classification is presented in Table 17. As in other methods presented in this document, a hazard index is given to each classification .

Table 17. Risk assessment criteria for evacuation of underground spaces through flooded stairs according to the Specific Force Per Unit Width parameter (Ishigaki et al., 2010).

| Population group | Hazard (M_o value in m^3/m) | | |
|------------------|-----------------------------------|--------------|--------|
| | Low | Medium | High |
| Young female | < 0,1 | 0,1 - 0,2 | > 0,2 |
| Young male | < 0,125 | 0,125 - 0,25 | > 0,25 |
| Old female | < 0,08 | 0,08 - 0,16 | > 0,16 |
| Old male | < 0,1 | 0,1 - 0,2 | > 0,2 |
| Index | 1 | 2 | 3 |

Following the same consideration as in the previous section, the volume of ridership of each metro station is a key aspect to consider when assessing the vulnerability of a metro station to flooding events. Hence, the vulnerability classification criteria presented in Table 15 will be also considered in this specific risk assessment, assigning vulnerability scores of 1 (low) to 3 (high) to each station.

Risk assessment

The risk for metro users associated with flooding of underground stations during urban flooding events will be determined considering the product of the hazard and the vulnerability score, associated with each scenario and location, that will provide a risk score. As shown in Table 16, risk sores of 1 to 2 correspond to low risk, 3 to 5 medium risk and 6 to 9 high risk.

2.6 Impacts on Natural areas

Detrimental effects on natural areas of flooding should be measured and accounted for in order to better understand the cost of inaction and take adaptation measures that protect ecosystems and the benefits that society obtains from the so-called ecosystem services. Although natural areas cover a broader scope, such as beaches or natural parks, following the objective of ICARIA on tangible damages, the estimates of monetary values of damages are proposed only for the agricultural sector to be evaluated in this framework.

2.6.1 Direct impact on agriculture

This section describes the effects caused by pluvial flood events in agricultural production in monetary terms. For agriculture, the damage is related to a loss in output when the yield is destroyed by floods. Therefore, the value added in Euros per hectare is used as the proxy for the damage value. From the methodology developed by the Joint Research Center (JRC) by Huizinga et al.,(2017), based on the World Development Indicators (WDI) (World Bank, 2023), the agricultural land per country (km²) and agriculture value added (€/year) are proposed as indicators to measure the damage of floods on agricultural systems. The proposed method will be downscaled for the CS with available data.

2.6.1.1 Scope and objectives of the impact assessment

The assessment focuses on agricultural production losses expected under each scenario selected by the consortium, considering climate change and different levels of adaptation.

2.6.1.2 Input datasets used in the model

Table 18. Impact assessment on vehicles, data requirements.

| Data requirements for impact assessment on vehicles | | |
|--|---|---|
| Data Group | Description | Source |
| Historic climate data | IDF curves of historic rain events | Results of Task 1.2 |
| Future climate projections | Future IDF curves considering different change scenarios scenarios and time horizons | Results Task 1.2 |
| Historical Agriculture Insurance payouts from extraordinary events | Dataset of Agriculture Insurance Company of Spain covering the production losses for agriculture producers related to all extreme events occurred in the past 25 years. | Insurance companies and entities (i.e. for AMB Case study: Seguro Agrario (Ministry of Agriculture)) |
| Agricultural land (past, present and future values) | Agricultural land use (sq. km) | National Statistical Office |
| | Value Added of agriculture (current Euros/year) | National Statistical Office |

2.6.1.3 Impact assessment model setup

The first step is to estimate the current value added per hectare of agricultural land use for the specific case study (Huizinga et al., 2017). This can be easily calculated using statistical datasets. The calculations should be done for the present, past and future values, in order to match the current scenarios with current or baseline expected damages, the past value of agriculture production with the past registered events and payouts, and future projections of value will be needed to match with the expected damages of future scenarios.

The methodology proposed by Hoes and Schuurmans (2006) relates historical flood events classified by return periods, to insurance payouts. Based on that methodology which estimates the EAD of the floods based on the definition of risk as probability times consequences:

$$EAD = \int S(h) f(h) dh \text{ [eq. 21]}$$

in which $f(h)$ is the Probability Distribution Function (PDF) of water level h and $S(h)$ is the damage caused by water level h . The integration is needed to deal with the complete range of all possible water levels. When determining the risk of flooding, two functions are needed: (1) the PDF already computed to check the water system to the standards; and (2) depth damage functions (Hoes and Schuurmans, 2006).

The approach to risk of Project ICARIA is the combination of hazard, exposure and vulnerability. Hazard is understood as the probability of flooding events (the flood depths for the different return periods). The most important flood parameter considered in the damage functions for agriculture in one of the reference studies is the flood depth (Huizinga et al., 2017). Whereas exposure is represented by the surface of agricultural land by production type, and vulnerability focuses on the probability of a given agricultural production of reducing its productivity when affected by the floods. Seasonality is also considered to be an influential parameter to assess crop damage, but it is not included in this study as it is quite complicated to apply due to differences in crop and climate. Therefore, the two functions mentioned by Hoes and Schuurmans (2006) will be adapted to the ICARIA trials and minitrials:

- **f(h):** the hazard function will be determined by the 1D/2D maps, providing flood depths for the synthetic return periods
- **S(h):** the damage function will be constructed from the historical damages claims and payouts from the agricultural insurance company, associated with a certain return period. The estimation of regular incomes obtained from the production in normal conditions will also be carried out.

The risk maps, hydrodynamic hazard, exposure and vulnerability maps will be modelled to set a baseline scenario, climate change projections' scenarios with different adaptation strategies, as mentioned in previous methodologies.

2.6.1.4 Expected outputs of the model

The agricultural land per CS (km² or ha) and agricultural value added (€/year) will be intermediate outputs of the model that will allow us to estimate the EAD in terms of euros per year for the given agriculture land use (ha) of the case study, for the different scenarios selected.

2.7 Impacts on Pedestrians produced by urban pluvial floods

As previously mentioned, although the focus of ICARIA is on tangible damage assessments, the intangible impacts of floods, as the impact on people's security of certain strong flood events are relevant for policy makers. It is known that "intangible losses" with an effect on human welfare are as important as the economic losses (UNFCCC, 2013).

2.7.1 Direct effects

2.7.1.1 Scope and objectives of the impact assessment

The impacts of pluvial floods in urban areas are not limited to damage and service disruption of critical infrastructure and services. A consensus exists on the fact that, during floodings, pedestrians are exposed to surface flows that can destabilise them (above certain thresholds) causing potential injuries and even, in extreme cases, fatalities. In fact, several authors indicate that most flood-related fatalities occur outdoors when people attempt to drive or walk in floodwaters (Kellar and Schmidlin 2012; Salvati et al. 2018; Fitzgerald et al. 2010). This reality can become especially critical in flash flood prone areas such as urban environments, where situations with low water depths and high velocity occur frequently (Abt et al., 1989; Martinez-Gomariz et al., 2016).

Hazard assessment

Several experimental campaigns carried out at the Technical University of Catalonia (UPC) have concluded that the hazard posed to pedestrians can be evaluated based on the product of water depth (y) and velocity (v) (see equation below). According to this criterion, it is possible to define threshold values that permit the classification of any depth and velocity combination in hazard levels (e.g. low, medium and high) (Russo et al., 2009; 2013 and Martinez-Gomariz et al., 2016), see Eq. 22.

$$\text{Hazard (m}^2\text{/s)} = \text{water velocity (m/s)} * \text{water depth (m)} \quad (\text{Eq. 22})$$

Project RESCCUE project did integrate a complex 1D/2D urban drainage model with this pedestrian hazard classification to carry risk assessment of floods for citizens (Evans et al., 2018). Crossing the results of the flooding models (expressed in terms of water height and velocity), it is possible to classify the hazard in every street and open space of the model domain.

Project ICARIA will follow the same methodology in its case studies to provide regional scale evaluations of this risk.

The flood hazard classification will be classified following the guidelines suggested in Martinez-Gomariz et al.,(2016). Figure 28 presents this classification graphically.

- Low hazard is below the product $(v \cdot y) = 0.16 \text{ m}^2/\text{s}$
- Medium hazard is compressed between $(v \cdot y) = 0.16 \text{ m}^2 \cdot \text{s}^{-1}$ and $0.22 \text{ m}^2/\text{s}$
- High hazard is beyond $(v \cdot y) = 0.22 \text{ m}^2/\text{s}$
- High hazard is assumed if water depth exceeds 0.15 m (regardless of the water velocity)
- High hazard is assumed if water velocity exceeds 1.88 m/s (regardless of the water depth)

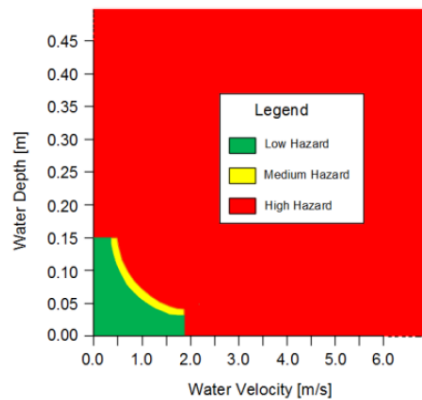


Figure 28. Hazard criterion proposed in project RESCCUE (Evans et al., 2018).

Exposure and Vulnerability assessment

As for the assessment of vulnerability to these events, project CORFU established a methodology that has been replicated in several other investigations. This methodology is based on information about the population census of the region's districts (e.g. total inhabitants, population density, age and number of foreign people). Based on this information, qualitative vulnerability indexes are given to each district based on the characteristics of their population as it is summarised in the table below. Parameter C accounts for the inherent vulnerability of inhabitants based on their age. Parameter F accounts for the fact that foreigners tend to travel more frequently, being more exposed to this risk. Parameter D reflects the exposure information, accounting for the fact that higher population densities imply a higher vulnerability (Evans et al., 2018). The combined exposure and vulnerability level of each district is determined based on the average value of these indexes.

Table 19. Thresholds to assess human vulnerability according to different criteria (Evans et al., 2018).

| Combined Exposure and Vulnerability index | Parameter C (% of inhabitants with age < 15 or > 65 years) | Parameter F (% of foreign people) | Parameter D (urban density) |
|---|---|--------------------------------------|--|
| 1 (low) | ≤ 33% | ≤ 33% | ≤ 10 houses/200m |
| 2 (medium) | 33% < X ≤ 50% | 33% < X ≤ 50% | 10 houses/200m < X ≤ average local density |
| 3 (high) | > 50% | > 50% | > average local density |

Table 20. Formulation to compute the total vulnerability level (Evans et al., 2018).

| Exposure and Vulnerability level | Criterion |
|----------------------------------|-----------|
|----------------------------------|-----------|

| | |
|--------|-----------------------|
| Low | $(D+C+F)/3 < 1.5$ |
| Medium | $1.5 < (D+C+F)/3 < 2$ |
| High | $(D+C+F)/3 > 2$ |

Risk assessment

Risk levels are quantified in a qualitative manner by significance levels such as “high”, “medium” and “low” resulting from the overlapping between the hazard and vulnerability maps. As mentioned in the previous paragraphs, both the hazard and vulnerability information are classified in “high”, “medium” and “low” levels too based on specific criteria. Scores of 1 to 3 are assigned accordingly. Based on this information, the risk value of each cell of the model domain is calculated as the product of the hazard and the vulnerability levels. Hence, risk values range from 1 to 9 where higher levels indicate higher risk (see Figure 24).

DRAFT

3 Drought Impact Assessment

As it is mentioned in Deliverable 2.1 of project ICARIA, in the scope of this project, drought will be assessed from the point of view of hydrological drought. In other words, the hazard assessment methodology is focused on quantifying the level of water availability in reservoirs for the regions of interest. To this end, rainfall and temperature patterns corresponding to different future climate projections will be used to forecast how water availability will evolve over the coming decades. The outputs of these models will allow us to estimate different tangible damages, presented in this section.

3.1 Impact on aggregated Economic sectors

Water is a critical element for the development of any economic activity and therefore a relevant productivity factor to consider. Many productivity activities could not be carried out without water, such agriculture, and most food & beverage industries. Under certain circumstances, water supply restrictions lead to diminished production, which in turn affects other activities through intersectoral relations in the economy (Freire, 2011).

The data sources are similar for both direct and indirect damages, thus they are presented in the following common section.

3.1.1 Input datasets used in the model

In the following table 22, input datasets required for the model are presented.

Table 22. Data requirements for the indirect tangible impact to all economic sectors of drought.

| Data requirements for the indirect tangible impact to all economic sectors of drought | | |
|---|---|--|
| Data group | Description | Source |
| Water consumption by sectors | Historic water demand/use by economic sector from network, own sources (wells) | Public Water Authorities, Statistics |
| Drought Special Action Plan | Water supply restrictions and allowances by economic sector established by the authorities to diminish water scarcity, with different drought scenarios | Relevant publications from public authorities |
| Economic data | Regionalized input-output tables; regional stock of net capital (capital), Employment datasets (labour) and value added datasets (aggregate production functions) | Economic Research Institutions; Public Statistics Agencies |

3.1.2 Direct effects - Estimation of Aggregate Production Function by Sector

The economic impact of drought has been widely studied, but mostly on the agricultural sector. This focus is appropriate for highly agricultural economic regions, it is of less relevance when assessing the potential impact of drought in economic regions that are less reliant on agriculture or which have a more

complex and diversified industrial structure (Freire, 2016). Due to the more frequent and persistent periods of water scarcity, in all types of economic structures, there is a need for a more general analytical framework that can assess impacts for all economic sectors and activities.

3.1.2.1 Scope and objectives of the impact assessment

Drought direct impact assessment on the economy aims to evaluate the sectoral impacts of water supply restrictions. This method follows the one described and applied by Freire (2011) in Catalonia that evaluated the economic impacts per sector of the water restrictions measures caused by the previous drought in the region during 2008.

The method proposes that direct economic losses originated from water restrictions over different economic activities can be estimated by calculating the elasticity of gross value added (GVA) by economic activity with respect to the water consumed (Freire-González, 2011; Freire-González et al., 2017; Jenkins et al., 2021). The methodology presented to quantify them is based on an input-output model, which is able to estimate the macroeconomic impact of water supply restrictions through the estimation of aggregate production functions that include water consumption by sectors.

There is a distinction between green water and blue water that determines the two main sources of direct economic impacts. On one hand, there is the green water, which is understood as the precipitation on land that does not run off or recharge the groundwater but is stored in the soil or temporarily stays on top of the soil or vegetation. Eventually, this part of precipitation evaporates or transpires through plants' (Freire, 2011). This type of water is mainly used by agricultural activities and therefore it is the sector that the lack of rainfall impacts the most. On the other hand, there is the blue water, which is the 'fresh surface and groundwater, in other words, the water in freshwater lakes, rivers and aquifers'. This is the main source of the water distribution network, being therefore linked to agriculture, manufacturing, energy, water suppliers, service sector and households. The first direct impacts are caused by reduction of green water. Blue water can potentially totally, or partially, offset the impacts of a drought if it is properly managed before, during and after a drought situation, therefore the economic impact of drought depends on the hydraulic capital, which sets the amount of blue water availability (Freire, 2016).

3.1.2.2 Impact assessment model setup

The method begins by collecting and analysing data on water supply restrictions by sector, ordered by Public Authorities during previous drought events, which allows synthetic modelling on specific sectoral restrictions.

Second, an econometric model developed by Freire-Gonzalez (2011) is carried out to estimate the effects of variations on water consumption by sector, included in the following Cobb-Douglas function:

$$Y_{it} = A_{it}^{\alpha} L_{it}^{\beta} W_{it}^{\gamma} \quad \text{[eq. 23]}$$

where Y_{it} is the total output of sector i in period t ; A represents the total factor productivity or the technological level of sector i in period t ; K_{it} is the stock of capital of sector i in period t ; L_{it} is the

employed population in sector i in period t ; W_{it} is the water consumption of sector i in period t ; α , β and γ are the output elasticities of capital, labour and water, respectively (Freire-Gonzalez, 2011).

Certain adjustments or aggregations of sectors may be required in order to obtain a correspondence among the available data of all the variables for all sectors. The sectors aggregated by Freire-Gonzalez are the following: Agriculture (AGR), Extractive industries (EXT), Manufacturing industries (MAN), Market services (MKT) and Non-Market services (NMKT), so the parameters of five models are simultaneously estimated.

Following, an estimation of an equations system with the number of specified models (5 in the reference taken) is performed, establishing common coefficients for the intercept and for the variables employed population and stock of capital. The estimation methodology is selected based on the robustness of the available econometric methods.

The estimated coefficients obtained from the econometric models transform variations of water supply into changes in the value added in a partial equilibrium context, described in the following section, that focuses on the indirect damages.

At this point, water restriction scenarios can be included to assess the direct impact per sector of the different water restrictions per level of emergency related to water scarcity and drought.

3.1.2.3 Expected outputs of the model

The model is expected to provide insights into the economic effects of water supply restrictions caused by drought in relevant economic sectors., given a particular production structure. It will serve to understand the restrictions and their impacts, and consequently, take better informed decisions. It is also the baseline to study the indirect impacts, which quantify the impact of water supply on macroeconomic indicators such as GDP, employment, and productivity in the following section. The findings will help inform policymakers and stakeholders in making decisions regarding water resource management and sustainable economic development.

3.1.3 Indirect effects - Macroeconomic Impact from the Leontief Supply Model

3.1.3.1 Scope and objectives of the impact assessment

From a macroeconomic perspective of general equilibrium, impacts of water supply restrictions can be assessed with the Input–output methodology. This methodology obtains the consequences of changing an exogenous variable over the productive structure of an economy (Freire, 2011).

The macroeconomic implications can be obtained by introducing the previously estimated values by sector in a general equilibrium model, such as the Input–output model. A general equilibrium perspective refers to the economic approach that examines the entire economy as a system of interrelated parts. It considers how various factors, such as supply and demand, prices, production, consumption, and resource allocation, interact with each other simultaneously.

Input-output models are commonly used to analyse the interdependencies between different sectors of the economy and assess the ripple effects of changes in water supply on various industries. These applied analysis models allow the simulation of policies and estimate their macroeconomic impact.

The simplifying assumptions proposed by Leontief's demand model, can provide the value added estimates per sector, thus allowing us to calculate the estimated loss of production and gross domestic product (GDP).

3.1.3.2 Impact assessment model setup

The model considers factors such as water scarcity, water management policies, and climate change projections to understand their impact on water supply and the economy. The model aims to simulate the impacts of policies, in terms of the relationship between water supply and macroeconomic indicators such as GDP, employment, and productivity. By considering these factors and using economic models, the model provides insights into the overall economic effects of water supply and quantifies its impact on macroeconomic indicators.

The first step is to obtain the estimate of the aggregate production function, in order to use as an input for the macroeconomic model, that provides the amount of water used by economic sectors on their aggregate production, which has been described in the previous section (direct damage).

The second step comprises the development of the input/output model, based on Leontief's demand model. The framework allows to empirically estimate the relations between economic sectors in a general equilibrium context based on input–output tables. In this case, the strategic variable, exogenously determined, is the value added, instead of the final demand. The present model takes analogous simplifying assumptions to the Leontief demand model:

1. Each sector produces a single product. This implies constant allocation coefficients (so there is no technical change) and no substitution between inputs. Allocation coefficients are the distributed amount of a good, expressed in monetary units, between the total production of a sector.
2. Consideration of the same number of supplier and consumer sectors. There should be a correspondence between the total number of products employed in production processes and the number of sectors that produce them.
3. The inputs of each sector are exclusively a function of the production level of that sector. That means that production functions are linear and homogeneous, so the inputs are proportional to the production level.
4. Exogeneity of values added. This assumption implies that values added of each sector are not explained within the model, but are considered as exogenous variables. A variation of this variable would lead to a change of total output, as a measure of economic impact.

Assuming a Walrasian general equilibrium context (Walras 1954), the total production of an individual sector j can be disaggregated as the sum of the productive inputs used in its production x_{ij} plus its added value:

Where x_i are the sectoral productions, d_{ij} are the allocation coefficients, g_i is the value added of each sector and t_{ri} are the net taxes on products of sector i . Finally:

$$x = g + t_r(l - D)^{-1} \quad \text{[eq. 31]}$$

Where the exogenous variables of the model are the VA and the net taxes on products.

Finally, the scenarios of synthetic restrictions on water supply to economic sectors are designed, based on the real special action plan developed by authorities for drought. They are applied to understand the indirect impacts on the territorial economy of the Case Study where the model will be applied.

3.1.3.3 Expected outputs of the model

Loss of production and variation of sectoral value added (VA) and Gross Domestic Product (GDP) as the sum of VAs in the Case Study regions are the main economic indicators we can obtain with the methodology.

Adapting slightly the methodology, there is also the possibility to obtain changes in indicators such as jobs, salaries, profits or taxes, depending on the I-O framework used.

3.2 Impact on the Water sector

3.2.1 Direct effect on supply side

3.2.1.1 Scope and objectives of the impact assessment

Assessing the risk associated with droughts is a complex matter (Hagenlocher et al., 2019). The definition of “drought conditions” is often defined by national or regional regulations that, based on the intrinsic characteristics of the regions, define threshold values to determine the severity of a drought situation. Usually, these thresholds are associated with drought management plans that determine and/or limit water resources management accordingly. Such regulations are diverse and present significant differences across regions. Hence, it is not reasonable to define a global threshold to assess the risk of hydrological drought for different case studies.

In ICARIA, it was suggested evaluating the risk associated with droughts based on the existing local regulations that determine the degree of risk based on volume or percentage (with respect to maximum reservoir capacity) of water resources availability. As an example, the following paragraphs presents the criteria that is applied to in the Barcelona Metropolitan Area (AMB). The same methodology could be applied to other locations if “drought risk assessment” criteria are adapted to the region of interest.

3.2.1.2 Impact assessment criteria

The figure below depicts the threshold values that are used to quantify the severity of an hydrological drought in the AMB based on the total volume of water stored in the water reservoirs. According to this, drought situations can be classified in levels of Alert, Excepcional and Emergency. These values are defined by the Catalan Water Agency (ACA), the governmental administration in charge of the management of water resources in Catalunya.

Such criteria is established in the “*Pla especial d’actuació en situació d’alerta i eventual sequera*” (Special management plan for alert situation and potential drought) developed by the ACA to improve

water management after the 2008 drought that affected this region. This plan involved a deep hydrological understanding of the catchments that contribute to the reservoirs, other water resources that also contribute to supplying this region and the average consumption of water per capita at different levels (households, industry, agriculture) in each season of the year (ACA 2019).

Importantly, this plan includes water use criteria that regulate the use of water for certain activities and the maximum daily water consumption per capita under each specific drought level.

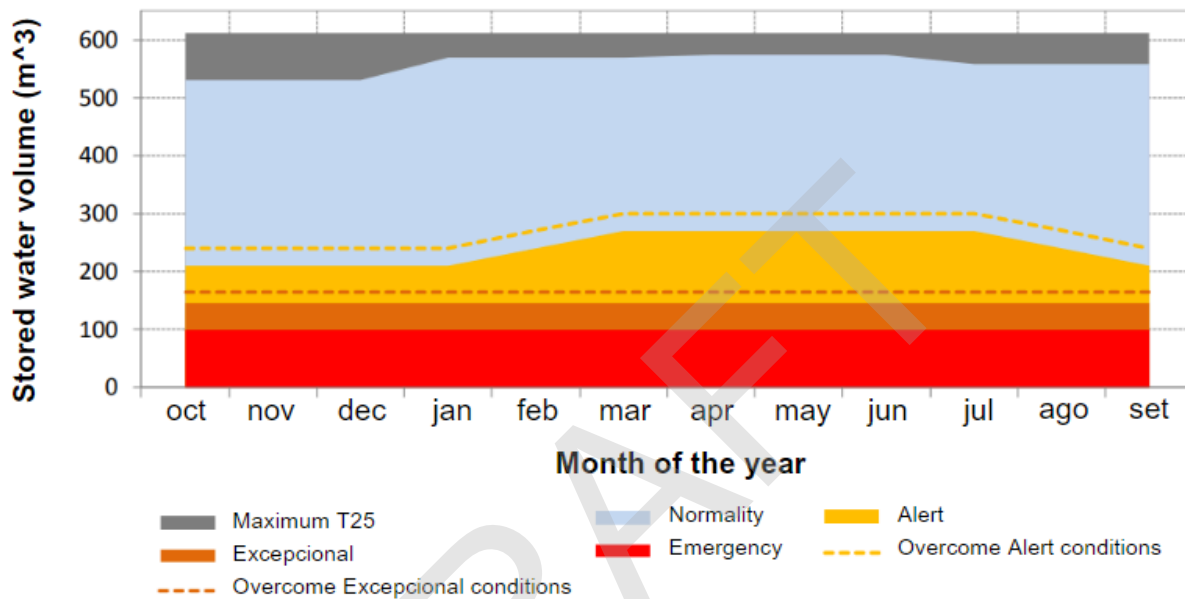


Figure 30. Criteria for assessing drought conditions in the surface water reservoirs of the AMB area. Source: ACA 2019.

The results of the hazard model will show the monthly total volume of water stored in the reservoirs upstream of the AMB for time series up to year 2100. This model will be run for several different climate change scenarios (based on the VI IPCC Report)

In order to evaluate the severity and frequency of future hydrologic drought events for different climate change scenarios, the results of the drought hazard model will be crossed with the criteria shown in the previous figure. This comparison will help to evaluate the number of events where drought conditions reach a certain degree of severity, for how long this situation lasts and how often does this occur. Based on this information, it will be possible to foresee periods of water restrictions for certain activities and even shortages of drinking water supply. Furthermore, this drought assessment criteria will help planners and researchers to evaluate how well different adaptation strategies help enhancing water resources management and reducing severity and duration of drought periods.

3.2.1.3 Expected outputs of the impact assessment methods

The figure below shows a graphical representation of the results that can be obtained with this approach. It shows a comparison between a projection of water storage in “Sau” and “Susqueda” reservoirs system, for the period between 1980 and 2100 according to the RCP 4.5 climate change projection projections

and compares it with the drought emergency levels defined by the administration for this specific reservoir.

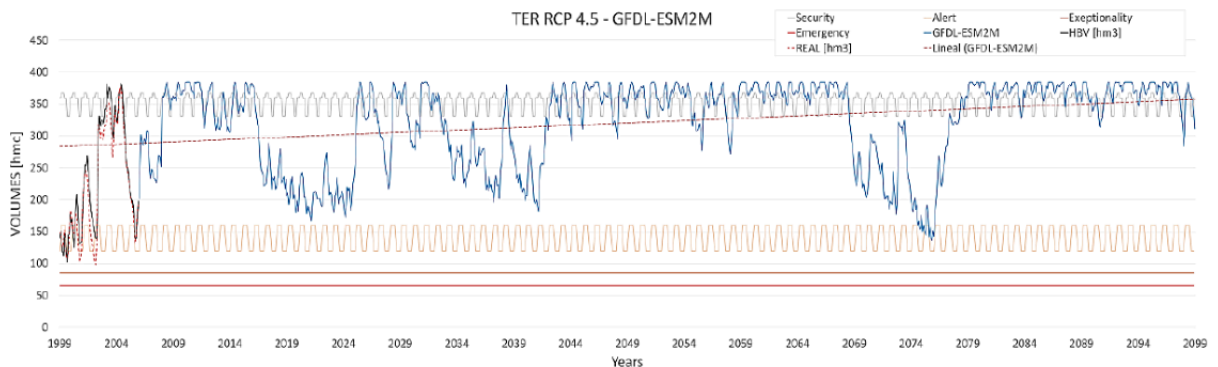


Figure 31. Results of drought impact assessment in Sau-Susqueda reservoir system developed in project RESCCUE or the RCP 4.5 climate change scenario (RESCCUE 2019).

3.2.1.4 Input datasets used in the model

The main data requirements to apply this impact assessment methodology can be summarised in two main groups. Firstly, a daily (or monthly) time series of stored water volume in surface water reservoirs. This information corresponds to the results of the drought hazard assessment model described in Deliverable 2.1 of project ICARIA. Secondly, an official criteria to assess the severity of drought situations in the area of study based on the total volume of stored water in its water reservoirs. This criteria is usually defined by governmental bodies or water resources management agencies.

3.2.2 Direct effect on demand side

3.2.2.1 Scope and objectives of the impact assessment

Water scarcity is a significant challenge in the xerothermic regions, such as the Mediterranean region, due to the limited availability of water resources and increasing demand for water due to population growth, tourism, urbanisation and agricultural development. In the Mediterranean region, according to CCP4 (Ali et al., 2022), the expected frequency and severity of droughts are projected to increase (severe emission scenarios). In addition to that, the overall trends in the hydrologic cycle indicate a decrease in river runoff, groundwater recharge and water availability in rivers and lakes (Spinoni et al., 2018). Climatic simulations for this region show that water scarcity in the studied region and the associated water quality decrease will be more profound in the future, based on RCP 4.5 and 8.5 scenarios (Rocha et al., 2020).

Within the scope of the ICARIA project, and specifically for the SAR region, rainwater harvesting effectiveness study will be carried out to assess the impact of climate change on the collected water by individual households. Rainwater harvesting is a technique used to collect and store rainwater for later use, especially in areas where water scarcity is a concern. The technique involves capturing rainwater from rooftops, roads and other surfaces, and storing it in tanks or underground reservoirs for later use.

3.2.2.2 Input datasets used in the model

High-resolution climate simulation precipitation datasets of 5 km horizontal resolution for the area of Greece were derived via the dynamical downscaling technique using the non-hydrostatic Weather Research and Forecasting model (WRF/ARW, v3.6.1)

Projected changes in drought severity and drought duration were estimated through the calculation of 12-month Standardized Precipitation Index (SPI).

Population Census and Touristic Arrivals will be also taken into account in the impact model.

3.2.2.3 Impact assessment model setup

Two water stress index approaches will be used:

- Falkenmark Water Stress Indicator (FWSI) (Falkenmark et al., 1989): This indicator considers only the available renewable water (rainfall not returned to the atmosphere via evaporation and evapotranspiration) per capita per year. FWSI defines a threshold of 1700 m³/p · year, below which the region is considered to experience water stress. As the water availability decreases further from this threshold, the negative effects become more severe. More specifically, water availability below 1000 m³/p · year is considered a limitation for economic development, while 500 m³/p · year is considered a life constraint.
- Basic Human Water Requirement (BHWR) (Gleick et al., 1996): This indicator defines the minimum requirement for daily water use per capita per day as 0.05 m³ (50 L/p · day) in order to cover the basic needs of each person corresponding to 18.25 m³/p · year. However, given the need of every individual, this minimum water requirement can reach up to 70 L/p · day, a total of 25.5 m³/p · year.

3.2.2.4 Expected outputs of the model

The effectiveness of RWH application is directly related to the population benefited and more specifically to the volume of water harvested per capita. Thus, the average harvested volume per capita per simulated period is calculated, presented and compared with historical data and the BHWR.

3.2.3 Indirect effect on WWTP

Drought episodes not only manifest important effects on the supply side of the water cycle but also manifest themselves in the sanitation part of the cycle. Drought events generate a reduction in the volume of rainwater and, above all, an increase in consecutive dry days (Mestre et al., 2013), being this the main climatic consequence of this hazard. Since the 1950s, human development has intensified extreme events of heat waves and drought, projecting a high probability increase in these episodes in the coming decades according to the sixth assessment report of IPCC (2023).

Drought events do not usually result in tangible direct damage to Wastewater Treatment Plants (WWTPs). Most damages are identified as indirect and are caused by a decrease in inflow and the associated concentration variations of the influent water volume. Usually, droughts are associated with water use restrictions on the supply side (Hughes et al., 2020 and Zouboulis et al., 2015). These restrictions generate variations in domestic flow, increasing the concentration of pollution due to reduced use for

low-polluting purposes (e.g. swimming pools, fountains or irrigation), effect demonstrated in two studies conducted in California by the Public Policy Institute of California (PPIC) during the 2012-2016 drought (Chappelle et al., 2019 and Tran et al., 2017). On the other hand, the reduction of rainwater volume, together with the reduction of infiltration and inflow from outside into pipes, also reduces water flow and contributes to maintaining elevated concentrations of domestic wastewater (Hughes et al., 2020).

3.2.3.1 Scope and objectives of the impact assessment

A transversal methodology is developed for the assessment of drought risks for any WWTP anywhere in the world, based on experimentation and information collected in the Barcelona study area and its treatment facilities. The model implementation will be carried out in the ICARIA Deliverable 4.2, related to the implementation of the damage assessment methodology presented here. Drought assessment in WWTP will be developed initially in Barcelona CS and will be replicable in other CS.

Within the current literature, there exist some qualitative studies on the vulnerability assessment of wastewater infrastructure to climate-related impacts such as drought episodes (Pocock et al., 2017; Hughes et al., 2020 and Spirandelli et al., 2018). These studies are characterised by a qualitative and general approach. More specifically, the effect of drought on the usual development of treatment processes in WWTPs has been studied in two projects on the California coast (USA). One of them carried out a survey of the different workplaces assessing the differences and treatment needs during drought years in the area (2012-2016) (Chappelle et al., 2019). The second project quantifies in general terms the extra cost of treatment in different drought scenarios compared to the usual unit cost in €/m³ of treated water (Tran et al., 2017).

This section focuses on the tangible impacts of long drought episodes and proposes a model for the economic quantification of indirect impacts (WWTP operative). The final objective of the proposed study is to develop a cost estimation model that relates the decrease in inflow to WWTPs to the increase in total costs of operation derived from the drought conditions. The following four stages are identified in the development of the model:

Table 23. Stages of the drought damage model.

| | |
|----------------|---|
| STAGE 1 | COLLECTION OF DROUGHT MEASUREMENTS AND DATA Drought indicators according to the water availability for the region are related to the inflows and concentrations data at the WWTP facilities. Different drought climate scenarios are indirectly evaluated in this section, as they modify the inflows reaching the treatment facility. |
| STAGE 2 | CREATION OF INFLOW-OPERATIVE COST CURVES Inflow-Operative Cost curves are one of the main internal development inputs required by the economic model. Two curves will be performed: the first one, relating the reduction in flow and the increase in concentrations with the increase in operative costs. The second, associating the flow reduction with sanctions for non-compliance with discharge regulations. |
| STAGE 3 | GENERATION OF THE DROUGHT DAMAGE MODEL In this phase, an internal process is conducted to develop the formulation of the relation between the decrease in flow rate and the associated total cost. At this stage, the curves developed in step 2, the extra costs associated with the cleaning and corrosion of pipes and equipment and the influence on the regeneration treatment (tertiary) are considered. |
| STAGE 4 | APPLICATION OF THE DROUGHT DAMAGE MODEL The final phase of the model is its application. Based on local data from the different case studies, the evaluation of total costs associated with the drought episode is developed. Results are presented |

for each WWTP and for all facilities in the study area. Different climate scenarios are reassessed based on the duration of the drought event as determined by the projections.

3.2.3.2 Input datasets used in the model

Inputs of the model are classified in two main categories: inputs related to the model application and information needed for model generation. The model can be contextualised for each study area or WWTP if all data used in the first application of the model by Aigües de Barcelona in the study of the Barcelona Metropolitan Area (AMB for its acronym in Catalan) are available. As a result, the Inflow-Operative Cost curves and the formulation of total costs can be locally contextualised. However, the model has been designed to be functional with only the data required in Stage 1. The model's basic inputs are those related to inflow records at the facilities (historical and future drought events projections) together with the location of the WWTPs. Additionally, inputs related to increased inflow concentrations and associated economic costs, such as penalties, chemical product and energy cost ratios, or expert information, are essential for the internal development of the model. Figure 32 illustrates this information.

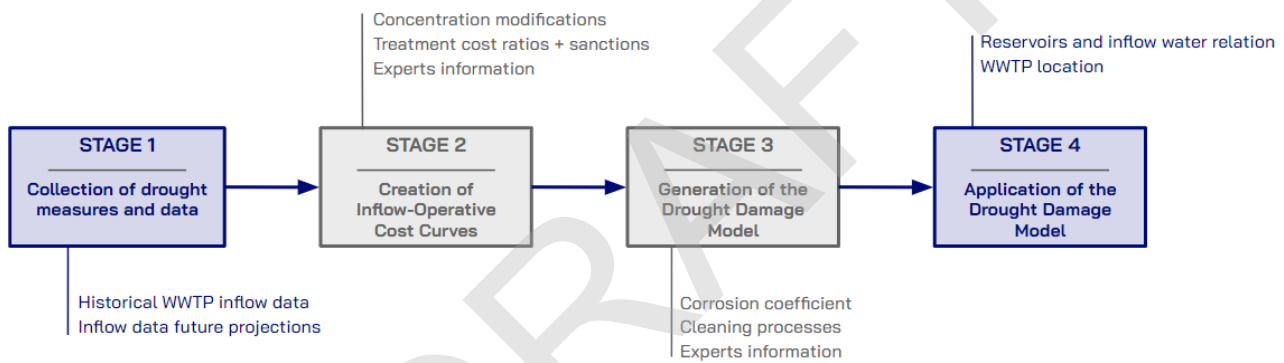


Figure 32. Organisation of the model's inputs in the different stages (in blue, essential; in grey, allow a better contextualisation to the local case).

To complete the stages 2 and 3 information, expert opinion will be obtained from interviews with the WWTP Plant Managers and other experts from WWTP local operator (Aigües de Barcelona in AMB CS) to understand the costs associated with pipe cleaning, treatment extra costs and corrosion episodes in case of higher inlet concentrations. Through the responses from the interviews in the AMB context, a proposal for the estimation of the economic indirect affectations will be presented. These data are required for internal model construction, but are not necessary for the application of the model in other case studies. Even so, local interviews are proposed as inputs to be carried out in each case (further transferability of the methodology to other places), different from the Barcelona case study, in order to use the most specific data possible. Finally, an extense review of regulations data and sanctions related with the discharge of insufficiently treated water must be conducted in each case study, as has been done assisted by the legal service of Aigües de Barcelona in this initial approach. Table 24 shows the inputs resume.

Table 24. Necessary input data for the economic drought damage evaluation model for WWTPs.

| Data requirements for the Drought Damage Model on WWTP | | |
|---|--|--|
| Data group | Description | Source |
| Water supply quantity historical data | Historical quantity data: flow input data to WWTPs in water flow (m ³ /s) historical evolution (monthly data). | Competent water management specific authority |
| Water supply quality historical data | Historical quality data: different concentration indicators (mg/L) historical evolution (monthly data). | Competent water management specific authority |
| Evolution of water volume in reservoirs | Drought projections carried out on the reservoirs in the case study area, to relate to the expected future values of inflows to WWTP. | ICARIA Task 2.1 results |
| WWTP locations and extents | 2D rendering (GIS support files) the WWTPs and effluent location for each of them. | Competent water management specific authority |
| Regulations and sanctions for discharges to effluents | Information on financial sanctions (indirect costs) for the discharge of treated water with high concentrations. Working in interval format (adapting to different countries and laws) | 91/271/EEC and implementing laws of the legislation in each case study |
| Experts information cost of extra treatment | Results of the interviews with WWTPs Plant Managers and other professionals. These allow the economic model to be defined and specified for each study case (extrapolation). | Local WWTP operator personnel On-site interviews |

3.2.3.3 Impact assessment model setup

The current project section aims to quantify economically the impacts of drought events on the usual performance of WWTPs following the first steps taken in two studies on the California coast during the 2012-2016 drought in that territory (Chappelle C. et al., 2019 and Tran Q. et al., 2017). In addition, the impact assessment pretends to follow the usual scheme **Risk (Impact) = Hazard x Exposure x Vulnerability** (see D1.1) used in studies on flooding in vehicles (Martínez-Gomariz et al., 2019), dams (Martínez-Gomariz et al., 2023), and linear infrastructures such as major roads (Douglass et al., 2014), adapting it to the drought hazard. The model is mainly based on the development of damage curves. In this case, the economic consequences of the hazard respond to increased operational costs, which are therefore indirect costs. In addition, other types of costs different from the treatment but associated with the drought episode are added for a full characterisation of the event. The feasibility of dealing with the

potential costs associated with penalties related to non-compliance with regulations on concentrations of discharges into the environment will be analysed.

Hazard assessment

Hazard assessment for the impact of drought on WWTPs is based on the analysis of the reduction in inflow into the facility in relation to the usual average monthly flow in times of usual climate (episodes without drought). Thus, the input of the model is the percentage reduction (%) of the flow (Q/Q_{max}), where Q (m^3/day) is the monthly average flow for the study month and Q_{max} (m^3/day) is the maximum possible treated flow in each WWTP. In addition, the thresholds that determine the start of the drought event will be defined from the beginning of the cost increases associated with the reduction of inflows (not necessarily equal to the drought thresholds adopted based on water availability).

Following the evolution of the presented methodology in the previous subsection, it is intended to relate the WWTP inflow reduction with a concentration increment of several pollution indicators in the first stage. Monthly historical data is available. The main objective in this section is to obtain a function by correlating both measurements. The results will be presented and argued. Figure 33 represents the concept of the expected relationship between a generic inflow concentration and the inflow reduction associated with a drought event.

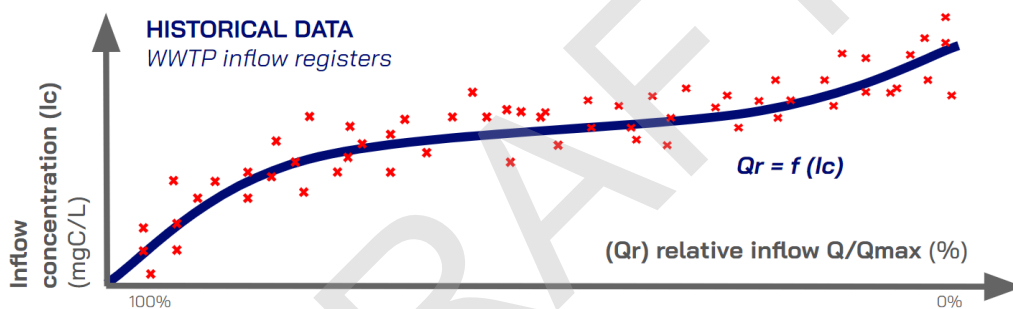


Figure 33. Exemplification of expected data relationship between inflow concentration and inflow reduction (monthly data).

Exposure and vulnerability assessment

Exposure of WWTPs to drought episodes manifests itself from the reduction of inflow and is the same for all facilities when the climate impact takes place. In other words, exposure is maximum when a drought event appears in a specific region.

Regarding vulnerability assessment, damage curves methodology proceeds in a similar way to Velasco et al., (2013), where this kind of curves were developed for a flood model that analysed flood events in the Raval neighbourhood (Barcelona). Other examples related to floods where similar methodologies are used are the assessment of urban flood resilience of the RESCCUE project (Russo et al., 2020 and Martínez-Gomariz et al., 2020), where depth (m) / damage ($€/m^2$) curves for properties were proposed. In these previous cases, the considered driver of the flood hazard is the flood depth (m). In the case of the current study, the driver of the drought for WWTPs is the decrease in inflow with respect to the maximum treatable flow in each WWTP (inflow %).

Inflow - operative cost curves development is the main objective in Stage 2. As it has been explained, the main curve to be developed is based on the increase in operative costs during water treatment at the facility. The formulation is based on increases in required chemicals and energy costs to produce one cubic metre of treated water when the inflow is reduced ($Δ€/m^3 - Q/Q_{max}$). Inflow-Operative Cost curves

related to extra treatment cost ($I-OCC_{Et}$) in the AMB trial case study are defined based on historical information obtained from a report conducted by the financial department of Aigües de Barcelona. To apply the methodology in other areas, the Barcelona curves can be applied or new localised curves can be generated, following the steps that will be presented in Deliverable 4.2 on the application of the methodology.

Regarding the economic sanctions associated with possible discharges with concentrations above the required thresholds as a consequence of an increase in the concentration of the initial inflow, it is also pretended to develop an extra cost curve (CC_{SAN}) ($\Delta\text{€}/\text{m}^3 - Q/Q_{max}$) based on existing regulations. These curves will be developed with the support of the legal department of Aigües de Barcelona for the AMB trial. This additional information will be analysed and the incorporation of costs into the general formulation will be assessed. This curve is associated with the Do Nothing Scenario (Business as Usual, BAU), although it is not presented as a feasible scenario because the company always ensures proper wastewater treatment. Both expected Inflow-Operative Cost curves are exemplified in Figure 34.

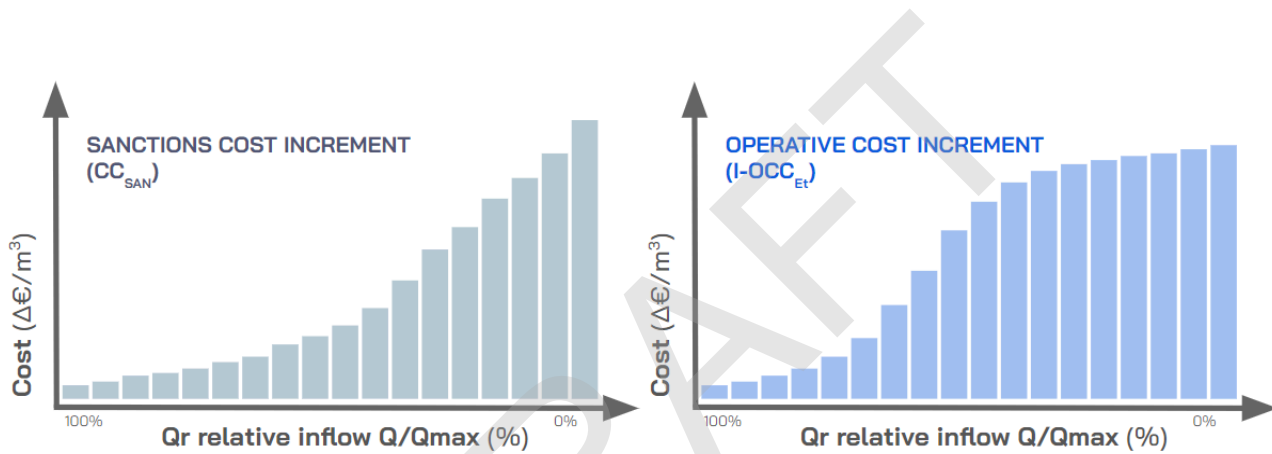


Figure 34. Exemplification of expected cost curves relating sanctions cost or extra treatment with inflow reduction (%) in each WWTP.

Impact assessment

Third stage of the model is associated with the impact assessment and the development of the general internal formulation, where data from the Inflow-Operative Cost curves are overlapped and other costs associated with drought episodes are added. There are detected and referenced two extra inputs that add costs derived from the drought episode, such as the increase in the frequency of pipe cleaning activities (White et al., 2017 and Hughes et al., 2020) and the possible modifications or changes of process equipment as a consequence of increased corrosion (long term direct impact) (Zouboulis et al., 2015 and Chappelle et al., 2019). A cost assessment formulation is proposed. The final cost of each drought episode affectation is performed as follows:

$$C_{TOT} = C_p(q_e) + C_c(Sc, q_e) + C_{CU}(q_e) \quad \text{being} \quad C_{CU} = CC_{SAN} + I-OCC_{Et} \quad \text{where} \quad q_e = f(Sc)$$

where C_{TOT} (€/month) is the total extra cost related to the drought episode, C_p (€/month) is the cost associated to the pressure water pipe cleaning processes, C_c (€/month) is a coefficient added in case of corrosion existence due to elevated concentration, q_e is an input variable related to the inflow reduction in each WWTP and C_{CU} (€/month) is the the curves cost. C_{CU} is calculated based on the cost curves defined in Stage 2. On one hand, the curve is associated with sanctions and regulations (Do Nothing

scenario) (CC_{SAN}) and on the other hand, the Inflow-Operative Cost Curve ($I-OCC_{Et}$) is associated with the extra operating costs. The model will be validated with historical data from local drought events records.

Finally, the application of the model is developed in stage 4. Different climate scenarios are associated with reductions in water volumes in the reservoirs. The state of the reservoirs in the study area is directly related to the reduction of inflows to the WWTPs. The climate scenarios modify the drought periods and thus the costs calculated in stage 3. Figure 35 shows a data flow diagram representing the performance of the entire drought model.

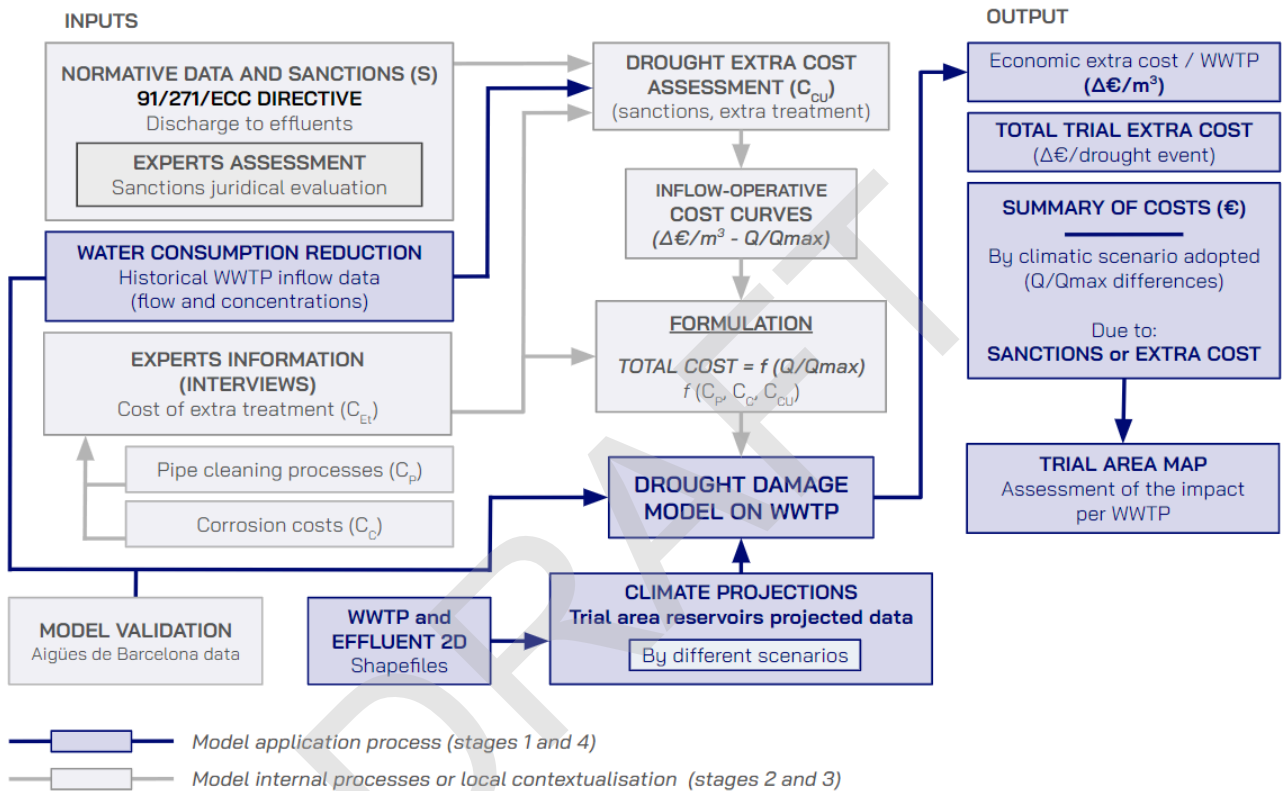


Figure 35. Data flow diagram representation of the Drought Damage Model (own elaboration).

3.2.3.4 Expected outputs of the model

Expected outputs for the model are a summary of the economic losses per WWTP and per water volume treated ($\Delta\text{€}/\text{m}^3$). With this result, and integrating it for the whole time of the drought event, an analysis of the total cost (€) of the drought episode in a given WWTP or in the whole study area is obtained. A generic illustration of the expected result of the temporal study is shown in Figure 36.

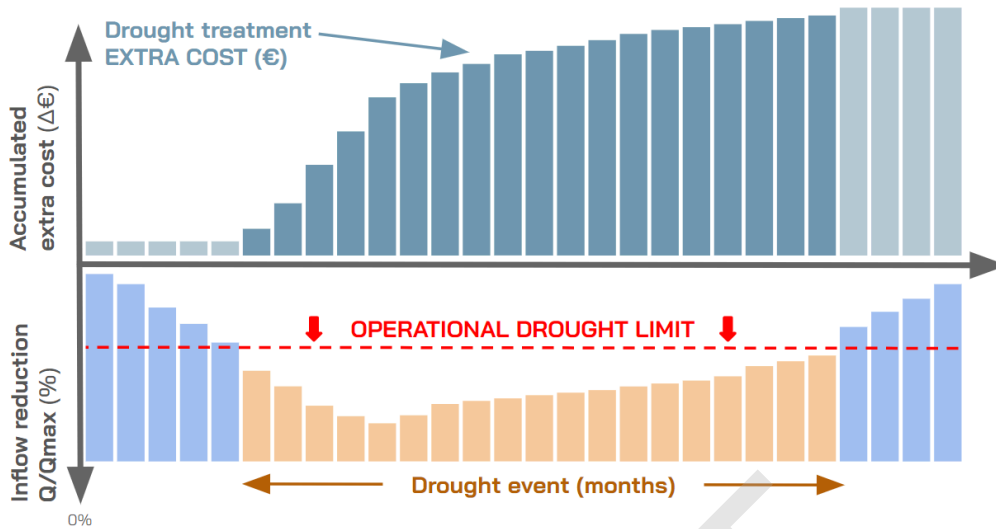


Figure 36. Generic exemplification of the expected result of accumulated extra cost during an drought event related with the WWTP inflow reduction.

A comparison between the results of the different climate scenarios will be presented in the summary of costs. In addition, the costs associated with the sanction curves (CC_{SAN}) are evaluated in the context of the scenario in which extra treatments are not carried out (i.e. do nothing scenario). Different climate scenarios with the same casuistry will be evaluated in the same procedure. As a general summary of the effects of drought in the study area, a global mapping of the WWTPs will be developed with visual information of their vulnerability to drought events.

Finally, an assessment of the cost of the feasibility of regeneration in WWTPs with tertiary treatment is added. There are maximum concentrations and salinity values in the outflow of the biological (secondary) treatment that do not allow water regeneration and therefore invalidate the operability of the tertiary treatment plants. For each WWTP, the volume of untreated water is related to the consecutive time of interrupted treatment. Then, by relating the cubic metre price of regenerated water ($€/m^3$) to the time of service interruption, the lost revenue due to non-treatment is shown, as is presented in Figure 37.

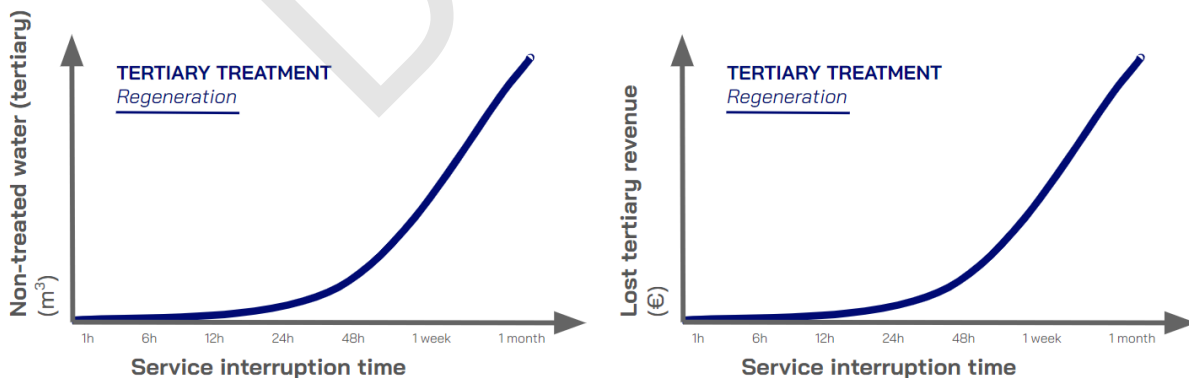


Figure 37. Tertiary treatment lost revenues in drought time assessment representation in €/time.

3.2.4 Cascading effect on electricity sector

3.2.4.1 Scope and objectives of the impact assessment

Severe drought also impacts the electrical sector, although not in terms of direct damages to the power system elements that may cause a decrease in the efficiency of the system, as seen in the impacts generated due to floods. Instead, there exists an inversely proportional relationship with the capacity for hydroelectric renewable energy generation, (Van Vliet M, T. *et al.*,2016). In other words, the more severe the drought in the studied territory, the less capable it becomes of generating hydroelectric energy. While this relationship may appear straightforward, it becomes challenging to find reliable models that quantify the actual impact of droughts on the electrical sector due to various external factors beyond technical aspects that can influence the real impact of drought, for instance, the water management policies specific to the territory.

Hence, the ICARIA project proposes to adopt the methodology put forth in the study by Naumann *et al.* (2015), aiming to quantify the impact caused by potential droughts in various European countries, including Spain, Austria and Greece. The methodology measures the amount of hydroelectric energy reduced due to such an event.

3.2.4.2 Input datasets used in the model

Table 25. Input datasets used in the model.

| Data requirements for the electricity sector damage model | | |
|---|---|--|
| Data group | Description | Source |
| Hydroelectric production | Hydroelectricity production data for each country or region. | World Bank database |
| Historic climate data | Meteorological drought indicators such as SPI or SPEI from historical records for accumulation periods. | EU/National/Regional meteorological agencies Meteorological databases (e.g. Copernicus) |
| Futures climate projection | Meteorological drought indicators such as SPI or SPEI projections for accumulation periods. | Results Task 1.2 |

3.2.4.3 Impact assessment model setup

In order to quantify the overall impact of the drought event, the model is based on the equations from the study by Hergarten (2004), where risk (R) is defined for any general disruptive event as the probability of the event occurring over time (N) multiplied by the average damage (D) it may cause. Therefore, we could define risk with the following equation (Eq. 32):

$$Risk = N \cdot D \quad (Eq. 32)$$

Eq. 32 should be adapted to represent all possible event sizes, their frequency of occurrence, and the damage corresponding to the event size. When considering all potential events, the variable N can be expressed through its cumulative probability density function (PDF), denoted as $p(s)$, where s denotes the severity of drought. In this context, the magnitude of s can be defined in various ways, such as absolute or relative drought severity, the extent of the area affected by a drought of a specific severity, or by a bivariate PDF considering both aspects, see Eq. 33.

$$p(s) = - \frac{p(s)}{ds} \quad (Eq. 33)$$

Following with $D(s)$ the expected damage. The expected overall damage is then given by Eq. 34:

$$\bar{D} = \int p(s) \cdot D(s) ds \quad (Eq. 34)$$

Taking into account the previous equations, the overall drought risk can be ascertained through Eq. 35:

$$R = N \cdot \bar{D} = N \cdot \int p(s) \cdot D(s) ds \quad (Eq. 35)$$

A simple power law dependence Eq. 36 is used to propose a connection between the drought severity and the damage it could cause, which for this study is the change in the quantity of hydroelectric energy generation.

$$D(s) = \alpha \cdot s^\beta \quad (Eq. 36)$$

Table 26 exposes the different types of relations they can have by changing the value of β . With a β equal to the unity, the relationship between the drought severity and the reduction of the hydroelectric energy in the is linear. The exponent can be smaller than the unity, given a limited growth relation, and greater than it if the relation is stronger than a linear relationship.

Table 26. β exponent values and type of relation.

| Exponent β | Type of relation |
|------------------|---------------------------------------|
| $\beta = 1$ | Linear relation |
| $\beta < 1$ | Limited growth relation |
| $\beta > 1$ | Power-law growth relation |
| $\beta = 0$ | No relation |
| $\beta \ll 0$ | Possible positive effects of droughts |

3.2.4.4 Expected outputs of the model

The direct output of the model is the reduction of the country's hydropower produced due to water scarcity. Of the three regions studied in the ICARIA project, only the Salzburg region has hydropower

plants. In this specific one, the impact of the reduction in power produced in the country could be disaggregated and indicate how much energy the region would no longer be capable of generating. Nevertheless, this result would not be satisfactory as it could not be applied in the AMB region or in the South Aegean region.

Thus, the final result focuses on the electric energy consumed by the population in each region and what percentage of it is hydroelectric. Therefore, the output is how much hydropower consumed from the region is reduced due to the drop in production from the entire country.

In order to calculate the cost of the hydropower generation reduction impact, it will be computed by the relationship between the drop in hydroelectric generation and the rise of the price of each region from historical data and look for how much this loss of generation is translated as a cost.

DRAFT

4 Heat waves impact assessment

4.1 Impacts on people

Following the same reasoning as for floods, intangible damages caused by heat waves were found relevant enough by policy makers and stakeholders to be included in ICARIA's scope. Therefore, this section shows a methodology proposed to be applied to relevant CS.

4.1.1 Direct effects

4.1.1.1 Scope and objectives of the impact assessment

Heat-related disease

Heatwaves can have serious and potentially life-threatening impacts on human health (Anderson and Bell, 2009; Basu and Samet, 2002; Campbell *et al.*, 2018; Hajat and Kosatky, 2010), with specific events noted as public health disasters such as in Chicago during July 1995 and in France during August 2003 (Krau, 2013; Chambers, 2020).

Merely attaining an elevated body temperature is insufficient for categorising the nature of heat-related predicaments. A comprehensive determination involves an amalgamation of associated symptoms and signs. Typically, these predicaments manifest under conditions characterised by:

- Elevated ambient temperatures
- Heightened relative humidity
- Physical exertion

Heatwaves or instances of anomalous thermal conditions manifest diverse impacts across individuals (Chambers 2020), with those considered vulnerable or belonging to specific societal sectors exhibiting heightened susceptibility. Broadly, risk factors can be categorised as follows:

- **Corporeal risk factors:** These include age over 70 years, obesity, cardiovascular disease, and other health conditions that may increase an individual's vulnerability to heat-related issues (Gasparrini *et al.*, 2015b; Campbell *et al.*, 2018; Guo *et al.*, 2017; Li *et al.*, 2015; Oudin Åström *et al.*, 2011).
- **Environmental factors:** Conditions such as the absence of trees, elevated humidity levels, prolonged and intense exposure to sunlight and other environmental factors contribute to the risk of heat-related health issues (Basu and Samet 2002; Watts *et al.*, 2018).
- **Specific living or working conditions:** Certain circumstances, such as social isolation, engaging in intense sports activities, undertaking heavy physical work and other lifestyle or occupational factors can amplify an individual's susceptibility to the adverse effects of heatwaves (Buscail *et al.*, 2012).

Depending on the factors mentioned above and the level of temperature increase, a spectrum of causes for heat-related hospitalizations emerges, encompassing conditions from low-impact heat-stress diseases to high-impact heat-stress diseases. High temperatures can cause heat stroke, heat exhaustion, heat syncope, and heat cramps, with heat stroke being particularly associated with sedentary elderly people (Kilbourne 1997).

Hospitalisation costs and Mortality rate increase during heat wave

The methodologies employed by the Heat Wave Local Effect model (HWLEM), developed within the framework of the H2020 CLARITY project (Zuccaro and Leone, 2021) are specifically tailored to evaluate the economic ramifications of heat waves on human health based on the effect of urban microclimate factors. Key output of the model include the assessment of hazard conditions in urban areas (assessed through the Tmrt - Mean Radiant Temperature and UTCI - Universal Thermal Climate Index indicators with a resolution of 5-250m, see D2.1), and the quantification of impacts in terms of mortality rate increase and hospitalisation costs (including both direct costs beared by the public health systems and indirect economic impacts related to the diminishing productivity due to the compromise of individuals' health).

As there is no European database for cost categories and parameters/indicators applicable to economic models, an analytical approach has been adopted. The damages thresholds are highlighted in Table 26.

Drawing from the most pertinent literature on hospitalisation costs related to heatwaves (N. i. England, 2020; Merrill et al., 2005), it is possible to correlate the type of treatment and related costs for each damage level (Table 35). The average hospitalisation stay following a heatwave is estimated to be 3.2 days. Approximately 80% of individuals hospitalised due to heat waves enter the hospital through the emergency department. Based on hospital reports from New York between 1991-2004 (Liss et al., 2017), the duration of hospital stay in days can be estimated, contingent upon the severity of the illness, as indicated in Table 27.

Table 27. Damage typologies for the six levels of damage and the corresponding level of medical care and time of hospital stay.

| Level of Damage | | Damage Typology | Level of medical care | Avg. hospital stay (days) |
|-----------------|-----------------|---|--|---------------------------|
| D0 | No Damage | - | Not needed | 0 |
| D1 | Caution | Fatigue, Possible discomfort | Few visits to doctors, generally no hospitalisation needed | 0,5 |
| D2 | Extreme caution | Sunstroke, heat cramps, heat exhaustion possible | Hospitalisation needed | 4,5 |
| D3 | Danger | Sunstroke, heat cramps, heat exhaustion likely, heatstroke possible | Hospitalisation needed | 7 |
| D4 | Extreme danger | Sunstroke and heat stroke highly likely | Hospitalisation needed | 10,5 |
| D5 | Critical danger | Death | - | - |

The duration of hospitalisation can have significant geographical variability among individuals affected by a heatwave, as evidenced by findings from a comprehensive analysis of a substantial hospitalisation database focused on heatwave-related cases (Liss *et al.*, 2017). The empirical observation indicates that the average daily cost of hospitalisation for the treatment of heat-related illnesses amounts to approximately 1,000 USD, based on a study conducted in the United States in 2004. This monetary equivalent corresponds to around 900 EUR at the prevailing exchange rate of USD/€ as of January 2023.

It is pertinent to note that due to a lack of specifically focused literature at EU level, further refinement of this figure depends on the availability of specific data at national/sub-national level. In the absence of specific European data, for all delineated damage classes (D1-D4) enumerated in Table 27, the standardised average cost per day of hospitalisation is stipulated at €900.

4.1.1.2 Input datasets used in the model

The table 28 below summarises the data needs of the heat wave impact model.

Table 28. Data required (model inputs) for the heat wave impact model.

| Data required or the heat wave impact model | | |
|---|--|--|
| Data Group | Description | Source |
| Historic climate data | Historic datasets of heat climate data | EU/National/Regional meteorological agencies Meteorological databases |
| Future climate projections | Projections of local climate data downscaled according to climate change scenarios | Results Task 1.2 |
| | Future IDF curves considering different change scenarios and time horizons | |
| Land use and terrain information | Building information (dimensions, roof material) | National/Regional/Local geography agencies; Copernicus |
| | Trees information (dimensions, species, foliage colour) | |
| | Digital Elevation Model and land cover data (crops/vegetation type, paving material) | |
| Exposure information | Distribution (number) of the population | EU/national statistics agencies |
| Vulnerability information | Composition (group of age) of the population | EU/national statistics agencies |
| Human Health Intervention Costs | Injured People (Number of person suffering during/after a Heat wave event) | EU/national statistics agencies; Literature review |
| | Average days of hospitalisation for each damage level | |

| | | |
|---|---|---|
| | Average cost per hospitalisation stay | |
| Value of statistical life of the deceased | Number of human lives lost | EU/national statistics agencies; Literature review (Table 28) |
| | Average cost of a human life | |
| Decrease in local value added due to hospitalisation effects (losses in productivity) | Number of persons hospitalised | EU/national statistics agencies; Literature review |
| | Average hourly GDP product by each worker in the specific country | |
| | Average rate of unemployment | |
| | Average hour per each work day | |
| | Average days of hospitalisation stay | |

4.1.1.3 Impact assessment model setup

HWLEM tools are specifically crafted to simulate impact assessments arising from various reference events, enabling a meticulous quantification of anticipated damage on selected elements at risk, contingent upon the availability of exposure and vulnerability data.

Once the hazard has been identified with sufficient resolution, the data pertaining to exposure and vulnerability are utilised to assess the anticipated impact of extreme heat and/or precipitation events in the HWLEM framework. The risk or impact assessment in HWLEM follows the conventional approach initially outlined in the field of risk science and decision theory (UNDRO, 1980; UN DHA, 1993; Coburn et al., 1994).

This approach conceptualises risk as a product, employing probabilistic convolution, of hazard (H), exposure (E), and vulnerability (V), as per the established relationship expressed as

$$Risk(Impact) = H \times E \times V \text{ (Eq. 37)}$$

In the context of heat waves, the main element at risk is the population and the expected impacts are related to perceived discomfort leading to various levels of illness and increased mortality. Levels of perceived discomfort are assessed using the UTCI indicator, which reflects levels of perceived heat stress in urban outdoor spaces and can be associated with a thermal discomfort scale related to the thresholds shown in Table 29.

Table 29. Damage scale correlating thermal discomfort as a function of the Universal Thermal Climate Index (UTCI).

| Damage scale related to thermal discomfort | | |
|--|---|---------------------|
| Damage Classes | Description | UTCI [°C] threshold |
| D0 | No Damage | < 32 |
| D1 | Caution level (modest thermal stress). | 32-38 |
| D2 | Caution level (moderate heat stress). | 38-42 |
| D3 | Damage (high thermal stress) | 42-46 |
| D4 | Extreme damage (extreme thermal stress) | > 46 |

Vulnerability classes are age-calibrated, focusing on the most vulnerable population groups, namely children under 15 and individuals over 65. Three classes (under 14, 15-64 and over 65) are defined, spatially distributed in each grid cell and ranked according to the probability of damage in relation to hazard thresholds. The use of vulnerability curves related to age groups depends on the availability of exposure data, i.e., the geolocation of the population in cities according to age groups (Zuccaro and Leone, 2021). Exposure concerns the number of people in the analysis cell with reference to the classes mentioned before.

Mortality rate increase

The assessment of mortality rate increase during heat waves is based on the following factors:

- Vulnerability functions (VF)
- Computation of the mortality proportion attributable to heat waves (AP)
- Computation of deaths (PD)
- Computation of heat waves days (HW_days)
- Generation of spatial distribution of deaths
- Generation of spatial distribution of deaths due to heat wave

Vulnerability curves for mortality rate increase developed in the context of the CLARITY project are based on the understanding of intrinsic adaptation to high temperature (with respect to physiological human thresholds) due to living in specific geographical areas in Europe, as suggested by Baccini *et al.*, 2008. These functions carefully consider variations between populations in Mediterranean and continental Europe, focusing specifically on discrepancies in temperature levels that result in conditions that lead to heat stress (Goler, 2020).

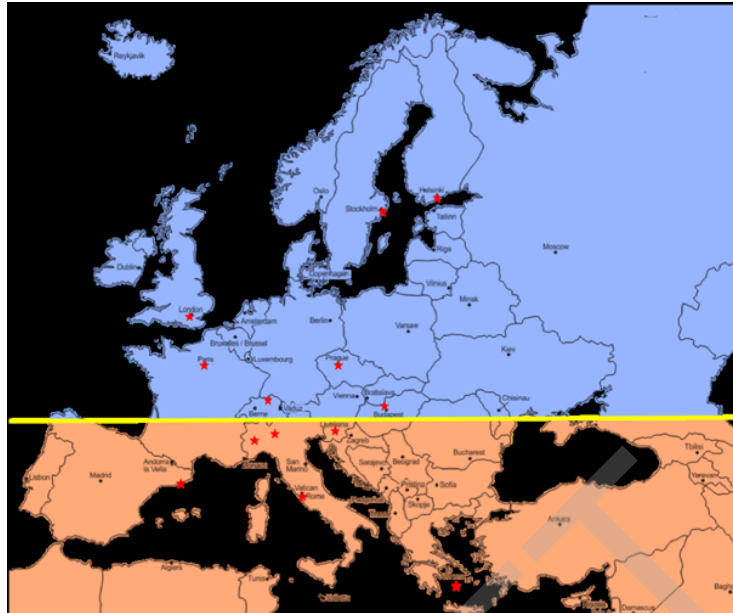


Figure 38. Identified European areas.

The expected increase in mortality in relation to the intensity of heat waves was evaluated in collaboration with the Department of Epidemiology of the Regional Health Service of ASL Roma 1, using data calibration from the relevant scientific literature (D'Ippoliti *et al.*, 2010). Percent change in natural mortality is linked to the value of apparent temperature, understood as the temperature equivalent perceived by humans, caused by the combined effects of air temperature, relative humidity and wind speed. Baccini *et al.*, 2008 reported the values used to generate the vulnerability functions.

South Europe

$$VF = 0.099 * e^{0.1246*x} \quad (Eq. 38)$$

North Europe

$$VF = 0.0087 * e^{0.2345*x} \quad (Eq. 39)$$

The percentage of mortality attributable to heat waves (AP) can be calculated using the formula given in Rothman, Greenland, & Associate, (2014)

$$AP = \frac{(VF\%/100 + 1) - 1}{VF\%/100 + 1} \quad (Eq. 40)$$

where *VF%* are the values of the vulnerability functions (variation of mortality attributable to heat wave). Predicted Deaths (*PD*) are calculated by extracting the historical number of deaths for the reference city. This data is retrieved from the open datasets of national or European statistical institutes (Eurostat).

Days of duration of the single heat wave are then computed based on the studies carried out within the CLARITY project. These data were calculated by combining urban climate simulations with long-term climate information from monitoring stations or regional climate projections from the EURO-CORDEX initiative (Goler, 2019). New CMIP6 projections are expected to further refine this key data input.

Then the spatial distribution of deaths is made using the following formula:

$$Deaths_i = PD * \frac{Pop_i}{\sum_i Pop_i} \quad (Eq. 41)$$

On the spatial unit (polygons in which the population is distributed), $\sum_i Pop_i$ should be calculated as the sum of the population of each polygon included in the study area. Dividing the deaths by summer days gives the estimated average daily mortality for each spatial unit, while multiplying the estimated average daily mortality for each spatial unit by heat wave days gives the number of average deaths (*MD*) observed on heat wave days.

$$MD = HW_{days} * \frac{Deaths_i}{summer_{days}} \quad (Eq. 42)$$

The obtained data are then distributed over the selected spatial unit.

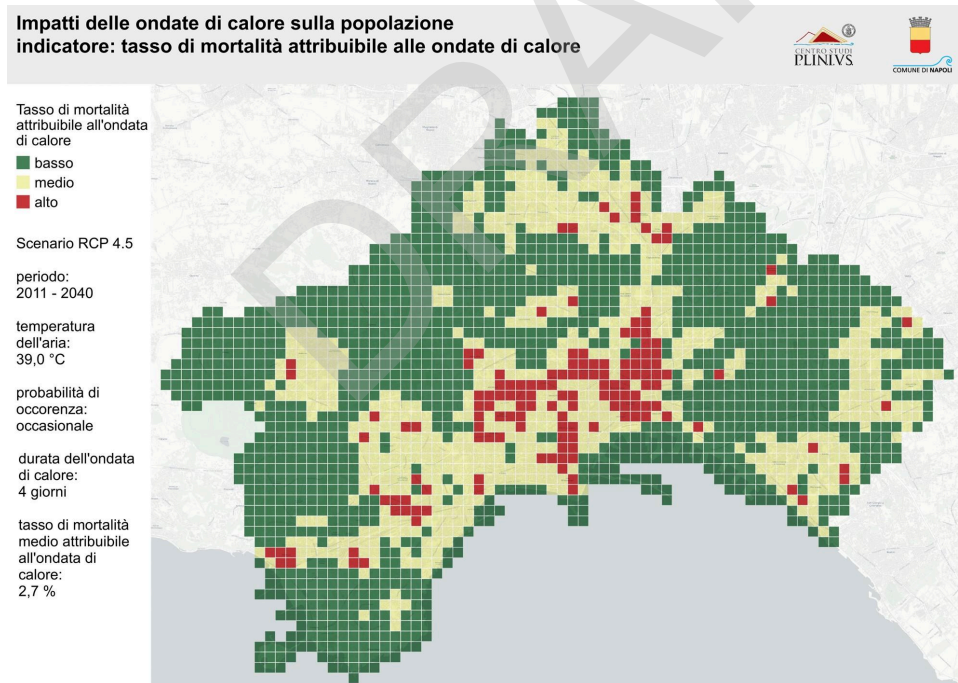


Figure 39. Spatialization of the impacts of heat waves with reference to mortality. Impact is referred to RCP4.5 current period occasional frequency.

Hospitalisation costs

The second impact that HWLEM is able to calculate is related to hospitalisation costs from morbidity attributable to heat waves. They include direct costs related to healthcare and indirect costs related to decreased local added value (lost productivity and loss of life).

Direct costs of health care is calculated by the following formula:

$$Heat\ Stress\ Direct = \%INJ_{person} * avgSTAY_d * avgSTAY_{cost} \quad (Eq. 43)$$

$\%INJ_{person}$ (percentage of injured person) and $avgSTAY_d$ (Days of average stay in hospital) are established based on the injury thresholds related to UTCI as shown in Table 30.

Table 30. Damage scale correlating thermal discomfort as a function of the Universal Thermal Climate Index (UTCI).

| UTCI threshold | $\%INJ_{person}$ | $avgSTAY_d$ |
|----------------|------------------|-------------|
| 1 | 0,00000 | 0,00 |
| 2 | 0,00003 | 0,50 |
| 3 | 0,00005 | 4,50 |
| 4 | 0,00010 | 7,00 |
| 5 | 0,00015 | 10,50 |

Average cost per hospitalisation stay ($avgSTAY_{cost}$) has been stable instead at 900€ as described in the previous paragraph.

Indirect costs related to the decrease in local added value are based on the following equation:

$$Heat\ Stress\ Indirect = (avgSTAY_d * LAB_{day_h}) * hPROD_c * nPERSON_c * (1 - UNEMP_c) * USDxchRATE \quad (Eq. 44)$$

Hospital occupancy days are again determined based on the UTCI thresholds in Table 31. The Hourly Average Daily Workforce is assumed to be 6 hours (LAB_{day_h}). The remaining parameters have been obtained from OECD data ([unemployment-rate](#); GDP-per-hour-worked). Since this global data is provided in USD dollars, we convert to euros at the discounted exchange rate ($USDxchRATE$).

The computation of indirect costs, beyond those associated with lost productivity resulting from fatalities, is executed by multiplying the statistical mean value of a human life (VSL_c) by the number of individuals exposed to the adverse effects, denoted as $Deaths_i$:

$$Mortality\ Indirect = VLS_c * Deaths_i \quad (Eq. 45)$$

In the equation 35 the statistical value of human life assigned to VLS_c is presumed to be €1.600.000 as per the determination by ISTAT (Italian Statistical Institute). The amount of fatalities due to heat waves ($Deaths_t$) emanates from the preceding mortality calculation.

4.1.1.4 Expected outputs of the model

The outputs of the model, encompassing direct and indirect hospitalisation costs as well as mortality attributed to the heat wave, can be presented through two primary formats:

- Spatial Maps:** Utilising Geographic Information System (GIS) tools allows the geographical representation of the data, enabling a visual representation of the impacts across different geographical locations within the analysed region. This approach provides a detailed and spatially explicit depiction of the distribution of hospitalisation costs and mortality associated with the heat wave. However, it is crucial to acknowledge that the map-based approach may have limitations and could be misleading. This methodology operates on the assumption that the population remains consistently exposed in the same location, neglecting the reality that people move within and outside the city. Additionally, it does not account for the potential influence of human behaviours, such as using air conditioning, which can significantly impact heat exposure and its health-related effects.

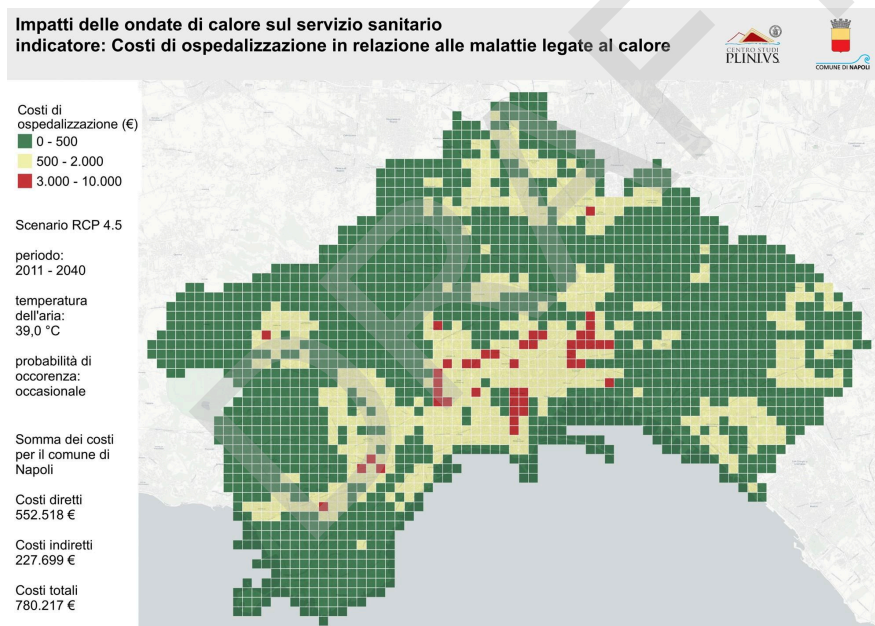


Figure 40. Graphical representation of the impacts of heat waves with reference to hospitalizations costs. Impact is referred to rcp scenario 4.5 current period occasional frequency.

- Aggregate Data:** Alternatively, the results can be presented in the form of aggregate data that consolidates the impacts for the entire region under consideration. This approach simplifies the information into summarised figures, offering an overall perspective of the direct and indirect costs and mortality burden across the entire analysed area and among is reducing the margin of error inherent in spatial maps

The choice between these presentation methods depends on the specific needs of the analysis and the preferences of the audience or stakeholders involved. Spatial maps are valuable for visualising spatial patterns, while aggregate data provides a more consolidated and high-level overview.

4.2 Impacts on the Electricity sector

4.2.1 Direct impact

4.2.1.1 Scope and objectives of the impact assessment

With the current climate change scenario and recognizing the increasing frequency and severity of heat waves at the local level, numerous studies like Eom et al. (2012) have sought to explore the relationship between the rising demands for electrical energy consumption to address prolonged periods of high temperatures. Generally, the energy demand for cooling increases as the ambient temperature deviates from a reference temperature.

Moreover, heatwaves are periods of abnormally hot weather that last enough to stress the power grid system not only because of the increase in the energy demand, but also can affect the electrical distribution, transmission and power generation. High temperatures during the heatwave make the majority of electrical elements lose their maximum capacity in working operation. So, by putting all the pieces together, it is possible to obtain a system that claims more energy to satisfy the demand, but at the same time, it has more losses due to the temperature, which can unbalance the system and lead to blackouts, as it is represented on the diagram of Figure 41.

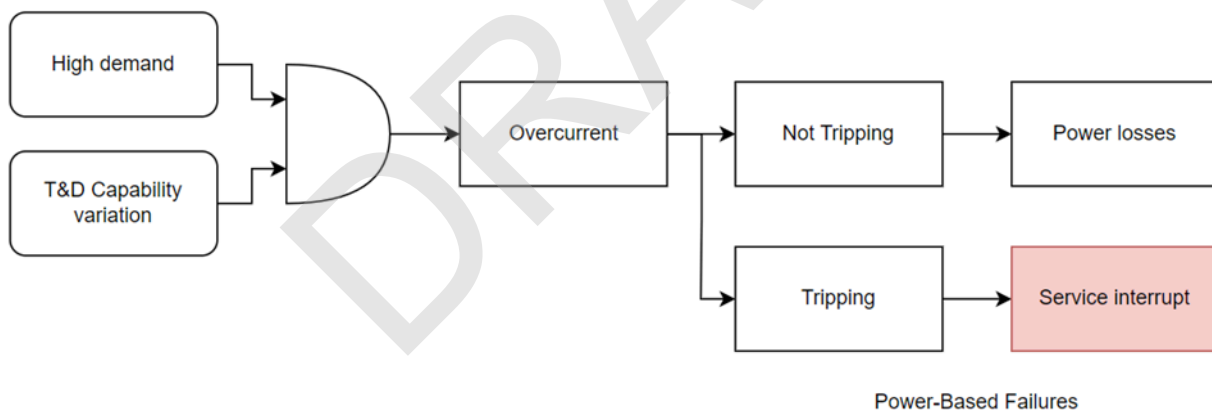


Figure 41. Flowchart for the electricity sector impact assessment model.

Power-based failures occur when the capacity of a circuit is inadequate to meet demand. Such failures may result from insufficient generation, an overcurrent condition in a transmission line, or an overcurrent situation in a substation.

4.2.1.2 Input datasets used in the model

Table 31. Data requirements for the electricity sector damage model.

| Data requirements for the electricity sector damage model | | |
|---|---|---|
| Data group | Description | Source |
| Futures climate projection | Climatic map with the temperatures of the heat waves' future scenarios. | Previous task |
| Power grid map | Power grid geolocation map of the elements that compounds it with their electrical data related to them | ENTSO-E OpenStreetMap Energy supply company (ENDESA for AMB CS) |

4.2.1.3 Impact assessment model setup

Demand

According to Allen et. al. (2016), the demand side of the power system changes due to two parameters during a heat wave event: the temperature and the latitude where the consumption is. Both values are manageable for each region of the ICARIA project, which is one reason to follow this study to quantify how much the demand would be affected in each territory. The equation that defines it, is the following one:

$$J = (5.33 - 0.067 \cdot L_{centroid}) \cdot \Delta T_F \quad (Eq. 36)$$

In the formula, J represents the percentage increase in electricity demand, $L_{Centroid}$ denotes the latitude in decimal degrees at the territory's centroid, and ΔT stands for the change in maximum annual temperature in degrees Fahrenheit since the study was conducted in the United States. Thus, to transform the formula to be used in Celsius degrees the next step is done:

$$\begin{aligned} J &= (5.33 - 0.067 \cdot L_{centroid}) \cdot (T_{F2} - T_{F1}) \\ &= (5.33 - 0.067 \cdot L_{centroid}) \cdot ((T_{C2} \cdot 1.8 + 32) - (T_{C1} \cdot 1.8 + 32)) \quad (Eq. 37) \end{aligned}$$

Eliminating the values of 32 and taking out the common factor of 1.8 by multiplying them in the element where the latitude is, the equation will be as follows:

$$J = (9.594 - 0.1206 \cdot L_{Centroid}) \cdot \Delta T_C \quad (Eq. 38)$$

The total demand of the territory (D) is the calculation of the average customer demand (D_{avg}) multiplied by the total number of customers (N) in it, and considering the percent increase of the demand due to the temperature rise and the latitude of the territory (J).

$$D = D_{av} \cdot N \cdot \left(1 + \frac{I}{100}\right) \quad (Eq. 39)$$

With this procedure explained above, the model calculates for each substation of the territory their increase in demand by knowing the temperature difference due to the heatwave and its latitude with its location. With the increment of the energy needed for each point multiplied by the total consumers supplied by each substation, we obtain the increase of the total demand of the whole territory.

Overhead lines

Aerial power lines are susceptible to heat that influences their capacity to transport energy from one point to another. The surface temperature of the conductor is determined by the ambient temperature and the current flow through it, part of which is converted into heat due to the Joule effect. In the study outlined by IEEE 738-1993, a first-order differential equation was proposed by taking into account the conductor's resistance and the heat gained from solar irradiance, as well as that dissipated through convection and radiation.

Choobineh et al. (2016) approximated this equation for aluminium conductors steel reinforced (ACSR), which are most commonly used in overhead lines, and derived Eq. 40. It represents how the power of the line decreases from 25°C upwards. It was subsequently employed in other studies, such as Choobineh et al. (2016). It considered a uniform temperature for the entire network's case study. However, for ICARIA, a specific temperature will be adopted for each line, aligning with the climatic map of each case of study.

$$\Delta P_{b,T}^{Line,max} = -0.768 \cdot T_t^a + 119.45 \quad (Eq. 40)$$

The adverse scenario of a heatwave reduces the line's capacity, and simultaneously, considering the growth in electricity demand in the system, it can lead some lines to operate above their nominal load capacity. When subjected to an increase in electrical current, these lines may experience failures. Lee et al. (2018) and Bhatt et al. (2009) presented a fragility curve that relates how loaded the line is operating and the probability of that line failing; Figure 42 displays the results.

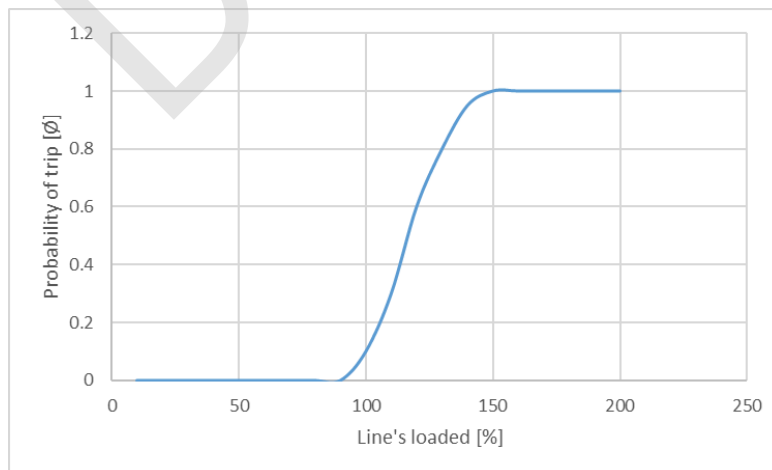


Figure 42. Fragility curve of how likely the line is to fail as a function of the load it supports.

Substations

Electric substations are not exempt from the impacts generated during a heatwave. In the literature, the maximum capacity of transformers has been considered and quantified as it decreases with increasing ambient temperature. For the ICARIA project, the results of Hashmi et al. (2008), are taken as a reference. This study has the advantage of providing the relationship between ambient temperature and capacity for two different types of transformers: power transformers and distribution transformers. Since the territories under study in ICARIA are extensive enough to have both kinds installed in the electrical network, the report yields two expressions (Eq. 41 and Eq. 42) that relate their respective behaviours as a function of temperature, which Figure 44 plots and determines that the distribution transformers are more susceptible to the higher temperatures than the power transformers.

$$\Delta P_T^{t.power} = -0.0098 \cdot T_t^a + 1.1961 \quad (\text{Eq. 41})$$

$$\Delta P_T^{t.dist} = -0.01 \cdot T_t^a + 1.2003 \quad (\text{Eq. 42})$$

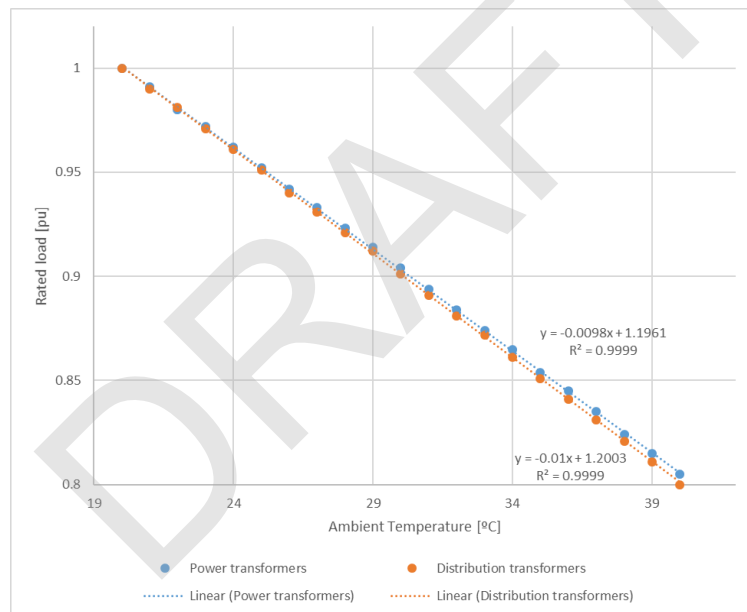


Figure 43. How the rated load (pu) is affected by ambient temperature (°C) for power and distribution transformers.

4.2.1.4 Expected outputs of the model

Recalling Figure 42 from section 4.2.1.3., the model outputs will encompass, on the one hand, the quantification of energy losses attributable to high temperatures. Additionally, the model identifies and locates the most susceptible points in the electrical network to fail due to electrical overcurrent, and how likely they are to trip. In this case, the total energy not supplied is quantified for the branches of the lines that go out of service.

When there is an interruption in the service there are also direct economic losses. For this matter, in order to calculate the costs due to service disruption, it is proposed to follow the same procedure

explained in section 2.4.1.4. in the output of the model to assess the risk on the electricity sectors on a flood risk event to quantify the monetary costs, which are the following ones:

1. **Damages over electrical assets:** The direct cost of failed components within the system, accounting for the required labour for replacement installation.
2. **Non-supplied electricity:** The cost associated with energy losses during the entire peril event.

4.2.2 Indirect impact

The indirect damages caused to the electricity sector due to heat waves are estimated through a model that values the economic costs due to the income lost due to service disruption and the additional costs caused by the emergency measures that have to be taken during the disruption events to provide electricity to the basic services.

4.2.2.1 Scope and objectives of the impact assessment

There are not only direct economic losses in the disruption of an electric service. To calculate those that are indirect, we recover the equations of section 2.4, where it is possible to differentiate the following impacts:

1. **Businesses earning losses provoked by the shortage:** The cost incurred due to the inability to meet the total energy demand.
2. **Expenditures associated with the renting of emergency electrical supply appliances:** Additionally, considering the network connections where significant project assets are located, an assessment is made to determine their vulnerability in the event of a system incident and the potential ramifications of a disruption in their electrical supply.

Another impact of heatwaves is the reduction in solar energy generation, which indirectly may necessitate an increase in non-renewable energy generation to compensate for its decrease.

4.2.2.2 Input datasets used in the model

Table 32. Data requirements for the electricity sector damage model.

| Data requirements for the electricity sector damage model | | |
|---|---|---|
| Data group | Description | Source |
| Futures climate projection | Climatic map with the temperatures of the heat waves' future scenarios. | Previous task |
| Power grid map | Power grid geolocation map of the elements that compounds it with their electrical data related to them | ENTSO-E OpenStreetMap Energy supply company (ENDESA for AMB CS) |
| PV panels map | Map of photovoltaic generating stations in the area under study and their nominal power ratings | OpenStreetMap Risk owners |

4.2.2.3 Impact assessment model setup

Evans and Florschuetz (1975) provided the linear expression for how the efficiency of a solar module or cell varies with ambient temperature, as shown in the following equation:

$$\eta_c = \eta_{ref} \cdot [1 - \beta_{ref} \cdot (T_c - T_{ref})] \quad [\text{eq. 43}].$$

Where T_{ref} , η_{ref} , and β_{ref} are typically provided by the manufacturer. However, the paper of Dubey et al., (2013) complemented a table from other sources with the values commonly adopted. Based on data in the table for $T_{ref}=25$, average $\eta_{ref}=0.12$ and average $\beta_{ref}=0.0045^\circ\text{C}$.

4.2.2.4 Expected outputs of the model

The result of the reduction in solar energy for the region would be the sum total of this. Additionally, knowing the increase in demand for the area proposed in the previous section on direct impacts, it is possible to determine how much energy from non-renewable sources is required to meet the demand, considering the reduced capacity of solar panels and their associated cost.

4.2.3 Cascading effects on the water sector

4.2.3.1 Scope and objectives of the impact assessment

The water sector can be impacted by failures in the electricity sector due to power failures in major water sector assets (Chen et al., 2019). Also water purifying and cleaning could be rendered inoperable and thus out of service. The available water supply volumes could be reduced, water pressure level not according to operating standards and customers can stay without water. Inoperable pumps at a drinking water utility can make firefighting activities difficult and cause local health care facilities. Pressure loss can allow contaminants to enter the drinking water distribution system from surrounding soil and groundwater.

*This work has been provided by DMKT without explicit participation in Task 3.1.

4.2.3.2 Input datasets used in the model

Water assets interconnected to the electricity network (Poudineh et al., 2017). Simulation of the electricity network and identification of power outages, especially on water related nodes and locations of water network assets (Zuloaga et al., 2020).

Identified dependencies of the Water Distribution Systems on the electricity networks : electricity for pumping throughout the water system from the source to the treatment facilities to the distribution system

4.2.3.3 Impact assessment model setup

- Receive electrical energy input from the electrical system.
- Perform water network simulation. to determine the actual demand pattern and pump operation that can be met with the available electrical energy input.
- Examine different solutions to assess if the water demand pattern can be satisfied during the limited electrical energy input.

4.2.3.4 Expected outputs of the model

The average annual amount of water customers not served and water utility loss of profits.

5 Forest fire impact assessment

The content of this section has been provided by DMKT without explicit participation in Task 3.1.

5.1 Impacts on Water sector

5.1.1 Direct impacts

5.1.1.1 Scope and objectives of the impact assessment

Wildfires increase susceptibility of watersheds to flooding and erosion and can have both short- and long-term impacts on water supplies, such as increased treatment costs, need for alternative supplies, and diminished reservoir capacity (Rey et al., 2023). High-intensity rainfall events in steep, burned watersheds are likely to move large amounts of suspended and dissolved material into downstream water supplies. Additionally, assets (e.g. distribution pipes and pumps) of the water system physical network may be exposed to direct impacts from the wildfires, such as melting of water pipes and taint water with chemicals, rendering water unsafe to drink (Wibbenmeyer et al., 2023, Meadows, 2022).

5.1.1.2 Input datasets used in the model

Table 33. Data requirements for the water sector damage model.

| Data requirements for the electricity sector damage model | | |
|---|--|----------------------|
| Data group | Description | Source |
| Wild fire simulation | Wild fire spreading simulations, burned areas. Fire induced heat flux (W/m ²), FIREAREA [0/1] value that indicates burned area | Previous task |
| Water network asset | Water network locations, and description of asset attributes | Water supply company |

5.1.1.3 Impact assessment model setup

The wildfire simulations from the WRF-FIRE will be used to make an assessment indicating the burned area. Following this analysis and considering the geolocation of the water assets, an intersection of burned areas with water network assets. Essentially, following this approach a binary damage function for the water assets is implemented deriving the water network assets that are damaged and non-operable. Following this assessment, the user should perform a water network assessment to identify service levels with assets out of service.

5.1.1.4 Expected outputs of the model

The cost of a power outage is the difference between normal operating conditions and the situation where an outage occurs. For businesses, this difference is often equal to the lost profits caused by the blackout (Reichl et al., 2013). The number of customers not served should be determined from the assessment of the water network simulation, considering the topology of the network and the water assets attributes.

From the solution of the water network simulation the number of not served customers can be determined and subsequently the associated cost, considering the downtime and potential damages to the water pipelines in the private houses.

5.2 Impacts on electricity sector

5.2.1 Direct effects

5.2.1.1 Scope and objectives of the impact assessment

In the case of Electricity Infrastructure, the damages are distinguished according to their influence on the asset. The main impacts on the electricity network are the melted / burned electricity network assets, although their capacity to withstand wildfire impacts depends a) on the wildfire thermal energy and b) the structural properties of the materials of the asset..

Table 34. Forest fires impact on electricity infrastructures and associated threshold by Sfetsos et al 2021.

| Forest fires impact on electricity infrastructures | | |
|--|---|---|
| | Asset | Impact Threshold |
| Electricity | Distribution lines Extra-High Voltage (EHV) transmission lines | Structural threshold: Temperature = 500–600 °C |
| | Distribution substations Transformer Electrical grid operation | Functional threshold: Temperature = 420 °C (melting point of zinc) |
| | Functional threshold: PM2.5 concentration is > 350 µg/m ³ | Functional threshold: PM2.5 concentration is > 350 µg/m ³ |
| | Step up/down substations | Same threshold values as described in EHV transmission lines. |
| | Wooden pylon | Flame temperature (>650 °C) |

5.2.1.2 Input datasets used in the model

Table 35. Data requirements for the electricity sector damage model.

| Data requirements for the electricity sector damage model | | |
|---|--|-----------------------|
| Data group | Description | Source |
| Wild fire simulation | Wild fire spreading simulations, burned areas. Fire induced heat flux (W/m ²), FIREAREA [0/1] value that indicates burned area | Previous task |
| Electricity network asset | Electricity network locations, and description of asset attributes | Energy supply company |

Wildfire spreading model and burned areas

Electricity network placement and asset attributes

5.2.1.3 Impact assessment model setup

The wildfire simulations from the WRF-FIRE will be used to assess the assets of the electricity network exposed to the wildfire and the burned area. Following this analysis and considering the location of the electricity assets, an intersection between them is performed to identify the assets that need further assessment. Depending on the characteristics of the wildfire and the asset structural elements the equations of Fig 44 and 45 can be implemented to identify if the assets are completely melted, become inoperable or could function as normal. Following this assessment, the user should perform a simulation of the electricity network to identify service levels with assets out of service

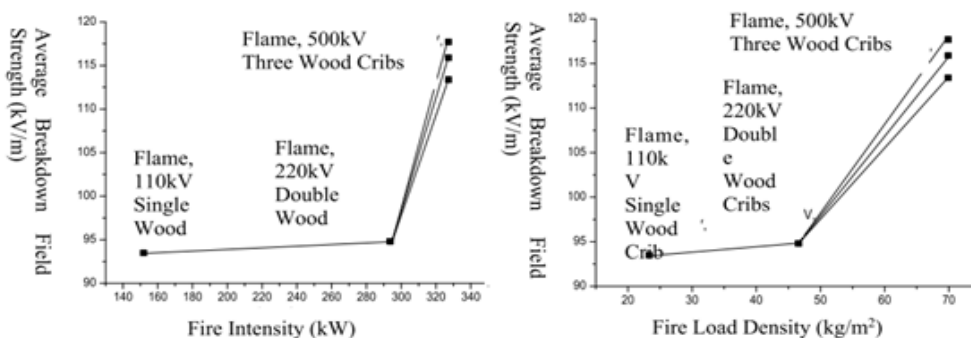


Figure 44. The effect of fire intensity and fire load density on breakdown voltage and distance in fire (You et al., 2013).

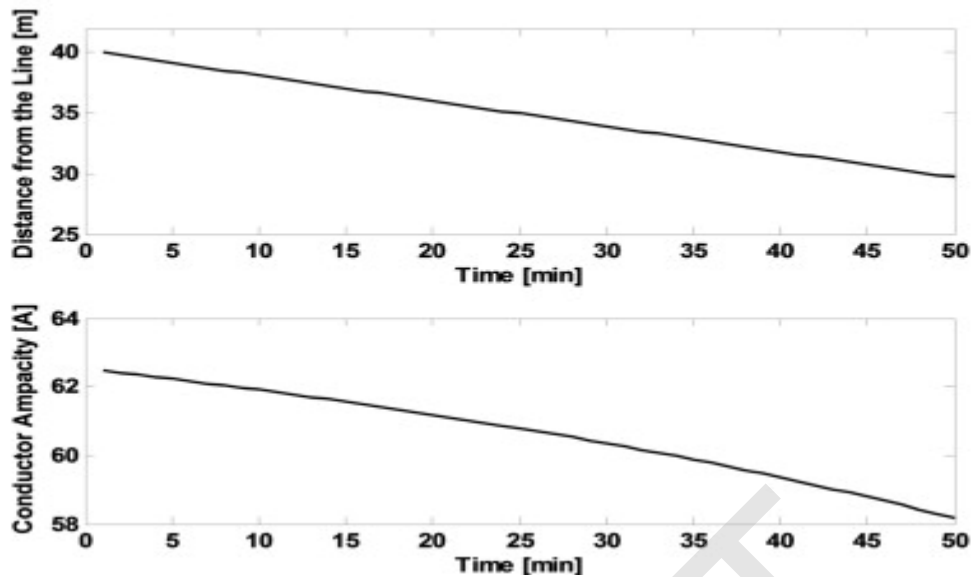


Figure 45. Variations in the conductor's ampacity as fire approaches the line (Choobineh et al., 2015).

5.2.1.4 Expected outputs of the model

This assessment needs to provide an assessment of the network operation considering the assets that are burned and thus out of service and identify the number of customers not served. The cost of a power outage is the difference between normal operating conditions and the situation where an outage occurs. For businesses, this difference is often equal to the lost profits caused by the blackout. Outage costs for all customer types depend on the following five factors:

1. **Perspective:** who/what experiences the loss of power.
2. **Timing:** when the outage occurs.
3. **Magnitude:** how much load is lost and overall impact.
4. **Duration:** how long the outage lasts.
5. **Advanced warning:** whether the outage is anticipated or unexpected.

A replacement cost should also be included in the analysis which is a direct sum of the burned area.

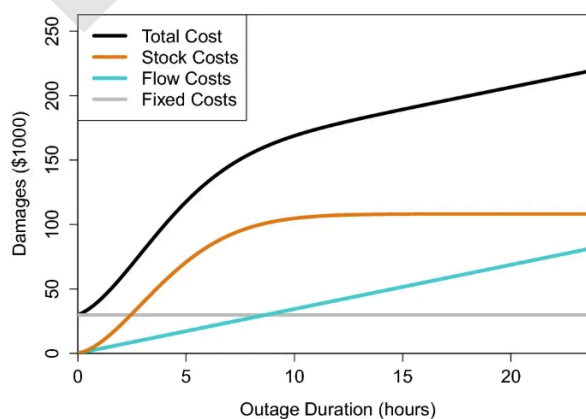


Figure 46. Total damages due to power outages.

6 Extreme winds impact assessment

This section shows the proposed methodologies to assess the damages caused by extreme winds in properties and the electricity sector. The potential impact to the rest of critical sectors have been evaluated and considered not relevant to be included in the study.

6.1 Impacts on properties

6.1.1 Direct effects

Severe wind storms directly affect properties through damages by detaching single parts (e.g. roofs) or by fallen trees or other debris. The impact of a storm event depends on the (maximum) wind velocity, the building characteristics and its surroundings.

6.1.2 Scope and objectives of the impact assessment

The objective is the assessment of expected economic damages to properties, relative to the (maximum) velocity of the wind storm events and their return periods with case study specific damage curves.

Thus, the hazard data (wind velocity), exposure (geographic area) and vulnerability (building specifics, surroundings) are needed to be linked with economic damages. A possibility to assess the direct damage is by applying vulnerability curves.

The damage due to wind storms can be assessed by using historical insurance data, a method also applied by Koks *et al.* (2020) who defined global damage curves based on previous estimates of construction costs, open street map (OSM) data etc. The open-source impact assessment model CLIMADA combines vulnerability curves (based on specific building types) with hazard data - in the case of extreme wind, wind gust data is applied.

6.1.3 Input datasets used in the model

Datasets needed within the impact assessment model chosen (CLIMADA) are:

- Hazard classes: units, intensity, frequency of each class
- Exposure classes: describing the assets, properties, people etc. exposed to a specific hazard, its value and impact function_id, allowing the definition of different hazards to the same asset
- Impact functions: relate different hazards and their intensity to impact on specific assets

Within CLIMADA, impact functions related to different hazard types have been pre-defined: e.g. tropical cyclones, winter storms, flooding, drought and crop yield. If data is available for specific regions, impact functions can be defined by the users.

Additionally, adaptation measures can be defined that alter the hazard and impact classes.

6.1.4 Impact assessment model setup

The impact model to be applied is the CLIMADA CB model (Fields *et al.*,2014).

6.1.5 Expected outputs of the model

Based on past events, location and characteristics of assets and hazard data, expected damage can be quantified. It is computed for:

- Each hazard event summarised over the whole domain
- Expected annual impact for each locations, summed over all events and weighted by frequency
- total annual average aggregated impact value (summed over events and locations)

6.2 Impacts on Electricity sector

6.2.1 Direct impacts

The electricity sector is impacted in different ways by extreme winds, on the one hand the supply can be impacted and on the other hand the network, for instance cables are damaged by fallen trees and therefore disrupting the electricity network. Regarding the energy supply, wind turbines as well as hydro power plants are affected.

6.2.2 Scope and objectives of the impact assessment

Extreme wind events can lead to direct impacts on the electrical grid at various levels. Firstly, they can cause damage to electricity generation, particularly to wind turbines. Wind turbines can be buckled by sustained high wind speeds. Additionally, outdoor transmission and distribution components such as electrical towers and power lines are also vulnerable to strong winds and can fail, resulting in disruptions to the normal operation of the grid.

6.2.3 Input datasets used in the model

Table 36. Data requirements for the electricity sector damage model.

| Data requirements for the electricity sector damage model | | |
|---|--|---|
| Data group | Description | Source |
| Weather wind map | Weather map with wind velocity and direction Future IDF curves considering different change scenarios scenarios and time horizons | Previous task |
| Power grid map | Power grid geolocation map of the elements that compounds it with their electrical data | ENTSO-E, OpenStreetMap ENDESA (for AMB CS) |
| Fragility curves data | Fragility curves for outdoor elements vulnerable to the strong winds such as lines and towers | Pantelli et. al 2016 |

6.2.4 Impact assessment model setup

The initial step in the development of the model for assessing the impact of network components affected by extreme winds consists of delimiting the elements to be considered and the corresponding fragility curves associated with these elements. In this context, the most susceptible transmission elements acknowledged are the electrical towers and the overhead power lines interconnecting them. For these components, we adopted the fragility curves presented in Figure 47, proposed by the scientific study conducted by Pantelli et al. (2016).

In a more recent article, they expounded the mathematical formulation of these fragility curves for both transmission lines and towers as follows:

$$P_{L,T}(w) = \{\bar{P}_{L,T}, \text{ if } w < w_{critical}\} \quad \text{[eq. 43]}$$

$$P_{L,T}(w) = \{P_{L,Thw}(w), \text{ if } w_{critical} \leq w < w_{collapse}\} \quad \text{[eq. 44]}$$

$$P_{L,T}(w) = \{1, \text{ if } w \geq w_{collapse}\} \quad \text{[eq.45]}$$

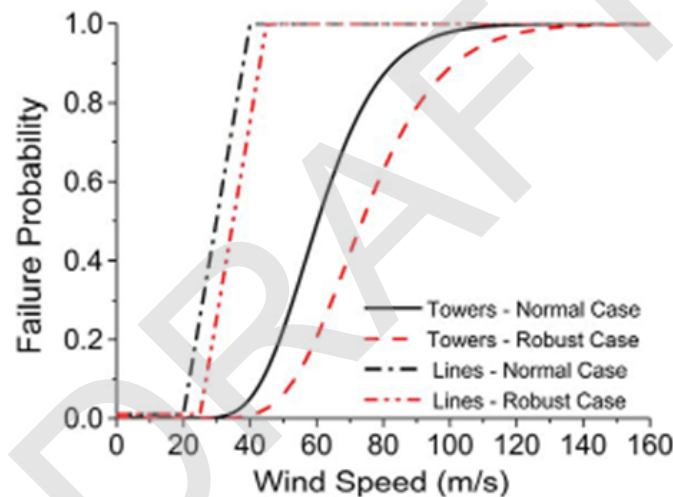


Figure 47. Fragility Curves used for assessing the impact of network components affected by extreme winds. Source: Pantelli et al. (2016).

Where $P_{L,T}(w)$ refers to the line (L) or tower (T) failure probability as a function of the wind speed w . \bar{P} is the “good weather conditions” failure rate, taken to be zero for towers and 10^{-2} for lines. P_{hw} is the failure rate under high wind speed, after some critical threshold $w_{critical}$ is reached. The wind speed beyond which the survival of transmission lines/towers is negligible is given by $w_{collapse}$.

Once the towers and power lines have been identified, each characterised by their respective fragility curves, they will be superimposed on the future climate map to assess the impact of wind on the grid elements under different future scenarios.

For the calculation of the probability of failure of electrical towers, it is assumed that failure is solely dependent on wind speed, regardless of wind direction. In other words, the tower’s failure probability remains unaffected by the wind’s direction, and, therefore, no additional transformation is required.

In the case of power lines, the wind speed is considered for the calculation of their failure probability. However, in contrast to towers, a more complex transformation is performed, taking into account the wind's direction concerning the line. The starting point is that the fragility curve quantifies the probability of line failure when the wind is completely perpendicular to it. Consequently, the less perpendicular the wind is relative to the line, the lower the likelihood of failure, as illustrated in Figure 48. Equation 46 seeks to exemplify this phenomenon mathematically. Taking into consideration, on one hand, the azimuth orientation of the line (O), in which it would remain constant, and on the other hand, the orientation at which the wind would strike upon the power line (WB). From these two orientations, the vertical component at which the wind impacts the line is calculated (resultant of the sine) and multiplied by the probability of element failure (P_L).

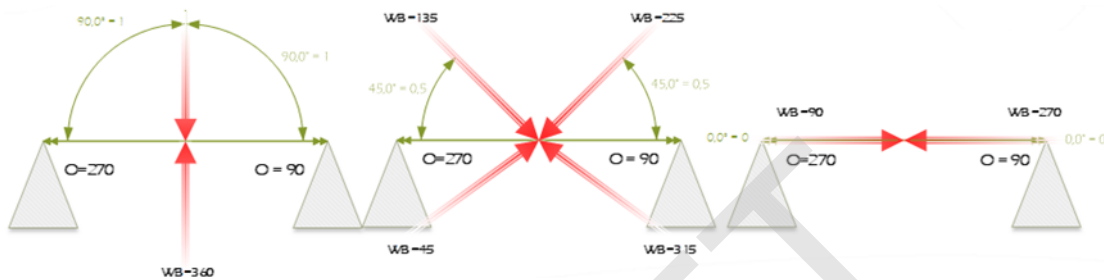


Figure 48. Wind impacts on the overhead line depending on the direction of the wind.

$$P_{windrisk} = P_L(w) \cdot \text{abs}(\sin(WB - O)) \quad \text{[eq. 46]}$$

Wind turbines can be approximated by simple wind power curves that determine the produced power depending on the wind speed. This function provides reasonable approximation, but can induce larger uncertainties (Lydia et al., 2014 and Marčiukaitis et al., 2017).

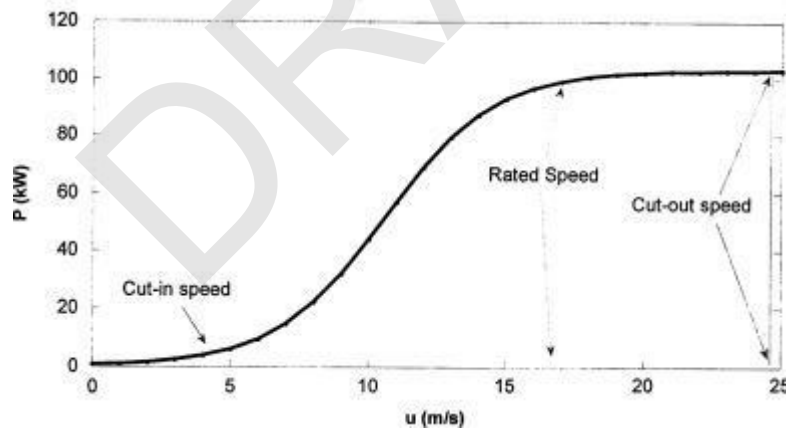


Figure 49. Wind turbine efficiency to wind speed.

Here the produced power (P) can be determined from $P = 0.5 C_p \rho \pi R^2 V^3$, where C_p is the coefficient of performance (efficiency factor, in percent), ρ is air density (in kg/m³), R is the blade length (in meters) and V is the wind speed (in meters per second). The wind should be estimated at the rotor hub height of the wind turbine.

6.2.5 Expected outputs of the model

The model's computed results, once the probability of failure for the elements in the electrical network is known, include the same monetary costs explained in section 2.4.1.4. in the output of the model to assess the risk on the electricity sectors on a flood risk event, which are the following ones:

1. **Damages over electrical assets:** The direct cost of failed components within the system, accounting for the required labor for replacement installation.
2. **Non-supplied electricity:** The cost associated with energy losses during the entire peril event.
3. **Businesses earning losses provoked by the shortage:** The cost incurred due to the inability to meet the total energy demand.
4. **Expenditures associated with the renting of emergency electrical supply appliances:** Additionally, considering the network connections where significant project assets are located, an assessment is made to determine their vulnerability in the event of a system incident and the potential ramifications of a disruption in their electrical supply.

DRAFT

7 ICARIA multi-risk perspective

The previous chapters of this document present the methodologies and impact models that will be applied in the ICARIA case studies to quantify the impact on critical assets and services when they are affected by extreme weather events. Such methodologies allow researchers (and any other users) to quantify in terms of economic damage, service disruption or intangible risk of people the impact of a given event.

Multi-hazard events may occur in various combinations of hazard types and dynamics between hazards, spatial and temporal scales, etc., and therefore requires comprehensive knowledge and modelling tools to simulate the involved processes. Most existing studies consider only one directional influence from one to another and ignore the feedback [Kappes et al., 2012].

The ICARIA multi-hazard risk/impact assessment framework starts from the assumption that the combination of multiple climate events and/or drivers puts society, assets, services, environment, etc. at risk in a combined manner. Depending on how the combination of these events occurs over time and space, receptors will suffer more severe damage than they would if a single event occurred, and the nature of damage will vary depending on both the complexity and interdependencies between hazards and/or impacts involved (Deliverable D1.1).

Within WP2, Tasks 2.1, 2.2 and 2.3 aim to reach a better understanding about interactions and joint probability among different hazards and investigate how to couple multiple state-of-the-art hazard models to reflect the dynamics among hazards and assess the impact of combined and compound multi-hazards.

In terms of multi-risk perspective, ICARIA applies two different modelling approaches:

1. Direct and indirect impacts on a specific risk receptor (main service, key asset, environment, etc.) can be analysed through a multi-risk assessment that takes into account different risks derived from single or linked (compound) hazards. For example, an electrical infrastructure can be affected by flooding, heat wave, heat wave + fire (compound events), etc.
2. Multi-risk assessment may also interest different risk receptors. In this case, for example, a flood may affect a specific sector (or a key infrastructure) and this situation produces other services drops or partial failures. This is the case of insufficient urban drainage networks that in case of heavy storm events can produce sewer floods with consequent transport disruptions, failures of key electrical infrastructures and economic damages in housing and other sectors. In this case, the direct and indirect impacts concern different risk receptors (services and infrastructures) though a chain of interrelated multi-sectoral consequences. In ICARIA, following the recent approach proposed by the RESCCUE project (Velasco et al., 2020), these kinds of situations have been defined as cascading effects. For this reason, even circumscribed and low-intensity hazards could generate broad cascading effects over time and space.

Both perspectives will be followed within ICARIA and, in some cases, implemented at the same time in ICARIA case studies to achieve a comprehensive climate-related risk assessment for complex regional systems with interdependencies among subsystems and infrastructures.

ICARIA project follows and try to improve the approach developed in RESCCUE project developing integrated or loosely coupled models and tools, where the outputs of certain models were used as inputs in others according to the scheme presented in Figure 51 (Evans et al., 2020, Forero-Ortiz et al., 2020, Martínez-Gomariz et al., 2019, Sánchez-Muñoz et al., 2020).

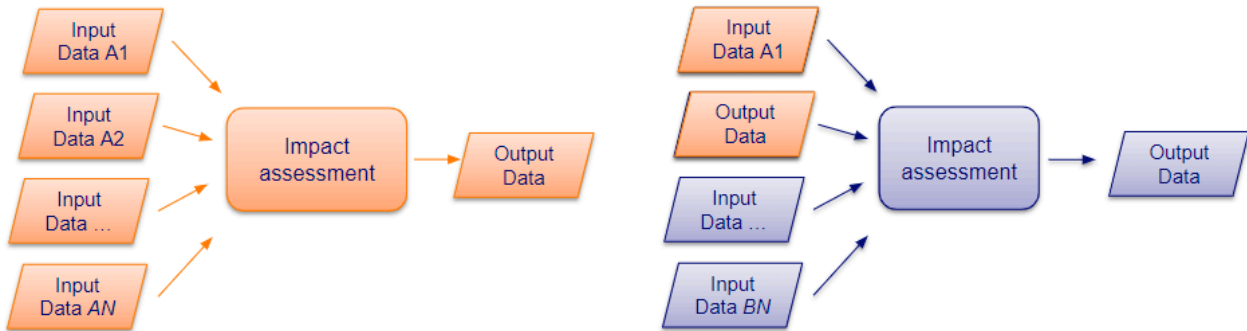


Figure 50. Scheme of loosely coupled model approach used for the cascading effect assessment.

This document acknowledges that there are enormous amounts of interdependencies between services and infrastructures in the case study regions. Their exhaustive identification, characterization and assessment would imply an enormous multidisciplinary effort beyond the reach of the project. Hence the assessment of chains of cascading effects in ICARIA is focused on a subset of assets according to the scope of the project and the previous background of the project consortium.

The following subsections look into the interdependencies existing among different risk-receptor assets and describe the main failure triggering mechanisms.

7.1 Cascading effects associated to the water sector

According to the scope of project ICARIA, the assets of the “water sector” encompass critical assets related to water management, including drinking water, pluvial water and wastewater, as well as drinking water supply.

Logically, drought episodes have a direct impact on the availability of water resources. Severe drought periods can lead to restrictions of water consumption in different economic sectors. In consequence, there are disruptions on productive sectors dependent on water inputs that cause cascading effects on connected economic activities in their supply chains.

During extreme rainfall events, urban areas can be affected by floods due to the lack of drainage capacity of its urban drainage system. The failure of this infrastructure is an intrinsic aspect of any flood assessment study of an urban area. The resulting accumulation of water in the city surface, can trigger various negative impacts (cascading effects) on different assets:

- Flooding of urban areas can lead to water intrusion in infrastructures related to electricity supply, leading to potential service disruption of the electricity distribution service. Such disruption can also trigger subsequent chains of cascading effects affecting other critical assets that were not directly affected by the flood.
- Transportation can also be affected by floods as the accumulation of water in streets and roads can lead to traffic cuts. Such cuts can subsequently hinder the activity of rescue and emergency services activated to face emergency situations. Similarly, interruptions can occur in underground metro and railway services.

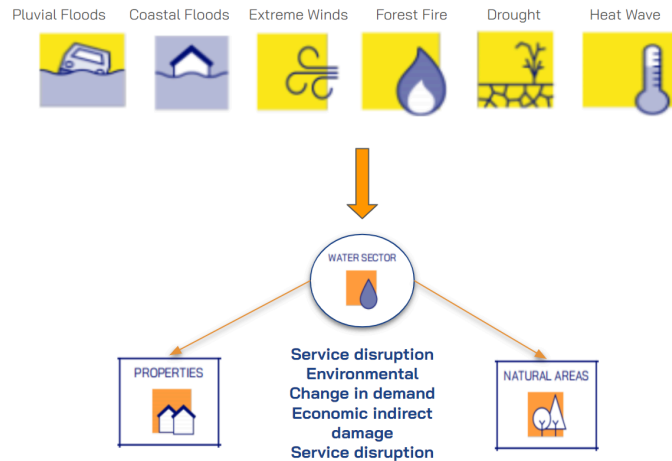


Figure 50. Water Sector Cascading Effects considered within ICARIA.

7.2 Cascading effects associated to the electricity

Electric grids are considered critical infrastructures, as ensuring their constant and safe operation is crucial for a region's security, health, and economy. Within the electricity sector, the ICARIA project encompasses assets ranging from energy generation elements to electric transmission and distribution components up to consumption or connection points. Throughout the document, methodologies have been presented for each specific hazard that could impair the optimal operation of the electrical system or cause direct damage, resulting in a complete loss of service.

Consequently, the cascade effects associated with electricity studied in the project involve examining the impact of a hazardous scenario on all non-electric assets connected to the electric grid and their risk of power outage. These impacts range from users being disconnected from their property, hindering their daily tasks, to transportation nodes unable to operate, affecting transportation services, or water sector assets unable to function correctly without electricity and provide essential services such as drinking water.

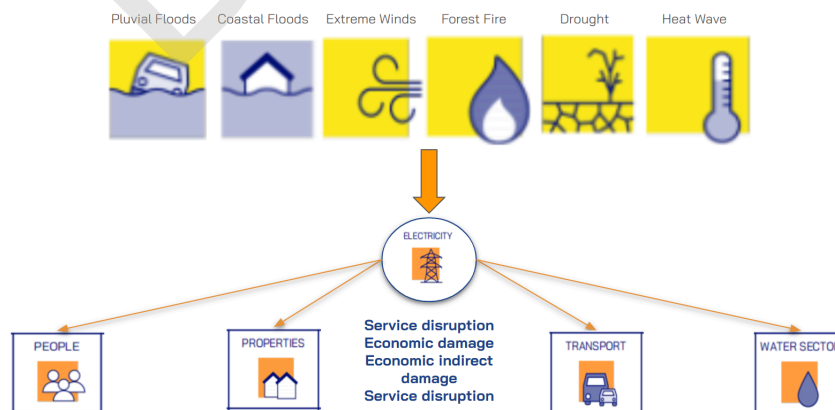


Figure 51. Electricity Sector Cascading Effects considered within ICARIA.

8 Conclusions

The comprehensive set of methodologies for assessing climate change impacts from a multi-hazard perspective presented in this deliverable is a stepping stone to develop an integrated assessment of the most relevant climate-related impacts at EU level. Including droughts, floods, heatwaves, forest fires and extreme winds ensures a holistic understanding of the potential impacts caused by Climate Change under the different scenarios presented in D1.2. This understanding will help to develop a set of adaptation scenarios that include different levels of investments in adaptation in the trials, and their consequences in terms of damages.

The methodologies presented are built mostly upon previous EU projects, and other consolidated international frameworks, ensuring a solid foundation for impact assessment. Leveraging the insights and experiences from projects like RESCCUE, CLARITY and others enhances the credibility and reliability of the proposed approach. Their selection was based on rigorous criteria, including robustness, suitability to hazards and risk receptors, adaptability to case studies, technical capability, and data availability.

This deliverable is expected to provide clear guidelines for conducting impact assessments in the three study regions - AMB, SAR and SBG in the following Tasks from WP4. These guidelines outline essential steps, from data collection to assessment methods, ensuring consistency and robustness across assessments.

The methodology caters to various critical sectors and services at risk, such as urban water, transport, energy, waste and natural areas (agriculture). By considering sector-specific vulnerabilities and impacts, the approach enables a targeted assessment of potential damages. This ensures that the chosen methods are appropriate for the context of the ICARIA project and its objectives.

The tangible impact assessment methods described in the deliverable play a crucial role in evaluating expected damages from climate hazards. By quantifying impacts in monetary terms, the methodologies facilitate a better understanding of potential consequences and support the identification of suitable adaptation solutions.

Ultimately, the outcomes of the impact assessments will contribute to promoting climate-resilient development. By providing insights into the costs and benefits of adaptation measures, the methodologies support decision-makers in identifying sustainable and cost-effective solutions to mitigate climate risks.

In conclusion, the ICARIA approach offers a robust and comprehensive methodology for assessing climate change impacts across various hazards and sectors. By providing clear guidelines, leveraging previous experiences, and prioritising sector-specific analysis, the approach facilitates informed decision-making for climate resilience and adaptation.

9 References

- Abt, S. R., Wittier, R. J., Taylor, A., & Love, D. J. (1989). Human stability in a high flood hazard zone 1. *JAWRA Journal of the American Water Resources Association*, 25(4), 881-890.
- Adhikari, P., Hong, Y., Douglas, K. R., Kirschbaum, D. B., Gourley, J., Adler, R., & Robert Brakenridge, G. (2010). A digitised global flood inventory (1998–2008): compilation and preliminary results. *Natural Hazards*, 55, 405-422.
- Agència Catalana de l'Aigua. (2023). Pla de sequera [Página web]. Recuperado de <https://aca.gencat.cat/ca/plans-i-programes/pla-de-sequera/>
- Agència Catalana de l'Aigua (2023). Regeneració, Gestió del Cicle de l'Aigua (ACA). Generalitat de Catalunya. Retrieved from: <https://aca.gencat.cat/ca/laigua/gestio-del-cicle-de-laigua/regeneracio/>
- Ali, E., Cramer, W., Carnicer, J., Georgopoulou, E., Hilmi, N.J.M., Le Cozannet, G., & Lionello, P. (2022). Cross-Chapter Paper 4: Mediterranean Region. In: *Climate Change 2022: Impacts, Adaptation, and Vulnerability. Contribution of Working Group II to the Sixth Assessment Report of the Intergovernmental Panel on Climate Change*. Cambridge University Press, Cambridge, UK and New York, NY, USA, pp. 2233-2272.
- Allen, M. R., Fernandez, S. J., Fu, J. S., & Olama, M. M. (2016). Impacts of climate change on sub-regional electricity demand and distribution in the southern United States. *Nature Energy*, 1(8), 1-9.
- Anderson, B. G., & Bell, M. L. (2009). Weather-related mortality: how heat, cold, and heat waves affect mortality in the United States. *Epidemiology (Cambridge, Mass.)*, 20(2), 205.
- Aparicio-Urbe, C., Russo, B., Tellez-Alvarez, J and Bladé, E. (2023) Análisis experimental y numérico del comportamiento hidráulico de escaleras de acceso a estaciones de metro. El caso de estudio de la estación de metro de Paral·lel en Barcelona. Proceedings of conference JIA 20203.
- Aulin-Ahmavaara, P. (1990). Dynamic Input–Output and Time. *Economic Systems Research*, 2(4), 329–344. <https://doi.org/10.1080/095353190000000023>
- Baccini, M., Biggeri, A., Accetta, G., Kosatsky, T., Katsouyanni, K., Analitis, A., ... & Michelozzi, P. (2008). Heat effects on mortality in 15 European cities. *Epidemiology*, 711-719.
- Baker, C. J., Hemida, H., & Quinn, A. D. (2016). The Operation of Trains through Flood Water. In *World Congress on Rail Research*, Milan.
- Baltagi, B. H., & Baltagi, B. H. (2021). Test of Hypotheses with Panel Data. *Econometric Analysis of Panel Data*, 75-108.
- Basu, R., & Samet, J. M. (2002). Relation between elevated ambient temperature and mortality: a review of the epidemiologic evidence. *Epidemiologic reviews*, 24(2), 190-202.
- Bhatt, N., Sarawgi, S., O'keefe, R., Duggan, P., Koenig, M., Leschuk, M., ... & Povolotskiy, M. (2009).

Assessing vulnerability to cascading outages. In 2009 IEEE/PES Power Systems Conference and Exposition (pp. 1-9). IEEE.

Bíl, M., Vodák, R., Kubeček, J., Bílová, M., & Sedoník, J. (2015). Evaluating road network damage caused by natural disasters in the Czech Republic between 1997 and 2010. *Transportation Research Part A: Policy and Practice*, 80, 90-103.

Burian, S. J., Walsh, T., Kalyanapu, A. J., & Larsen, S. G. (2013). Climate Vulnerabilities and Adaptation of Urban Water Infrastructure Systems. In *Climate Vulnerability* (Vol. 5, pp. 87–107). Elsevier.
<https://doi.org/10.1016/B978-0-12-384703-4.00509-8>

Building Arena. (2023). Railway Sleeper Sizes and Weights. Retrieved 7/11/2023 from <https://www.buildingarena.co.uk/companies/railwaysleepers-com1/products/railway-sleeper-sizes-and-weights>.

Buscail, C., Upegui, E., & Viel, J. F. (2012). Mapping heatwave health risk at the community level for public health action. *International journal of health geographics*, 11(1), 1-9.

Campbell, S., Remenyi, T. A., White, C. J., & Johnston, F. H. (2018). Heatwave and health impact research: A global review. *Health & place*, 53, 210-218.

Catalan Statistical Office. (2023). Inici. Recuperado de <https://www.idescat.cat/>

Cavanaugh, J. E., & Neath, A. A. (2019). The Akaike Information Criterion: Background, derivation, properties, application, interpretation, and refinements. *WIRES Computational Statistics*, 11(3).

Chambers, J. (2020). Global and cross-country analysis of exposure of vulnerable populations to heatwaves from 1980 to 2018. *Climatic Change*, 163(1), 539-558.

Chappelle, C., McCann, H., Jassby, D., Schwabe, K., & Szeptycki, L. (2019). *Managing wastewater in a changing climate*. San Francisco, CA: Public Policy Institute of California.

Chen, A. S., Hammond, M. J., Djordjević, S., Butler, D., Khan, D. M., & Veerbeek, W. (2016). From hazard to impact: Flood damage assessment tools for mega cities. *Natural Hazards*, 82, 857-890.

Chen, X., Ma, Z., Tan, X., Zhao, Y., Liu, C., Tan, F., & Yang, F. (2019). Analysis of Water Resource Benefits Due to Power Grid Interconnections Using the Virtual Water Method. *Global Energy Interconnection*, 2(3), 276-284. ISSN 2096-5117. doi:10.1016/j.gloei.2019.07.021.

Choi, H. il. (2019). Spatial assessment of damage vulnerability to storms based on the analysis of historical damage cost data in the Korean Peninsula. *Sustainability (Switzerland)*, 11(21).
<https://doi.org/10.3390/su11216051>

Choobineh, M., Ansari, B. and Mohagheghi, S. (2015), "Vulnerability assessment of the power grid against progressing wildfires", *Fire Safety Journal*, Vol. 73, pp. 20–28.

Choobineh, M., Tabares-Velasco, P. C., & Mohagheghi, S. (2016). Optimal energy management of a distribution network during the course of a heat wave. *Electric Power Systems Research*, 130, 230-240.

Climate Adapt Europe (2023) . CLIMADA adapt model. Retrieved from:
<https://climate-adapt.eea.europa.eu/>

Coburn, A. W., Spence, R. J. S., and Pomonis, A. (1994). Vulnerability and Risk Assessment. 2nd Edition. Cambridge, UK: UNDP Disaster Management Training Programme

Evans, D. L., & Florschuetz, L. W. (1977). Cost studies on terrestrial photovoltaic power systems with sunlight concentration. *Solar Energy*, 19(3), 255-262.

D'Ippoliti, D., Michelozzi, P., Marino, C., de'Donato, F., Menne, B., Katsouyanni, K., ... & Perucci, C. A. (2010). The impact of heat waves on mortality in 9 European cities: results from the EuroHEAT project. *Environmental Health*, 9(1), 1-9.

D2.4 MULTI-HAZARDS ASSESSMENT RELATED TO WATER CYCLE EXTREME EVENTS FOR CURRENT SCENARIO (PUBLIC SUMMARY). Retrieved from:

https://toolkit.resccue.eu/wp-content/uploads/2020/12/d2.4_multi-hazards_assessment_related_to_water_cycle_extreme.pdf

David M. Rey, Martin A. Briggs, Michelle A. Walvoord, Brian A. Ebel, (2023). Wildfire-induced shifts in groundwater discharge to streams identified with paired air and stream water temperature analyses, *Journal of Hydrology*, Volume 619, 129272, ISSN 0022-1694, <https://doi.org/10.1016/j.jhydrol.2023.129272>

DOCE (1991), Directiva 91/271/CEE del Consejo, de 21 de mayo de 1991, sobre el tratamiento de las aguas residuales urbanas, Bruselas.

Douglass, S. L., Webb, B. M., Kilgore, R., & Keenan, C. (2014). Highways in the coastal environment: Assessing extreme events (No. FHWA-NHI-14-006). United States. Federal Highway Administration.

Douglass, S. L., Webb, B. M., & Kilgore, R. (2014). Highways in the Coastal Environment: Assessing Extreme Events. *Hydraulic Engineering Circular No. 25 (Volume 2)*.
<https://www.fhwa.dot.gov/engineering/hydraulics/pubs/nhi14006/nhi14006.pdf>

Dubey, S., Sarvaiya, J. N., & Seshadri, B. (2013). Temperature Dependent Photovoltaic (PV) Efficiency and Its Effect on PV Production in the World – A Review. *Energy Procedia*, 33, 311-321.
doi:10.1016/j.egypro.2013.05.072

Energy Networks Association article. (2018). Resilience to Flooding of Grid and Primary Substations .
https://www.ena-eng.org/ena-docs/DOC3XTRACT/ENA_ET_138_-_Annex_Extract_180902050351.pdf.

Eom, J., Clarke, L., Kim, S. H., Kyle, P., & Patel, P. (2012). China's building energy demand: Long-term implications from a detailed assessment. *Energy*, 46(1), 405-419.

European Commission. (2022). DIRECTIVE OF THE EUROPEAN PARLIAMENT AND OF THE COUNCIL concerning urban wastewater treatment (recast) (Text with EEA relevance).
<https://eur-lex.europa.eu/legal-content/EN/TXT/?uri=CELEX%3A52022PC0541>

Evans, B. (2019). Impact Assessments of Multiple Hazards in Case Study Areas. Deliverable 3.4; RESCCUE EU H2020 Project. Internal report.

Evans, B., Chen, A. S., Prior, A., Djordjevic, S., Savic, D. A., Butler, D., Goodey, P., Stevens, J.R., and Colclough, G. (2018). Mapping urban infrastructure interdependencies and fuzzy risks. *Procedia engineering*, 212, 816-823.

Evans, B.; Chen, A.S.; Djordjevi, S.; Webber, J.; Gonzalez, A.; Stevens, J. (2020). Investigating the Effects of Pluvial Flooding and Climate Change on Traffic Flows in Barcelona and Bristol. *Sustainability*, 12, 2330.

Evans, B., Eigbogba, S., Muldoon, C., Campbell, A. G., Brewer, P. A., & O'Hare, G. M. (2019). Supporting participative pre-flood risk reduction in a UNESCO biosphere. *Journal of Flood Risk Management*, 12(S2), e12520.

FEMA. (2009). Multi-hazard Loss Estimation Methodology: Flood Model.
https://www.fema.gov/sites/default/files/2020-09/fema_hazus_flood-model_technical-manual_21.pdf

Faisst W., (1987). The impact of the Drought and Wastewater Treatment Plants and their Operation. California - Nevada AWWA Conference. Brown and Caldwell.
<https://brownandcaldwell.com/papers-and-reports/the-impact-of-the-drought-on-wastewater-treatment-plants-and-their-operation/>

Falkenmark, M.; Lundqvist, J.; Widstrand, C.(1989), Macro-scale water scarcity requires micro-scale approaches: Aspects of vulnerability in semi-arid development. *Nat. Resour. Forum* , 13, 258–267

Field, C. B. (Ed.). (2012). *Managing the risks of extreme events and disasters to advance climate change adaptation: special report of the intergovernmental panel on climate change*. Cambridge University Press.

Field, C. B., Barros, V., Stocker, T. F., Qin, D., Dokken, D. J., Plattner, G.-K., Ebi, K. L., Allen, S. K., Mastrandrea, M. D., Tignor, M., Mach, K. J., & Midgley, P. M. (Eds.). (2012). *Managing the Risks of Extreme Events and Disasters to Advance Climate Change Adaptation: Special Report of the Intergovernmental Panel on Climate Change*. Carnegie Institution for Science.

Field, C. B., & Barros, V. R. (Eds.). (2014). *Climate change 2014–Impacts, adaptation and vulnerability: Regional aspects*. Cambridge University Press.

FitzGerald, G., Du, W., Jamal, A., Clark, M., & Hou, X. Y. (2010). Flood fatalities in contemporary Australia (1997–2008). *Emergency Medicine Australasia*, 22(2), 180-186.

Forero-Ortiz, E., Martínez-Gomariz, E., Cañas Porcuna, M., Locatelli, L., & Russo, B. (2020). Flood risk assessment in an underground railway system under the impact of climate change—a case study of the Barcelona Metro. *Sustainability*, 12(13), 5291.

Forero-Ortiz, E., Martinez-Gomariz, E., & Canas Porcuna, M. (2020). A review of flood impact assessment approaches for underground infrastructures in urban areas: a focus on transport systems. *Hydrological Sciences Journal*, 65(11), 1943-1955.

Freire-González, J. (2011). Assessing the Macroeconomic Impact of Water Supply Restrictions Through an Input–Output Analysis. *Water Resources Management*, 25(9), 2335–2347.
<https://doi.org/10.1007/s11269-011-9811-4>

Freire-González, J., Decker, C. A., & Hall, J. W. (2017). A Scenario-Based Framework for Assessing the Economic Impacts of Potential Droughts. *Water Economics and Policy*, 03(04), 1750007.

<https://doi.org/10.1142/s2382624x17500072>

Friedrich, E., & Kretzinger, D. (2012). Vulnerability of wastewater infrastructure of coastal cities to sea level rise: A South African case study. *Water SA*, 38(5), 755–764. <https://doi.org/10.4314/wsa.v38i5.15>

Gámez R. (2021). “Programas piloto de adaptación al riesgo de inundación. Lote 2 instalaciones e industria” Tarea 5.5 Informe diagnóstico de la situación del riesgo de inundación de las EDAR de Butarque (Término municipal de Madrid).

Gámez R. (2021). “Programas piloto de adaptación al riesgo de inundación. Lote 2 instalaciones e industria” Tarea 5.5 Informe diagnóstico de la situación del riesgo de inundación de las EDAR de La China (Término municipal de Madrid).

Gasparrini, A., Guo, Y., Hashizume, M., Lavigne, E., Zanobetti, A., Schwartz, J., ... & Armstrong, B. (2015). Mortality risk attributable to high and low ambient temperature: a multicountry observational study. *The lancet*, 386(9991), 369-375.

Generalitat de Catalunya. Departament de Territori i Sostenibilitat, Agència Catalana de l'Aigua. (2019). Memòria 2019.

Ghosh, A. (1958). Input-Output Approach in an Allocation System. *Economica*, 25(97), 58. <https://doi.org/10.2307/2550694>

Goler R.(2019). in CLARITY D3.1. Science Support v1. available at: <http://www.clarity-h2020.eu>

Gleick, P.H.; Iwra, M. (1996). Basic Water Requirements for Human Activities: Meeting Basic Needs. *Water Int.* 21, 83–92

Gujarati, D. N., Porter, D. C., & Pal, M. (2021). *Basic econometrics*. Mcgraw-Hill Education.

Guo Y, Gasparrini A, Armstrong BG, Tawatsupa B, Tobias A, Lavigne E, Coelho M d SZS, Pan X, Kim H, Hashizume M, Honda Y, Guo YL et al (2016) Temperature variability and mortality: a multi-country study. *Environ. Health Perspect* 124:1554–1559. <https://doi.org/10.1289/EHP149>

Hagenlocher, M., Meza, I., Anderson, C. C., Min, A., Renaud, F. G., Walz, Y., ... & Sebesvari, Z. (2019). Drought vulnerability and risk assessments: state of the art, persistent gaps, and research agenda. *Environmental Research Letters*, 14(8), 083002.

Hajat S, Kosatky T (2010) Heat-related mortality: a review and exploration of heterogeneity. *J Epidemiol*

Hashmi, G. M., Lehtonen, M., & Millar, R. J. (2008). Transformer Loading Conditions for Future Thermally Unfavourable Environments. In *International Conference on Electrical and Control Technologies, ECT08*, Kaunas, Lithuania, May 8-9, 2008.

Community Health 64:753–760. <https://doi.org/10.1136/jech.2009.087999>

Hergarten, S. (2004). Aspects of risk assessment in power-law distributed natural hazards. *Natural Hazards and Earth System Sciences*, 4(2), 309-313.

Hsiao, S. C., Chiang, W. S., Jang, J. H., Wu, H. L., Lu, W. S., Chen, W. B., & Wu, Y. T. (2021). Flood risk influenced by the compound effect of storm surge and rainfall under climate change for low-lying coastal areas. *Science of the Total Environment*, 764. <https://doi.org/10.1016/j.scitotenv.2020.144439>

Hsu, M. H., Lin, S. H., Fu, J. C., Chung, S. F., & Chen, A. S. (2010). Longitudinal stage profiles forecasting in rivers for flash floods. *Journal of hydrology*, 388(3-4), 426-437.

Huang, Q., Wang, J., Li, M., Fei, M., & Dong, J. (2017). Modeling the influence of urbanization on urban pluvial flooding: a scenario-based case study in Shanghai, China. *Natural Hazards*, 87, 1035-1055.

Hughes, J., Cowper-Heays, K., Oleson, E., Bell, R., & Stroombergen, A. (2021). Impacts and implications of climate change on wastewater systems: A New Zealand perspective. *Climate Risk Management*, 31, 100262. <https://doi.org/10.1016/j.crm.2020.100262>

Huizinga, J., Moel, H. de, Szewczyk, W. (2017). Global flood depth-damage functions. Methodology and the database with guidelines. EUR 28552 EN. Publications Office of the European Union, Luxembourg, doi: 10.2760/16510.

Hummel, M. A., Berry, M. S., & Stacey, M. T. (2018). Sea level rise impacts on wastewater treatment systems along the U.S. coasts. *Earth's Future*, 6, 622–633. <https://doi.org/10.1002/2017EF000805>

IEEE. (1993). IEEE Standard for Calculating the Current-Temperature of Bare Overhead Conductors. In IEEE Std 738-1993 (pp. 1-48). doi: 10.1109/IEEESTD.1993.120365.

ICARIA. (2023). ICARIA Hollistic Modelling Framework. Hollistic Modelling Framework, D1.1. www.icaria-project.eu

Institut d'Estadística de Catalunya (IDESCAT). (2023). Idescat. <https://www.idescat.cat/>.

Intergovernmental Panel on Climate Change. (2018). Managing the risks of extreme events and disasters to advance climate change adaptation (Informe completo). Recuperado de https://www.ipcc.ch/site/assets/uploads/2018/03/SREX_Full_Report-1.pdf

International Monetary Fund. (2009). Export and Import Price Index Manual. International Monetary Fund.

IPCC, 2023: Summary for Policymakers. In: Climate Change ,(2023). Synthesis Report. Contribution of Working Groups I, II and III to the Sixth Assessment Report of the Intergovernmental Panel on Climate Change [Core Writing Team, H. Lee and J. Romero (eds.)]. IPCC, Geneva, Switzerland, pp. 1-34, doi: 10.59327/IPCC/AR6-9789291691647.001

Ishigaki, T., Asai, Y., Nakahata, Y., Shimada, H., Baba, Y., & Toda, K. (2010). Evacuation of aged persons from inundated underground space. *Water science and technology*, 62(8), 1807-1812.

Jefferson F. Flood and Lawrence B. Cahoon,(2011). "Risks to Coastal Wastewater Collection Systems from Sea-Level Rise and Climate Change," *Journal of Coastal Research* 27(4), 652-660. <https://doi.org/10.2112/JCOASTRES-D-10-00129.1>

Jenkins, K., Dobson, B., Decker, C., & Hall, J. W. (2021). An Integrated Framework for Risk–Based Analysis of Economic Impacts of Drought and Water Scarcity in England and Wales. *Water Resources Research*, 57(8). <https://doi.org/10.1029/2020wr027715>

Kappes, M. S., Keiler, M., von Elverfeldt, K., & Glade, T. (2012). Challenges of analyzing multi-hazard risk: a review. *Natural hazards*, 64, 1925-1958.

Kando (2023). What effects do droughts have on Wastewater Treatment Plants?
<https://www.kando.eco/what-effects-do-droughts-have-on-wastewater-treatment-plants/>

Karagiannis, G.M., Cardarilli, M., Turksezer, Z.I., Spinoni, J., Mentaschi, L., Feyen, L., & Krausmann, E. (2019). *Climate Change and Critical Infrastructure—Storms*. Luxembourg: European Union. ISBN 9789279964039.

Kellar, D. M. M., & Schmidlin, T. W. (2012). Vehicle-related flood deaths in the United States, 1995–2005. *Journal of flood risk management*, 5(2), 153-163.

Kerpelis, P. N., Alexakis, D. E., & Golfinopoulos, S. K. (2022). A Qualitative Approach to the Seismic Estimation of Wastewater Treatment Plants and Potential Impacts on the Hydrosphere. *Water (Switzerland)*, 14(20). <https://doi.org/10.3390/w14203225>

KILBOURNE, E. M. (1996). *Heat Waves and Hot Environments. The Public Health Consequences of Disasters*.

Koks, E. E., & Haer, T. (2020). A high-resolution wind damage model for Europe. *Scientific reports*, 10(1), 6866.

Krau, S. D. (2013). The impact of heat on morbidity and mortality. *Critical Care Nursing Clinics*, 25(2), 243-250.

Lee, S. T. (2008). Estimating the probability of cascading outages in a power grid. *Proc. of 16th PSCC, Glasgow, Scotland*, 14-18.

Leontief W (1941) *The structure of the American economy 1919–1939*. New York, Oxford

Leontief, W. W. (1951). Input-Output Economics. *Scientific American*, 185(4), 15–21.
<https://www.jstor.org/stable/24945285>

Li, J., Li, X., Liu, H., Gao, L., Wang, W., Wang, Z., Zhou, T., & Wang, Q. (2023). Climate change impacts on wastewater infrastructure: A systematic review and typological adaptation strategy. In *Water Research (Vol. 242)*. Elsevier Ltd. <https://doi.org/10.1016/j.watres.2023.120282>

Li, M., Gu, S., Bi, P., Yang, J., & Liu, Q. (2015). Heat waves and morbidity: current knowledge and further direction—a comprehensive literature review. *International journal of environmental research and public health*, 12(5), 5256-5283.

Liss, A., Wu, R., Chui, K. K. H., & Naumova, E. N. (2017). Heat-related hospitalizations in older adults: An amplified effect of the first seasonal heatwave. *Scientific reports*, 7(1), 39581.

Lyu, H. M., Shen, S. L., Zhou, A., & Yang, J. (2019). Perspectives for flood risk assessment and management for mega-city metro system. *Tunnelling and Underground Space Technology*, 84, 31-44.

M. Lydia, S. Suresh Kumar, A. Immanuel Selvakumar, G. Edwin Prem Kumar, (2014). A comprehensive review on wind turbine power curve modeling techniques, *Renewable and Sustainable Energy Reviews*, Volume 30, Pages 452-460, ISSN 1364-0321, <https://doi.org/10.1016/j.rser.2013.10.030>.

M. Panteli and P. Mancarella, (2015). "Modeling and Evaluating the Resilience of Critical Electrical Power Infrastructure to Extreme Weather Events," IEEE Systems Journal, Volume: 11, Issue: 3.

M. Panteli, C. Pickering, S. Wilkinson, R. Dawson and P. Mancarella, (2016). "Power system resilience to extreme weather: Fragility modelling, probabilistic impact assessment, and adaptation measures," IEEE Transactions on Power Systems.

Mantas Marčiukaitis, Inga Žutautaitė, Linas Martišauskas, Benas Jokšas, Giedrius Gecevičius, Athanasios Sfetsos, (2017) Non-linear regression model for wind turbine power curve, Renewable Energy, Volume 113, Pages 732-741, ISSN 0960-1481, <https://doi.org/10.1016/j.renene.2017.06.039>

Maranzoni, A., D’Oria, M., & Rizzo, C. (2023). Quantitative flood hazard assessment methods: A review. *Journal of Flood Risk Management*, 16(1), 1–31. <https://doi.org/10.1111/jfr3.12855>

Marleni, N., Gray, S., Sharma, A., Burn, S., & Muttill, N. (2012). Impact of water source management practices in residential areas on sewer networks - A review. In *Water Science and Technology* (Vol. 65, Issue 4, pp. 624–642). <https://doi.org/10.2166/wst.2012.902>

Martínez-Gomariz, E., Gómez, M., & Russo, B. (2016). Experimental study of the stability of pedestrians exposed to urban pluvial flooding. *Natural hazards*, 82(2), 1259-1278.

Martínez-Gomariz, E., Gómez, M., Russo, B., & Djordjević, S. (2018). Stability criteria for flooded vehicles: A state-of-the-art review. *Journal of flood risk management*, 11, S817-S826.

Martínez-Gomariz, E., Gómez, M., Russo, B. (2017). A new experiments-based methodology to obtain the stability threshold for any real vehicle exposed to flooding. *Urban Water Journal*. 14(9), 930-939.

Martínez-Gomariz, E., Guerrero-Hidalga, M., Russo, B., Yubero, D., Gómez, M., & Castán, S. (2019). Desarrollo y aplicación de curvas de daño y estanqueidad para la estimación del impacto económico de las inundaciones en zonas urbanas españolas. *Ingeniería del agua*, 23(4), 229-245.

Martínez-Gomariz, E., Locatelli, L., Guerrero, M., Russo, B., & Martínez, M. (2019). Socio-Economic Potential Impacts Due to Urban Pluvial Floods in Badalona (Spain) in a Context of Climate Change. *Water*, 11(12), 2658. <https://doi.org/10.3390/W11122658>

Martínez-Gomariz E, Gómez M, Russo B, Sánchez P, Montes J-A., (2019). Methodology for the damage assessment of vehicles exposed to flooding in urban areas. *J Flood Risk Management*. 12:e12475. <https://doi.org/10.1111/jfr3.12475>

Martínez-Gomariz, E., Forero-Ortiz, E., Guerrero-Hidalga, M., Castán, S., & Gómez, M. (2020). Flood Depth–Damage Curves for Spanish Urban Areas. *Sustainability*, 12(7), 2666. <https://doi.org/10.3390/su12072666>

Martínez-Gomariz, E., Forero-Ortiz, E., Russo, B., Locatelli, L., Guerrero-Hidalga, M., Yubero, D., Castan, S., (2021). A novel expert opinion-based approach to compute estimations of flood damage to property in dense urban environments. Barcelona case study. *J. Hydrol.* 598, 126244. <https://doi.org/10.1016/j.jhydrol.2021.126244>

Martínez-Gomariz, E., Barbero, C., Sanchez-Juny, M., Forero-Ortiz, E., & Sanz-Ramos, M. (2023). Dams or ponds classification based on a new criterion to assess potential flood damage to roads in case of failure. *Natural Hazards*, 117(1), 625-653.

Martínez-Gomariz, E., Guerrero-Hidalga, M., Forero-Ortiz, E., Castán, S., Velasco Droguet, M., Villanueva Blasco, Á., (2020). Inundaciones pluviales en zonas urbanas españolas: un modelo de estimación de daños basado en la experiencia pericial. *Conorseguros Rev. Digit.* 15.

Martínez-Gomariz, E.; Russo, B.; Gómez, M.; Plumed, A. (2019). An approach to the modelling of stability of waste containers during urban flooding. *J. Flood Risk Manag.* 13, e12558.

Martínez-Gomariz, E., Guerrero-Hidalga, M., Forero-Ortiz, E., & Gonzalez, S. (2021). Citizens' Perception of Combined Sewer Overflow Spills into Bathing Coastal Areas. *Water, Air, & Soil Pollution*, 232(9), 370. <https://doi.org/10.1007/s11270-021-05305-x>

Matthew Wibbenmeyer, Matthew R Sloggy, José J Sánchez, (2023). Economic Analysis of Wildfire Impacts to Water Quality: A Review, *Journal of Forestry*, Volume 121, Issue 4, Pages 374–382

Meadows, R., (2022) How Do Wildfires Affect Water Systems? *ACS Cent Sci.* May 25;8(5):504-506. doi: 10.1021/acscentsci.2c00511.

Merrill, C. T., Miller, M., & Steiner, C. (2011). Hospital Stays Resulting from Excessive Heat and Cold Exposure Due to Weather Conditions in US Community Hospitals.

Mestre, I., Casado, M. J., & Rodríguez, E. (2013). Cap 2- Tendencias observadas y proyecciones de cambio climático en España.

Miller, R. E., & Blair, P. D. (2009). *Input-output analysis : foundations and extensions*. Cambridge University Press.

Mundlak, Y. (1978). On the Pooling of Time Series and Cross Section Data. *Econometrica*, 46(1), 69. <https://doi.org/10.2307/1913646>

N. i. England, "Sito ufficiale del Sistema Sanitario del Regno Unito," [Online]. Available: <http://www.nhs.uk/Conditions/Heat-exhaustion-and-heatstroke/Pages/Diagnosis.aspx>. [Accessed 31 January 2020].

Naumann, G., Spinoni, J., Vogt, J. V., & Barbosa, P. (2015). Assessment of drought damages and their uncertainties in Europe. *Environmental Research Letters*, 10(12), 124013.

OECD. (2023). Real GDP long-term forecast (indicator). doi: 10.1787/d927bc18-en

Oudin Åström, D. , Bertil, F., & Joacim, R. (2011). Heat wave impact on morbidity and mortality in the elderly population: a review of recent studies. *Maturitas*, 69(2), 99-105.

OpenStreetMap. (2023). Retrieved from <https://www.openstreetmap.org/>

Penning-Rowsell, E., Viavattene, C., Pardoe, J., Chatterton, J., Parker, D., & Morris, J. (2010). The benefits of flood and coastal risk management: A handbook of assessment techniques. Flood Hazard Research Centre, Middlesex University, London, UK.

Pocock, G., Joubert, H., (2017). Effects of reduction of wastewater volumes on sewerage systems and wastewater treatment Plants. Water Research Commission, Gezina, South Africa. Retrieved from <http://www.wrc.org.za/wp-content/uploads/mdocs/2626-1-18.pdf>.

- Poudineh, R., & Jamasb, T. (2017). The Energy Journal Vol. 38, No. 1 (January 2017), pp. 51-76.
- Pregnoiato, M., Ford, A., Robson, C., Glenis, V., Barr, S., & Dawson, R. (2016). Assessing urban strategies for reducing the impacts of extreme weather on infrastructure networks. Royal Society open science, 3(5), 160023.
- Pregnoiato, M., Ford, A., Wilkinson, S. M., & Dawson, R. J. (2017). The impact of flooding on road transport: A depth-disruption function. Transportation research part D: transport and environment, 55, 67-81.
- Pyatkova, K. (2018). Flood Impacts on Road Transportation. University of Exeter (United Kingdom). ProQuest Dissertations Publishing, 30397792.
- Pyatkova, K., Chen, A.S., Djordjević, S., Butler, D., Vojinović, Z., Abebe, Y.A., Hammond, M., (2019). Flood Impacts on Road Transportation Using Microscopic Traffic Modelling Techniques, in: Simulating Urban Traffic Scenarios, Lecture Notes in Mobility. Springer, Cham, pp. 115–126. DOI: 10.1007/978-3-319-33616-9_8.
- Rail Safety and Standards Board. (n.d.). Safety Culture Maturity Model: Guidance Document. Retrieved 6/11/2023 from <https://www.rssb.co.uk/research-catalogue/CatalogueItem/T1052>
- Railroad Rails. (n.d.). UIC60 Rail. Retrieved 6/11/2023 from <https://railroadrails.com/railroad-rail-for-sale/uic60-rail/>
- Reichl, J., Schidthaler, M., Schneider, F.(2013): The value of supply security: the costs of power outages to Austrian households, firms and the public sector. Energy Econ. 36, 256–261
- RESCCUE 2019. Deliverable 2.3 Multi-hazards assessment related to water cycle extreme events for future scenarios (business as usual) - Project RESCCUE
- RESCCUE 2019. Deliverable 2.4 Multi-hazards assessment related to water cycle extreme events for current scenario – summary version - Project RESCCUE
- Review of the rules for the operation of trains through flood water (T1052) Retrieved from: <https://www.rssb.co.uk/research-catalogue/CatalogueItem/T1052>
- Rocha, F., & VISEU, T. (2016). Guidance on implementation of BINGO WP4–Assessment of impacts of extreme weather events. *Establishing the context for the risk management process. Relatório, 168*, 2016.
- Rocha, J., Carvalho-Santos, C., Diogo, P., Beça, P., Keizer, J.J., & Nunes, J.P. (2020). Impacts of climate change on reservoir water availability, quality and irrigation needs in a water scarce Mediterranean region (southern Portugal). Science of The Total Environment, 736, 139477.
- Rose, S., Jaramillo, P., Small, M. J., Grossmann, I., & Apt, J. (2012). Quantifying the hurricane risk to offshore wind turbines. Proceedings of the National Academy of Sciences, 109(9), 3247-3252.
- Rothman, K. J., Greenland, S., & Associate, T. L. L. (2014). Modern Epidemiology, 3rd Edition. In The Hastings Center report.
- Russo, B. (2010). Design of surface drainage systems according to hazard criteria related to flooding of urban areas (Doctoral dissertation, Universitat Politècnica de Catalunya (UPC)).

Russo, B., Gómez, M., & Macchione, F. (2013). Pedestrian hazard criteria for flooded urban areas. *Natural hazards*, 69, 251-265.

Russo, B., Velasco, M., Locatelli, L., Sunyer, D., Yubero, D., Monjo, R., ... & Gómez, A. G. (2020). Assessment of urban flood resilience in Barcelona for current and future scenarios. The RESCCUE project. *Sustainability*, 12(14), 5638.

Russo, B., Gómez, M., & Macchione, F. (2013). Pedestrian hazard criteria for flooded urban areas. *Natural hazards*, 69, 251-265.

Russo, B., Valentín, M. G., & Tellez-Álvarez, J. (2021). The relevance of grated inlets within surface drainage systems in the field of urban flood resilience. A review of several experimental and numerical simulation approaches. *Sustainability*, 13(13), 7189.

Salvati, P., Petrucci, O., Rossi, M., Bianchi, C., Pasqua, A. A., & Guzzetti, F. (2018). Gender, age and circumstances analysis of flood and landslide fatalities in Italy. *Science of the total environment*, 610, 867-879.

Sánchez-Muñoz, D., Domínguez-García, J. L., Martínez-Gomariz, E., Russo, B., Stevens, J., & Pardo, M. (2020). Electrical Grid Risk Assessment Against Flooding in Barcelona and Bristol Cities. *Sustainability*, 12(4), 1527. <https://doi.org/10.3390/su12041527>

Sangsefidi, Y., Bagheri, K., Davani, H., & Merrifield, M. (2023). Data analysis and integrated modelling of compound flooding impacts on coastal drainage infrastructure under a changing climate. *Journal of Hydrology*, 616. <https://doi.org/10.1016/j.jhydrol.2022.128823>

Sfetsos A, Giroud F, Clemencau A, Varela V, Freissinet C, LeCroart J, Vlachogiannis D, Politi N, Karozis S, Gkotsis I, et al., (2021); Assessing the Effects of Forest Fires on Interconnected Critical Infrastructures under Climate Change. Evidence from South France. *Infrastructures*. 6(2):16. <https://doi.org/10.3390/infrastructures6020016>

Sharpe R., Caddis B., Bewsher D., Grech P. (2012). Ballina Floodplain Risk Management Study, Volume 1, Exhibition Version.

Spinoni, J., Vogt, J.V., Naumann, G., Barbosa, P., & Dosio, A. (2018). Will drought events become more frequent and severe in Europe? *International Journal of Climatology*, 38, 1718-1736.

Spirandelli, D., Babcock, R., & Shen, S. (2018). Assessing the Vulnerability of Coastal Wastewater Infrastructure to Climate Change. University of Hawaii Sea Grant College Program. www.kew.org/msbp/samara

Sugimoto, K., Okuoka, K., & Tanikawa, H. (2018). Establishment of three-dimensional subway GIS data for inundation analysis in urban area. *J Jpn Soc Civ Eng Ser G (Environ Res)*, 73, I_283-I_289.

Tran, Q. K., Jassby, D., & Schwabe, K. A. (2017). The implications of drought and water conservation on the reuse of municipal wastewater: Recognizing impacts and identifying mitigation possibilities. *Water research*, 124, 472-481.

UN-DHA (1993). Internationally Agreed Glossary of Basic Terms Related to Disaster Management. DNA193136. Geneva: United Nations Department of Humanitarian Affairs

UNDRO (1980). Natural Disasters and Vulnerability Analysis. Report of Experts Group Meeting of 9-12 July 1979. Geneva: UNDRO

UNFCCC (2013). Non-economic losses in the context of the work programme on loss and damage. Technical paper. UNFCCC, Geneva, Swiss, 65 pp

Vamvakeridou-Lyroudia, L. S., Chen, A. S., Khoury, M., Gibson, M. J., Kostaridis, A., Stewart, D., Wood, M., Djordjevic, S., & Savic, D. A. (2020). Assessing and visualising hazard impacts to enhance the resilience of Critical Infrastructures to urban flooding. *Science of The Total Environment*, 707, 136078.
<https://doi.org/10.1016/J.SCITOTENV.2019.136078>

Vandellós i Delgado, L. (2023). Metodologia d'avaluació de la vulnerabilitat climàtica de les plantes de tractament de residus. Universitat Politècnica de Catalunya

Van Vliet, M. T., Sheffield, J., Wiberg, D., & Wood, E. F. (2016). Impacts of recent drought and warm years on water resources and electricity supply worldwide. *Environmental Research Letters*, 11(12), 124021.

Velasco, M., Cabello, À., & Russo, B. (2016). Flood damage assessment in urban areas. Application to the Raval district of Barcelona using synthetic depth damage curves. *Urban Water Journal*, 13(4), 426–440.
<https://doi.org/10.1080/1573062X.2014.994005>

Velasco, M., Russo, B., Kersting, T., & Cabello, À. (2013). Flood vulnerability assessment considering climate changes impacts. Application to Barcelona case study using relative depth damage curves. *International Conference on Flood Resilience: Experiences in Asia and Europe*, 11.

Velasco, M., Russo, B., Martínez, M., Malgrat, P., Monjo, R., Djordjevic, S., Fontanals, I., Vela, S., Cardoso, M. A., Buskute, A., (2018). Resilience to cope with climate change in Urban Areas—A multisectorial approach focusing on water—The RESCCUE Project. *Water*, 10(10), 1356.

Velasco, M., Russo, B., Monjo, R., Paradinas, C., Djordjević, S., Evans, B., ... & Pacheco, D. (2020). Increased Urban Resilience to Climate Change—Key Outputs from the RESCCUE Project. *Sustainability*, 12(23), 9881.

Walras, L. (1954) *Elements of Pure Economics*. Translated by Jaffe, W., Allen and Unwin, London.

Watts, N., Amann, M., Ayebe-Karlsson, S., Chambers, J., Hamilton, I., Lowe, R., ... & Latifi, A. M. (2018). The Lancet Countdown on health and climate change: from 25 years of inaction to a global transformation for public health (vol 391, pg 540, 2017). *The Lancet*, 391(10120), 540.

White, G.F. (1945) *Human Adjustment to Floods: A Geographical Approach to the Flood Problem in the United States*. Ph.D. Dissertation, University of Chicago, Chicago, MA, USA.

White, I., Storey, B., Owen, S., Bell, R., Charters, F., Dickie, B., Zammit, C., (2017). *Climate Change & Stormwater and Wastewater Systems*. Motu Economic and Public Policy Research, Wellington. Retrieved from:
<https://motu.nz/our-work/environment-and-resources/climate-change-impacts/climate-change-and-stormwater-and-wastewater-systems/>

Winne, S., Horrocks, L., Kent, N., Miller, K., Hoy, C., Benzie, M., & Power, R. (2012) *Increasing the climate resilience of waste infrastructure*. Final Report under Defra contract ERG 1102. AEA group, published by Defra.

World Bank. (n.d.). World Development Indicators. Retrieved 19/12/2023 from <http://databank.worldbank.org/data/views/variableSelection/selectvariables.aspx?source=world-development-indicators>.

Zhang, C., Tang, H., Ishigaki, T., Kawanaka, R., Onishi, Y., Shimada, H., ... & Baba, Y. (2009). Assessment of safety on evacuating route during underground flooding. In *Advances in Water Resources and Hydraulic Engineering: Proceedings of 16th IAHR-APD Congress and 3rd Symposium of IAHR-ISHS* (pp. 141-146). Springer Berlin Heidelberg.

Zouboulis, A., & Tolkou, A. (2015). Effect of Climate Change in Wastewater Treatment Plants: Reviewing the Problems and Solutions. In *Springer Water* (pp. 197–220). Springer Nature. https://doi.org/10.1007/978-3-319-10467-6_10

Zuccaro, G., De Gregorio, D., & Leone, M. F. (2018). Theoretical model for cascading effects analyses. *International journal of disaster risk reduction*, 30, 199-215.

Zuccaro, G., & Leone, M. F. (2021). Climate Services to Support Disaster Risk Reduction and Climate Change Adaptation in Urban Areas: The CLARITY Project and the Napoli Case Study. *Frontiers in Environmental Science*, 9, 693319.

Zuloaga, S., Khatavkar, P., Vittal, V. and Mays, L.W. (2020), Interdependent electric and water infrastructure modelling, optimisation and control. *IET Energy Syst. Integr.*, 2: 9-21.

DRAFT

Annex 1: Data Management Statement

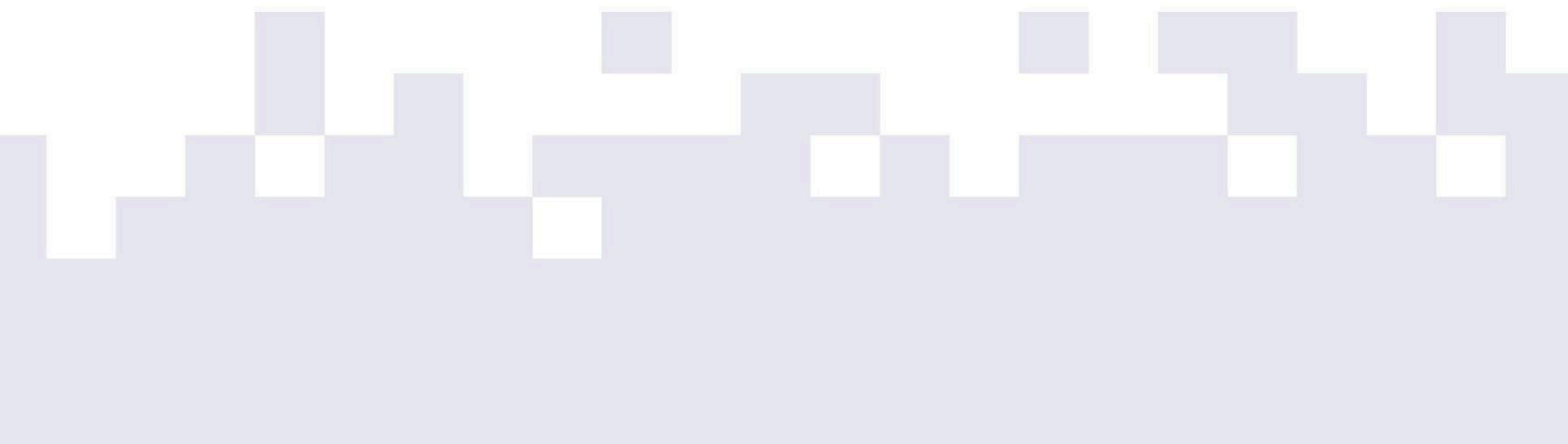
Table A1.1. Data used in preparation of ICARIA Deliverable 3.1

| Dataset name | Form at | Size | Owner and re-use conditions | Potential Utility within and outside ICARIA | Uniqu e ID |
|--------------|---------|------|-----------------------------|---|------------|
| n/a | | | | | |

Table A1.2. Data produced in preparation of ICARIA Deliverable 3.1

| Dataset name | Form at | Size | Owner and re-use conditions | Potential Utility within and outside ICARIA | Uniqu e ID |
|--------------|---------|------|-----------------------------|---|------------|
| n/a | | | | | |

DRAFT



More info: www.icaria-project.eu



This project has received funding from the European Union's Horizon Europe research and innovation programme under grant agreement No. 101093806. The publication reflects only the authors' views and the European Union is not liable for any use that may be made of the information contained therein.